© 2012

Adam K. Tressler

ALL RIGHTS RESERVED

THE CORRELATION BETWEEN POST- *IN SITU* CHEMICAL OXIDATION CONCENTRATION REBOUND AND MOLECULAR DIFFUSION

By

ADAM KARL TRESSLER

A dissertation submitted to the

Graduate School-New Brunswick

Rutgers, The State University of New Jersey

in partial fulfillment of the requirement

for the degree of

Doctor of Philosophy

Graduate Program in Environmental Sciences

Written under the direction of

Professor Christopher G. Uchrin

and approved by

_____

_____

_____

_____

_____

New Brunswick, New Jersey

October, 2012

ABSTRACT OF DISSERTATION

Correlation between Post-ISCO Concentration Rebound and Molecular Diffusion

by ADAM KARL TRESSLER

Dissertation Director:
Dr. Christopher G. Uchrin

Sodium permanganate and potassium permanganate have been used for *in situ* chemical oxidation (ISCO) projects for approximately two decades now. After decades of application, concentration rebound has emerged as a common problem for this remediation strategy. Unfortunately after decades of research on ISCO, there has been very little research on the question of concentration rebound. Most research on the topic of ISCO has focused on demonstrating effectiveness, estimating kinetics, or quantifying the effects of reaction products. Only one study has demonstrated that a correlation between concentration rebound and hydrogeological parameters exists. This study uses a numerical solution to an advection-dispersion-reaction equation in order to quantify a correlation between the rate of rebound and molecular diffusivity in pure water. It accomplishes this by simulating a variety of sites contaminated with tetrachloroethene or trichloroethene that also had an ISCO with permanganate. Each simulation included advection, two-dimensional dispersion, oxidation, concentration rebound, natural oxidant demand, and retardation. Six sites were suitable for simulation and nine cells were delineated within the six sites. These cells allowed for a variety of soils, contaminants,

injection methods (i.e. frequency, depth, mass of oxidant, duration, etc...), time scales, spatial scales, and hydrogeological variables to be examined. A robust correlation (R^2=0.9257) was identified with a regression analysis between the molecular diffusion coefficient in pure water and the rate of concentration rebound. The correlation identified by this research offers several useful applications. One application of this research is that it is now possible to optimize the information gained by a thorough site characterization. For example, a more predictable rate of concentration rebound can be used to optimize the time intervals between oxidant injections. In addition, choosing injection well locations can be optimized by modeling the boundaries of an oxidant's effectiveness. Another application of this research is that a more predictable rate of concentration rebound can be used to compare the effectiveness of ISCO to other remediation technologies. This reduces a variety of uncertainties by allowing more informed decisions between very expensive remediation strategies.

Without troublesome work, no one can have any concrete, full idea of what pure mathematical research is like or of the profusion of insights that can be obtained from it.

-Edmund Husserl

Acknowledgements

I have many people to thank for their support. First, I would like to thank my advisor, Dr. Christopher Uchrin, for all of his guidance, insight, and wisdom. I have no doubt that my project is much better than originally conceptualized because of your help. I would also like to thank Sue Dickison for all of the encouragement, access to data, networking, and reassurance that this project matters.

I was very fortunate to have a supportive and constructive committee, so I would like to thank Mr. Stewart Abrams, Dr. Daniel Gimenez, Dr. Weilin Huang, and Dr. Peter Strom for allowing me to muddle through this project. In addition to the support of my committee there are many members of the professional community that provided invaluable information about a various contaminated properties. I would like to thank Rich Bonczek, Pamela Dugan, Jennifer Hiatt, Mark Kauffman, Bruce Rundell, Michelle Simon, and Andy Vitolins for their time and generosity.

Dedication

This thesis is dedicated to my friend and mentor, Dick Soderberg. You were right that I had to go back and finish a Ph.D.

Table of Contents

Abstract ii

Quotation iv

Acknowledgements v

Dedication vi

Table of Contents vii

List of Tables ix

List of Figures x

List of Equations xii

Chapter 1: Introduction 1

Chapter 2: Background & Literature Review 4
- 2.1. Fate and Transport of PCE and TCE before ISCO 4
- 2.2. Fate and Transport of PCE and TCE during ISCO 9
- 2.3. Fate and Transport of PCE and TCE after ISCO 15
- 2.4 Summary 18

Chapter 3: Model Development 19
- 3.1 Fundamental Concepts and Definitions 19
- 3.2 Advection Dispersion Reaction Equation 23
- 3.3 Numerical Method and Solution 23
- 3.4 Method to Assess Mass Conservation 25
- 3.5 Uncertainty Analysis 29
- 3.6 Calibration Algorithm & Parameter Estimation 31
- 3.7 Sensitivity Analysis Approach 34
- 3.8 Mass Reduction Analysis Approach 34
- 3.9 Precipitate Accumulation Analysis Approach 36
- 3.10 Limitations and Assumptions 36

Chapter 4: Results 44
- 4.1 Site Descriptions and Concentration Rebound Rates 44
- 4.2 Results of Uncertainty Analysis 51
- 4.3 Results of Sensitivity Analysis 52
- 4.4 Mass Reduction Analysis Results 55

4.5 Precipitate Accumulation Analysis Results 56
4.6 Molecular Diffusion/Rate of Concentration Rebound Correlation Results 56

Chapter 5: Discussion 148
5.1 Uncertainty Analysis Conclusion 148
5.2 Sensitivity Analysis Conclusions 149
5.3 Mass Reduction Conclusions 150
5.4 Precipitate Accumulation Conclusions 151
5.5 Molecular Diffusion/Rate of Concentration Rebound Correlation Conclusions 151
5.6 Recommendations 152

References 153

Vita 162

List of Tables

Table 3.5.1: Location Specific Ranges for Monte Carlo Analysis 43

Table 4.1.1: Estimated Parameters for the Busch Campus Site 58

Table 4.1.2: Estimated Parameters for the Cape Canaveral Sites 62

Table 4.1.3: Estimated Parameters for the Chemplex Site 68

Table 4.1.4: Estimated Parameters for the PGDP 72

Table 4.1.5: Estimated Parameters for the Valmont Sites 76

Table 4.1.6: Estimated Parameters for the Watervliet Sites 82

Table 4.1.7: Summary of Estimated Parameters 88

Table 4.2.1: Standard Deviations for the Busch Campus Cell 89

Table 4.2.2: Standard Deviations for the Cape Canaveral 2S Cell 94

Table 4.2.3: Standard Deviations for the Cape Canaveral 5S Cell 100

Table 4.2.4: Standard Deviations for the Chemplex Cell 106

Table 4.2.6: Standard Deviations for the PGDP Cell 111

Table 4.2.7: Standard Deviations for the Valmont EW-1 Cell 112

Table 4.2.8: Standard Deviations for the Valmont EW-5 Cell 115

Table 4.2.9: Standard Deviations for the Watervliet IW-1 Cell 118

Table 4.2.10: Standard Deviations for the Watervliet IW-4 Cell 124

Table 4.4.1: Mass Reduction Summary 143

Table 4.5.1: Precipitate Accumulation in Pore Volumes 144

Table 4.6.1: Rejection of Outliers 145

List of Figures

Figure 3.2.1: Conceptual Schematic 38

Figure 3.4.1: Curve Generated by 1-Dimensional Analytical Solution 39

Figure 3.4.2: Regression Analysis for Mass Fixer 40

Figure 3.4.3: Two-Dimensional Plot for Comparison to Analytical Plot 41

Figure 3.4.5: Comparison of Three Solutions 42

Figure 4.1.1: Busch Campus Garage Well Locations & Initial Concentration 59

Figure 4.1.2: Busch Campus Garage Site Natural Oxidant Demand Calibration 60

Figure 4.1.3: Busch Campus Garage Concentration Rebound Rate Calibration 61

Figure 4.1.4: Cape Canaveral (2S) Well Locations & Initial Concentration 63

Figure 4.1.5: Cape Canaveral (5S) Well Locations & Initial Concentration 64

Figure 4.1.6: Cape Canaveral Sites Natural Oxidant Demand Calibration 65

Figure 4.1.7: Cape Canaveral (2S) Concentration Rebound Rate Calibration 66

Figure 4.1.8: Cape Canaveral (5S) Concentration Rebound Rate Calibration 67

Figure 4.1.9: Chemplex Well Locations & Initial Concentration 69

Figure 4.1.10: Chemplex Site Natural Oxidant Demand Calibration 70

Figure 4.1.11: Chemplex Concentration Rebound Rate Calibration 71

Figure 4.1.12: PGHP Well Locations & Initial Concentration 73

Figure 4.1.13: PGDP Site Natural Oxidant Demand Calibration 74

Figure 4.1.14: PGDP Concentration Rebound Rate Calibration 75

Figure 4.1.15: Valmont (EW-1) Well Locations & Initial Concentration 77

Figure 4.1.16: Valmont (EW-5) Well Locations & Initial Concentration 78

Figure 4.1.17: Valmont Sites Natural Oxidant Demand Calibration 79

Figure 4.1.18: Valmont (EW-1) Concentration Rebound Rate Calibration 80

Figure 4.1.19: Valmont (EW-5) Concentration Rebound Rate Calibration 81

Figure 4.1.20: Watervliet (IW-1) Well Locations & Initial Concentration 83

Figure 4.1.21: Watervliet (IW-4) Well Locations & Initial Concentration 84

Figure 4.1.22: Watervliet Sites Natural Oxidant Demand Calibration 85

Figure 4.1.23: Watervliet (IW-1) Concentration Rebound Rate Calibration 86

Figure 4.1.24: Watervliet (IW-4) Concentration Rebound Rate Calibration 87

Figure 4.3.1: Sensitivity Analysis for Advection 134

Figure 4.3.2: Sensitivity Analysis for Dispersivity 135

Figure 4.3.3: Sensitivity Analysis for α_L/α_T 136

Figure 4.3.4: Sensitivity Analysis for Retardation Factor 137

Figure 4.3.5: Sensitivity Analysis for Solubility 138

Figure 4.3.6: Sensitivity Analysis for Rate of Natural Oxidant Demand 139

Figure 4.3.7: Sensitivity Analysis for Rate of Oxidation 140

Figure 4.3.8: Sensitivity Analysis for Rate of Concentration Rebound 141

Figure 4.3.9: Figure 13: Hydraulic Conductivity Reduced at 250 days 142

Figure 4.6.1: Regression Analysis 146

Figure 4.6.2: Regression Analysis 147

List of Equations

Equation 2.1.1: Gilland-Sherwood Model 6

Equation 2.2.1: Mass Balance of Permanganate and PCE 9

Equation 2.2.2: Mass Balance of Permanganate and TCE 10

Equation 3.1.1: Average Linear Velocity 19

Equation 3.1.2: x-Direction Dispersion 20

Equation 3.1.3: y-Direction Dispersion 20

Equation 3.1.4: Retardation Factor 21

Equation 3.1.5: Dissolution Flux 21

Equation 3.1.6: Fate & Transport of Permanganate Injection 22

Equation 3.2.1: General Solution 23

Equation 3.3.1: Numerical Solution 24

Equation 3.3.2: Initial Concentration Estimation 24

Equation 3.3.3: ADI First Half Step 25

Equation 3.3.4: ADI Second Half Step 25

Equation 3.4.1: Two Dimensional Analytical Solution with First Order Kinetics 26

Equation 3.4.2: Mass Transport with Dissolution 26

Equation 3.4.3: Modified x-Dispersion 27

Equation 3.4.4: Mass Fixer 27

Equation 3.4.5: C Coefficient Correction 28

Equation 3.4.6: C_{error} 28

Equation 3.8.1: Aqueous Phase Estimation 35

Equation 3.8.2: Solid Phase Estimation 35

Equation 3.9.1: Mass Balance of NOD & Permanganate 36

Chapter 1: Introduction

Tetrachloroethene (PCE) and trichloroethene (TCE) are just two of the many products that are part of a toxic legacy from the twentieth century. In "A History of the Production and Use of Carbon Tetrachloride, Tetrachloroethylene, Trichloroethylene, and 1,1,1-Trichloroethane in the United States: Part 1 – Historical Background; Carbon Tetrachloride and Tetrachloroethylene," Richard Doherty (2000a) lists the most common uses of PCE.

> Until approximately 1996, the highest-volume use of PCE was as a cleaning fluid by the dry-cleaning industry. Dry-cleaners favored PCE because of its relatively low toxicity, good cleaning properties, nonflammability, high stability, and moderate cost. As a metal cleaning and degreasing solvent, PCE was preferred for aluminum cleaning because of its high stability, and for melting of wax and resin residues because of its high boiling point. It was considered well suited for sulfur recovery, rubber dissolution, paint removal, printing ink bleeding, soot removal, catalyst regeneration and electroplating pre-cleaning operations.

Later, in Doherty (2000b), he summarizes the historical uses and ubiquity of TCE.

> Trichloroethylene, also known by a variety of chemical and trade names, was a widely used degreasing solvent that achieved public notoriety for its role in contaminating drinking water wells in Woburn, Massachusetts in the 1960s. As of 1997, TCE was reported as being present at 852 of 1430 National Priority List sites, making it one of the most commonly found contaminants at Superfund sites.

MacDonald and Kavanugh (1994) demonstrated that the conventional treatment of groundwater contaminants has been widely ineffective for treating PCE and TCE. Conventional treatment of groundwater contamination drills wells for monitoring and drills another group of wells to pump contaminated groundwater to the surface for treatment. In some cases, the groundwater is shipped to a water treatment facility. In other cases, the groundwater is treated on site by flushing through granular activated carbon (GAC), an air stripping tower, or a catalytic oxidation (CatOx) chamber. After the latter group of treatments, the water is usually injected back into the subsurface.

Due to the ineffectiveness of pump and treat, there is a demand for a more effective and cost-efficient solutions to PCE and TCE in groundwater. One of the approaches emerging to address PCE and TCE is *in situ* chemical oxidation (ISCO). ISCO is an approach that pumps an oxidant into the source zone in order to initiate chemical reactions that render a contaminant harmless. Huang et al. (1999) state that permanganate became the preferable oxidant "because of not only its high aqueous solubility but also its relatively longer half-life in the subsurface. It offers the additional benefit of safe handling of a solid at room temperature and convenient delivery to the subsurface as a liquid injection."

ISCO has also been shown to be an effective treatment option. Early studies that demonstrated the effectiveness of ISCO include West et al. (1997) who demonstrated the effectiveness of ISCO on chlorinated ethenes with field studies and Schnarr et al. (1998) who demonstrated effectiveness with both laboratory and field investigations. Practical applications are not the only support for the wide spread use of permanganates. Research completed by Crimi and Siegrist (2005) compared the effectiveness and efficiency of potassium permanganate to catalyzed hydrogen peroxide. They compared both oxidants with the following five criteria: 1) soil oxidant demand (SOD), 2) contaminant oxidant demand, 3) reaction rates of oxidant consumption and dense non-aqueous phase liquid (DNAPL) destruction, 4) total percent destruction of DNAPLs, and 5) relative treatment efficiency[1]. Their investigation demonstrated that potassium permanganate is superior to catalyzed hydrogen peroxide for all criteria except the fifth.

After the mass of any oxidant has passed though a source zone, entrapped and untreated DNAPLS begin to migrate again. This results in a rebound of DNAPL

[1] The amount of mass remaining compared to the initial mass.

concentration. An unpredictable rate of concentration rebound leaves professionals in a position where decisions regarding ISCOs must be made with very little guidance from scientific studies. To address this problem, this study tests whether or not a correlation can be found between the diffusion coefficient in pure water and the rate of concentration rebound.

This study is organized into five chapters. The next chapter is a review of the publications that are relevant to the topic. Chapter three explains the model that was used to estimate the rate of concentration rebound and that model's numerical solution. Chapter four presents a summary of the results. Finally, in chapter five a summary of the conclusions is presented along with recommendations to further advance the field of study.

Chapter 2: Background and Literature Review

This chapter is organized into four subsections. The first summarizes the relevant literature regarding the fate and transport of DNAPLS such as PCE and TCE in the subsurface in order to understand how the spatial and temporal distribution of PCE and TCE develops. Subsection two presents the research that has been published about the relevant phenomena (such as kinetics and precipitates) that occur during permanganate injections. The third presents the studies that have examined what occurs after the permanganate has been consumed or flushed out of a contaminant source zone. The fourth is a brief recapitulation of the literature review.

2.1. Fate and Transport of PCE and TCE before ISCO

The general behavior of DNAPLs such as PCE and TCE in a saturated zone has been understood for decades now. Mercer and Cohen (1990) described a DNAPL's descent through the vadose zone and through the saturated zone until it settles in a location and condition that impedes the movement of a DNAPL (such as bedrock, low permeability formations, capillary pressure...). Illangasekare et al. (2006) listed six variables that will influence the spatial and temporal distribution of a DNAPL once it is released into the subsurface. Those variables include the volume of DNAPL released, the area of infiltration, time duration of the release, the properties of the DNAPL, properties of the porous media, subsurface flow conditions.

Illangasekare et al. (2006) also described how the spatial distribution will be affected by the fingering, preferential flow, and soil heterogeneities. In zones with high saturation, pools and macro-scale entrapment zones will form, whereas, in zones with

low saturation residual blobs and ganglia can be expected. However in earlier work Illangasekare et al. (1995a and b), it was demonstrated that a mix of pools and residual zones can be expected at all sites contaminated by DNAPLs. These pools, entrapments, and ganglia function as long term sources of contamination (McKay & Cherry, 1989; Schwille, 1998). Feenstra and Cherry (1996) argued that the entire extent of an aquifer that contains free phase DNAPL will function as a source of contamination. Several groups of investigators (Schwille, 1988; Kueper et al., 1989; Kueper et al., 1993; Kueper and Frind, 1991a and b) have demonstrated that most contaminated sites have multiple DNAPL source zones. The local variation in ganglia, fingers, and similar phenomena is caused by heterogeneities in capillary pressure in the subsurface (Poulson & Kueper, 1992; Kueper et al., 1993).

Even with all the of the previously identified relationships, the varying spatial and temporal distribution of DNAPLs in heterogeneous soils makes locating DNAPL sources in the field a difficult, time-consuming, and complicated task as demonstrated by Parker et al. (2003). However, proper characterization of source zones is important because it is in these locations that groundwater flows through generating aqueous phase PCE and TCE and carrying them to locations that may present ecological and human health hazards. Therefore, estimating rates of dissolution and the factors that influence how dissolution occurs are important in order to understand contaminant transport (Soga et al., 2004). As with most scientific endeavors, our understanding of a process began with laboratory experimentation.

Several column studies have examined mass transport coupled with mass transfer (Miller et al., 1990; Imhoff and Pinder, 1993; Powers et al., 1992; Powers et al., 1994;

Imhoff et al., 1998; Bradford et al., 2000; Saeton and Illangesekare, 2003; and Fure et al., 2006). There is also a commonly accepted empirical correlation, the Gilland-Sherwood model, which predicts mass transfer rates in columns (Bird et al., 1960).

$$\mathrm{Sh_{natl}} = \alpha(\mathrm{Re})^{\beta}(\mathrm{Sc})^{\gamma}\left(\frac{\theta_n d_{50}}{\tau L^*}\right)^{\mu} \qquad \text{(Equation 2.1.1)}$$

where:

$\mathrm{Sh_{natl}}$: Sherwood Number
α: Empirical coefficient
Re: Reynolds Number
β: Empirical coefficient
Sc: Schmidt Number
γ: Empirical coefficient
θ_n: Volumetric content of NAPL
d_{50}: Median grain size [L]
τ: Empirical coefficient
L^*: Distance from dissolution surface [L]
μ: Empirical coefficient

and:

$$\mathrm{Sh_{natl}} = \frac{k\,\mathrm{L}}{\mathrm{D}}$$

$\mathrm{Sh_{natl}}$: Sherwood Number
k: mass transport coefficient [L/T]
L: System Length [L]
D: Mass Diffusivity [L^2/T] (Weber, 2001)

Unfortunately, there are many complications that pose problems when applying the Gilland-Sherwood model to field studies. Bradford et al. (2003) demonstrated that mass transfer in the field is influenced by the particular spatial distributions of DNAPLs. Saba and Illangasekare (2000) showed that the reduction of permeability due to entrapped DNAPLs reduces the flow, and therefore, the rate of dissolution. They also proposed that dissolution rates may be at least an order of magnitude less in the field than proposed by the Gilland-Sherwood model. Saba (1999) demonstrated that estimating large scale mass transfer coefficients with small scale mass transfer coefficients (i.e., the Gilland-Sherwood model) is confounded by varying hydraulic conductivity found in any heterogeneous media.

More complications are identified in the study published by Nambi (2000) who used a regression analysis to include the varying hydraulic conductivities in the field in order to develop a modified Gilland-Sherwood model. However, Illangasekare et al. (2006) criticized this study because it assumed that the DNAPL distribution is homogenous. Parker and Park (2004) also demonstrated that field estimations of dissolution were much lower than column experiments with three-dimensional models. Parker and Park (2004) re-affirmed that dissolution rates are correlated to groundwater velocity, amount of DNAPL, and the source architecture (i.e., fingers, pools) of DNAPL distribution, but Illangasekare et al. (2006) criticized this publication for ignoring soil heterogeneity. Christ et al. (2006) and Guilbeault et al. (2005) further demonstrated that source zone architecture must be considered to effectively estimate the rates of dissolution in field settings.

Many of these complications must have been assumed before the previously mentioned studies confirmed that they are non-negligible. Fortunately, field studies have been conducted on DNAPLs in groundwater since the 1980s that can offer a little more insight into these dilemmas. Many of the early studies (Sudicky et al., 1983; Sutton and Barker, 1985; McKay et al., 1986; Freyberg, 1986; Roberts et al., 1986; Curtis et al. 1986; Sudicky, 1986; Barker et al., 1989; and Rivett, 1991) were conducted at the Borden Air Force base in Ontario, Canada. All these experiments can be briefly summarized as placing known quantities of DNAPLs in a sandy aquifer and monitoring the plume in order to establish many of the fundamentals concepts that are still in use.

Once the general behavior and fundamental processes were established, modeling DNAPL plumes still had to grapple with the problem of dissolution estimation at specific

locations. One problem that needed to be investigated was to ask why in column studies concentrations would approach solubility as length increased, but this phenomenon did not occur in the field. Andersen et al., (1992a and b) used three dimensional models to demonstrate that in the field solubility will never be reached due to the influence of source architecture. Later Gonullu (1996) supported Andersen et al. (1992a and b) when he observed that pool formation and reduced dissolution rates also occurred in column studies.

However, it was clear that other variables needed to be considered in order to estimate dissolution in the field. Johnson and Pankow (1992) published a study that related the rate of dissolution in the field to molecular diffusion, dispersivity, groundwater velocity, path length, and solubility. According to Hansen and Kueper (2007), two approaches developed for modeling source zone dissolution in the field with the variables identified by Johnson and Pankow (1992). The first was a numerical approach that attempted to include the complexities of temporal and spatial distributions. Four examples of this approach include Geller and Hunt (1993) Lee and Chrysikopoulos (1995), Frind et al. (1999), and Parker and Park (2004). The second approach combined analytical solutions in a series of time steps. Examples of this approach include Guiger (1993), Lee (2002), and Roy et al. (2002).

One approach that does not fit the categories proposed by Hansen and Kueper (2007) was published by Sale and McWhorter (2001) who used a semi-analytical model to determine two conclusions. First, they demonstrated that in the field the rate of dissolution is strongly influenced by advection and dispersion as well as the source architecture. Sale and McWhorter (2001) also concluded that field scale dissolution rates

will change very slowly over time due to very slow source reduction. Grant and Gerhard (2007) summarized the rate of dissolution in the field as a function of two factors. The first is the interfacial geometry of the DNAPL/water contact surface. The second factor is the relationship between the solute advection and mass diffusion of the DNAPL. Evidence of the claims stated by Grant and Gerhard (2007) can be found in Pfannkuch (1984), Sale and McWhorter (2001), Parker and Park (2004), and Park and Parker (2005).

Grant and Gerhard (2007) stated one of the current research questions well.

> Numerical modeling studies that compare published correlation expressions have shown predicted dissolution rates to be highly sensitive to the local-scale expression utilized to simulate behavior in large-scale (Zhu and Sykes, 2000) or heterogeneous (Mayer and Miller, 1996; Grant and Gerhard, 2004) systems. Imhoff et al, 1993 compared the correlation expressions of Miller et al., 1990, Parker et al., 1991, Powers et al., 1992, and Geller and Hunt, 1993 and found that they produced [Gilland-Sherwood model] values that span over three orders of magnitude for a fixed set of conditions. Imhoff et al., 1993 attributes this lack of agreement to laboratory methods, including the different techniques used for establishing residual NAPL within the porous media. These studies suggest that empirical correlation expressions may have limited applicability, related to the conditions under which they were derived.

Later in this project, concentration rebound and its causes will be reviewed and it will be assumed that the same factors (groundwater velocity, path length, dispersivity, diffusion, and solubility) that drive dissolution before ISCO will also drive dissolution (and therefore concentration rebound) after the oxidant leaves the system.

2.2. Fate and Transport of PCE and TCE during ISCO

The ultimate goal of injecting permanganate into a contaminant plume is to cause reactions that render the contaminants harmless. Schnarr et al. (1998) summarized the reactions between PCE, TCE, and permanganate with Equation 2.2.1 and Equation 2.2.2.

$$C_2Cl_4 + 2MnO_4^- \rightarrow 2Cl^- + 2CO_2 + 2MnO_{2(s)} + Cl_2 \qquad \text{(Equation 2.2.1)}$$

$$C_2HCl_3 + 2MnO_4^- \rightarrow 3Cl^- + 2CO_2 + 2MnO_{2(s)} + H^+ \quad \text{(Equation 2.2.2)}$$

However, the basic stoichiometry does not fully represent all the important information that may be required for a well designed ISCO. It may offer guidance to estimate the necessary amount of permanganate required for treating the contaminant (if the natural oxidant demand (NOD) is well characterized) and it shows the reaction products, but it does not present the rate that reactions will proceed.

The pathways and reaction rates of the reduction/oxidation reactions summarized above have been identified by several authors (Yan and Schwartz, 1999; Hood et al., 2000; Huang et al., 2001; Huang et al., 2002a; and Dai and Reitsma, 2004). All of the authors observed an overall second order reaction and that as chlorination increased the reaction rate decreased. Kao et al. (2008) suggested that the decreased reaction rates may occur in alkaline conditions because they are hindered by a rind of MnO_2 precipitates that forms between the DNAPL/water interfaces. The rind retards the reaction rate because it reduces the contact surface area between the permanganate and chlorinated ethenes. However, a rind does not form in acidic or weakly acidic conditions because the MnO_2 remains in solution.

In addition to oxidation reactions, another influential process is dissolution. It has been generally accepted that dissolution is the rate limiting step in ISCO. Early studies and modeling approaches (Schnarr et al., 1998; Zhang and Schwartz, 2000; and Hood et al., 2000) assumed that the concentration gradient changes of chlorinated ethenes caused by the oxidation of chlorinated ethenes by permanganate would increase the rate of dissolution. The conceptual model proposed by Schnarr et al. (1998) applied the single

stagnant film model summarized in Feenstra and Guiguer (1996). Schnarr et al. (1998) and Hood et al. (2000) also assumed that the rate of dissolution will increase with respect to the oxidant concentration because permanganate destroys the mass of chlorinated solvent in aqueous phase, thereby increasing the concentration gradient.

Reitsma and Dai (2001) attempted to quantify this increased rate of dissolution. They made an observation that the increased rate of dissolution happens when two macro-processes (advection and dispersion) are occurring. In short, in the sections of a system where advection and dispersion were functioning, the rate of dissolution increased. However, in sections where neither advection nor dispersion occurred, the rate of dissolution did not increase. This dilemma revealed that something was missing from understanding dissolution's role during ISCO.

Urynowicz and Siegrist (2005) supplied the missing piece to this puzzle. They published their laboratory experiments that compared dissolution under static versus non-static conditions and yielded the same observations as Reitsma and Dai (2001). However, Urynowicz and Siegrist (2005) proposed a model to explain the seemingly contradictory results. Urynowicz and Siegrist (2005) appealed to a model of dissolution coupled with first order reactions proposed by Hatcher (1986). Urynowicz and Siegrist (2005) (like Kao et al. (2008) later claimed) proposed that a very thin colloidal film of manganese oxides form at the interface of aqueous chlorinated ethenes and aqueous permanganates that retard the rate of dissolution. Urynowicz and Siegrist (2005) appealed to a single stagnant film model, but whereas previous authors assumed that the aqueous phase chlorinated ethene and aqueous phase permanganate would approach zero

at their respective interface, this model proposed a colloidal film developed when advection and dispersion are not present.

In summary, the rate of dissolution may be increased or decreased depending on whether or not advection and dispersion is occurring in the location of the reaction. Where advection or dispersion occurs, the colloidal film of manganese oxides that retards the rate of dissolution does not accumulate and concentration gradient changes increase the rate of dissolution. However, in situations where advection and dispersion do not occur a colloidal film retards the rate of dissolution. This retarded rate of dissolution is further supported by MacKinnon and Thomson (2002) and West et al. (2008) who both demonstrate that the MnO_2 can significantly reduce the rate of mass transfer.

This presents a dilemma for ISCO. Liquid phase chlorinated ethenes are commonly found in pools or residuals that generate the aqueous phase of chlorinated ethenes (Kueper & McWhorter, 1996) or diffuse into the less permeable rock matrix (Parker et al., 1996). These pools and residuals form because capillary pressure blocks their entry into other spaces and results in pockets of trapped liquid phase chlorinated ethenes. These stationary pools or residuals may or may not have advection and dispersion occurring at their water-solvent interface. Vanderkwaak and Sudicky (1996) concluded that rates of dissolution "is a function of flow and transport properties of the fracture network and rock matrix." Since it is impossible to characterize all of these interfaces in field settings, the coefficients for the rate of dissolution during an ISCO project may be very difficult to accurately estimate because it cannot be known where colloidal films of manganese oxides have rendered an increased rate of dissolution

(caused by a concentration gradient) to a location where diffusion into the matrix is occurring (due to reduced transport).

The reaction products may cause additional problems besides reducing reaction rates. Another question regarding the effect of ISCO on the hydrogeology of a subsurface system is whether or not the reaction products (i.e., manganese oxides) have an adverse effect on the flow regime of that subsurface system. One publication that offers evidence that reaction products do not reduce porosity is Struse et al. (2002) who concluded that reaction products only have a negligible effect on the subsurface system. However, the literature in favor of reaction products affecting the hydrogeology is, by comparison, overwhelming.

Early evidence that porosity is reduced was published by Li and Schwartz (2000), who made their claims based on the observations of MnO_2 deposition within column studies. In a subsequent column study published by Schroth et al. (2001), the permeability of a porous media was demonstrated to be reduced by MnO_2 production and Seol et al. (2003) support the claims of Schroth et al. (2001). Other laboratory studies published by MacKinnon and Thomson (2002) and Huang et al. (2002b) also concluded that MnO_2 precipitates will result in decreased velocity. In addition, Lee et al. (2003) confirmed that MnO_2 accumulation produced by reactions will reduce the velocity of a subsurface system with a study that employed a sand filled tank. Finally, Tunnicliffe and Thomson (2004) demonstrated that reaction products also reduce the flow regimes within fractured media.

It may seem that the evidence in favor of reduced permeability by reaction products far outweighs the evidence against it. However, the most reasonable answer to

the question about whether or not reaction products affect a subsurface system is that it depends on the conditions in the subsurface system. Crimi and Siegrist (2004) demonstrated that accumulation of reaction products depends upon four factors in the subsurface: "(1) particle size, (2) particle concentrations[2] (3) the time allowed for development, and (4) the impact of matrix conditions on the ability of particles to agglomerate[3]." Another example of conditions governing the accumulation of reaction products is offered by Petri et al. (2008) who demonstrated that the relationship between oxidant concentration and subsurface velocity will determine the accumulation of deleterious reaction products. For example, applications using high concentrations of permanganate with low subsurface system velocities will result in altered mass transfer rates (Petri et al., 2008). Finally, Heiderscheidt et al. (2008) concluded that reaction products formed based upon the configuration of the source zone. A few examples include source zones that had little or no flow underwent substantial reduction in mass transfer due to reaction products and pools versus ganglia experience difference patterns of reaction product formation. Heiderscheidt et al. (2008) also made the observation that mass transfer can be reduced along with hydrogeological parameters such as porosity or hydraulic conductivity.

Changes to the rates of mass transfer are a relevant factor to the rate of oxidation. Firstly, rate of mass transfer influences that amount of DNAPL that will be treatable while the oxidant is in the system. Secondly, the rate of dissolution offers guidance to the amount of DNAPL that will not be treated by the oxidant, which is one of the topics addressed in the following subsection.

---

[2] The number of particles in the aqueous phase.
[3] The degree to which particles are soluble/colloidal in form or particulate in form.

2.3. Fate and Transport of PCE and TCE after ISCO

As mentioned previously, it has been assumed that dissolution would be the rate limiting process during ISCO. It is also assumed that as the oxidant is exhausted by natural oxidant demand or flushed out of the system, concentration rebound will occur because of the dissolution of remaining DNAPLs. It is improbable that all DNAPLs will be treated in a single (or even multiple) injections. Thomson et al. (2007) attributed the remaining PCE after several permanganate injections to source architecture. However, they could not rule out the effects of precipitates. Brusseau et al. (2007) attributed the concentration rebound they observed in a large scale study that characterized an extensively contaminated site in Tucson, AZ, to the mass transfer from untreated DNAPLs with identical processes as those described in section 2.1. However, it should not be assumed that dissolution solely drives the concentration rebound.

Multiple publications show back diffusion is an important process that must be considered for effective remediation (Ball et al., 1997; Liu and Ball, 2002; Chapman and Parker, 2005; and Parker et al., 2008), but only recently have studies been published that considered back diffusion with respect to ISCO of chlorinated ethenes. Goldstein et al. (2004) monitored the rebound of PCE from fractured shale beneath the Watervliet Arsenal near Albany, NY, and documented that the concentration of PCE rebounded to nearly pretreatment levels within six months. They also attributed the concentration rebound to back diffusion as opposed to the dissolution of pooled or residual chlorinated ethenes. Goldstein et al. (2004) came to this conclusion by comparing the concentrations of VOCs in groundwater from fractures to VOC concentrations in the rock matrix both before and after permanganate treatments.

The reasons that back diffusion can also be an important process (in addition to the expected dissolution) at a particular site is threefold. Firstly, aqueous solutions of permanganate can react with the aqueous and liquid phases of a chlorinated ethene. Therefore, pooled liquid PCE and residual liquid PCE can be treated along with aqueous PCE.

Secondly, permanganate injections will most likely flow past some DNAPLs that have diffused into the matrix before the permanganate can treat it. Contaminants that have diffused into permeable rock matrix will have much less contact time (if any) with the oxidant injection. In these cases, the oxidizer will be flushed through before a reaction can occur and the concentration gradient that diffused chlorinated ethenes into the rock matrix begins to work in reverse. Further evidence of this can be found in Mundle et al. (2007). In their experiment, TCE is flushed through a column for a time period long enough for TCE to diffuse from the fractures into the clay matrix. Afterwards, permanganate is flushed though. The TCE mass in the fractures is reduced, but once the permanganate is exhausted back diffusion from the matrix to the fractures is observed.

Further evidence of the significance of back diffusion can be found in Marble et al. (2010). They observed varying rates of precipitate formation near lower permeability zones and attribute these phenomena to reactions with DNAPLs that are diffusing out in the lower permeability zone.

Thus, evidence of the back diffusion as a second driving force of concentration rebound has been collected from both laboratory studies and field studies. However, there is also third and final reason for concentration rebound. DNAPLs diffused into the

rock matrix are also less likely to be oxidized because organic matter in rock matrix consumes most of the permanganate before it oxidizes the diffused contaminants. Honning et al. (2007) offers evidence of this speculation with laboratory studies that were compared to a site in Denmark. In addition, Marvin et al. (2004) claim that soil oxidant demand (SOD) can be 1000 times greater than the mass required to treat the contaminant.

Once the field evidence and laboratory evidence of back diffusion's influence is considered, it can be reasonably assumed that back diffusion must be considered to be a co-dominant process driving concentration rebound for this conceptual model. Thus, the model described in upcoming sections will assume that back diffusion is one of two dominant processes driving concentration rebound.

As a final note on the matter of fate and transport of PCE and TCE, a comment on the role of biodegradation is needed. Many models include a term to account for biodegradation of PCE and TCE. It is widely accepted that reductive dechlorination and aerobic cometabolism occurs in the field and has an important role in mass reduction. However, for this work it will be assumed that a large injection of a strong oxidizer will largely kill the bacteria that metabolize any DNAPL, despite the two studies (Hrapovic et al. (2005) and Sahl et al. (2007)) that have observed a slight rebound in the populations of bacteria that can metabolize chlorinated ethenes after permanganate injections. Therefore, the large body of literature regarding biodegradation will be omitted in this literature review.

2.4 Summary

This literature review analyzed three roles that mass transfer plays for an ISCO with permanganate intended to treat PCE and TCE. First, it established the role that mass transfer plays in the development and complexity of a PCE or TCE source zone. Next, it examined how the rate-limiting step of dissolution is altered by an oxidant's impact on hydrogeological parameters as well as retarded kinetics. Finally, it argues that dissolution along with back diffusion will cause a concentration rebound of PCE and TCE as the slug of permanganate wanes. The objective of this study is to test whether or not the rate of concentration rebound is correlated with the diffusion coefficient in pure water. The following section presents the model that was used to estimate the rates of concentration rebound from ISCO projects that used permanganate to treat PCE or TCE.

Chapter 3: Model Development

The following chapter is also organized into several subsections. The first presents the terms of the advection-dispersion-reaction equation that will be presented in subsection two. The third presents the numerical solution. After the numerical solution is presented, the mass conservation confirmation approach and uncertainty analysis are presented. Subsection six describes how each parameter is estimated for the numerical simulation. The last three subsections present the sensitivity analysis, the mass reduction estimation approach, and the precipitate accumulation estimation approach.

3.1 Fundamental Concepts and Definitions

In order to construct a model that can incorporate all of the aspects examined in the previous literature review, each of those aspects must be defined. The variables that will be used in the following subsection include advection, dispersion, retardation, dissolution, oxidation kinetics, and natural oxidant demand (NOD).

Advection is the transport of mass by fluid from one location to another location. Fetter (1993) defines advection with Equation 3.1.1.

Average Linear Velocity

$$u_x = \frac{k}{n_e}\frac{dh}{dl} \qquad \text{(Equation 3.1.1)}$$

where:

u_x: Average linear velocity [L/T]
k: Hydraulic conductivity [L/T]
n_e: Effective porosity
dh: Change in head [L]
dl: Change in length [L]

The next parameter is a function of average linear velocity and dispersivity. Although there are several types of dispersion, dispersion in groundwater is primarily caused by mechanical dispersion. Fetter (1993) summarizes three causes for the mechanical dispersion in groundwater.

1. As fluid moves through the pores, it will move faster through the center of the pores than along the edges.
2. Some of the fluid particles will travel along longer flow paths in the porous media than other particles to go to the same linear distance.
3. Some pores are larger than others, which allows the fluid flowing through these pores to move faster.

Fetter (1993) states that dispersion is commonly expressed as a function of average linear velocity and dispersivity (Fetter, 1993).

Dispersion

$$D_x = \alpha_x u_x + D_* \qquad \text{(Equation 3.1.2)}$$

$$D_y = \alpha_y u_x + D_* \qquad \text{(Equation 3.1.3)}$$

where:

D_x: Longitudinal Dispersion Coefficient [L^2/T]
D_y: Transverse Dispersion Coefficient [L^2/T]
α_x: Longitudinal Dispersivity [L]
α_y: Transverse Dispersivity [L]
D_*: Diffusion [L^2/T]
u_x: Average linear velocity [L/T] (see Equation 3.1.1)

Both advection and dispersion are affected by the adsorption of organic solvents to the surfaces of the media that they move through. Adsorption is incorporated into groundwater models with retardation. Although there are several models of adsorption (e.g., Freundlich, BET, Langmuir), the linear retardation model found in Fetter (1993) will be employed for this project.

Retardation Factor

$$R = 1 + K_{OC} f_{OC} \frac{\rho}{n} \qquad \text{(Equation 3.1.4)}$$

where:

R: Retardation factor
K_{OC}: Octanol/water partition [V/M]
f_{OC}: Fraction organic carbon
ρ: Density of aquifer media [M/V]
n: Porosity

As chlorinated solvents move through the ground they also undergo transformations. The first transformation is phase change from a liquid phase to an aqueous phase. Several models of phase change can be employed, but this model will utilize the stagnant single film model as described in Weber (2001).

Dissolution

$$N = k_{cr}(C_s - C) \qquad \text{(Equation 3.1.5)}$$

where

N: Mass flux due to dissolution [M/ (VT)]
k_{cr}: Reaction rate [1/T]
C_s: Concentration at water/solvent interface (assumed to be the solubility) [M/V]
C: Aqueous concentration [M/V]

and:

$$k_{cr} = \frac{D}{\delta} SSA$$

k_{cr}: Reaction rate [1/T]
δ: Thickness of interfacial film [L]
D: Diffusion Coefficient [L^2/T]
SSA: Specific Surface Area [L^2/L^3]

The second transformation is oxidation. Two sets of redox reactions must be estimated in order to model the concentration rebound of chlorinated ethenes. Huang et al. (2001) has already published the second order reaction rates between permanganates and chlorinated ethenes, so their reaction rates were employed.

Since the reaction rate between a chlorinated solvent and permanganate is dependent upon the concentration of permanganate, the natural oxidant demand (NOD) must also be estimated. NOD must be estimated because as the permanganate is consumed by naturally occurring organics the rate that it reacts with a chlorinated ethene decreases. NOD rate estimation will use the two-dimensional advection-dispersion-reaction equation found in Holzbecher (2007).

Fate and Transport of Permanganate Injection

$$C_{MnO_4^-}(x,y,t) = \frac{M}{4\pi t\sqrt{D_x D_y}} \exp\left(\frac{-1}{4t}\left(\frac{(x-u_x t)^2}{D_x} + \frac{y^2}{D_y}\right) - k_{NOD}t\right) \qquad \text{(Equation 3.1.6)}$$

where:

$C_{MnO_4^-}(x,y,t)$: Permanganate concentration with respect to time and x, y coordinates
t: Time [T]
D_x: x-Direction dispersion [L^2/T]
D_y y-Direction dispersion [L^2/T]
x: Length [L]
y: Width [L]
u_x: Average linear velocity [L/T]
k_{NOD}: Rate of consumption by natural organic matter [1/T]
M: mass of permanganate [M]

Equation 3.1.6 was used to estimate the amount of permanganate available for chlorinated ethene treatment as it is consumed by NOD at each unit length. This approach assumes that NOD will consume so much more permanganate than the chlorinated ethene that it is intended to treat that we can assume the consumption by any chlorinated ethene to be negligible.

The following subsection expresses all of the variables presented in this subsection with one equation in order to show the relationship between all of the variables.

3.2 Advection, Dispersion, Reaction Equation

By applying a mass balance approach, the following general equation is generated. It represents all of the previously discussed parameters to simulate the concentration rebound of PCE or TCE. A conceptual schematic has been included in Figure 3.2.1.

General Solution

$$R\frac{\partial C}{\partial t} = D_x\frac{\partial^2 C}{\partial x^2} + D_y\frac{\partial^2 C}{\partial y^2} - u_x\frac{\partial C}{\partial x} + k_{CR}(C_s - C) - (k_{ox}C_{perm})C \qquad \text{(Equation 3.2.1)}$$

where:

t: Time [T]
R: Retardation factor
C: DNAPL aqueous concentration [M/V]
D_x: x-Direction dispersion [L^2/T]
D_y: y-Direction dispersion [L^2/T]
x: Length [L]
y: Width [L]
u_x: Average linear velocity [L/T]
k_{ox}: Rate of oxidation by oxidant [1/T]
k_{CR}: Rate of concentration rebound [1/T]
C_{perm}: Permanganate concentration [M/V]
C_s: Concentration at water/solvent interface (assumed to be the solubility) [M/V]

This equation includes retardation, two-dimensional dispersion, oxidation, and advection. It also incorporates a stagnant single film model to represent concentration rebound rates.

3.3 Numerical Solution

Due to the complexity of this differential equation, a numerical solution was used. An Alternating Direction Implicit (ADI) (Remson et al., 1971) approach with an upstream weighting is employed. The general equation from the previous section can be expressed numerically with the following equation.

Numerical Solution

$$R\left(\frac{C_{xy}^{t+1}-C_{xy}^{t}}{\Delta t}\right)=D_x\left(\frac{C_{x+1y}^{t+1}-C_{xy}^{t+1}+C_{x-1y}^{t+1}}{\Delta x^2}\right)+D_y\left(\frac{C_{xy+1}^{t+1}-C_{xy}^{t+1}+C_{xy-1}^{t+1}}{\Delta y^2}\right)-u_x\left(\frac{C_{xy}^{t+1}-C_{x-1y}^{t+1}}{\Delta x}\right)-$$

$$(k_{ox}C_{perm})C_{xy}^{t+1}+k_{CR}(C_s-C_{xy}^{t+1}) \qquad \text{(Equation 3.3.1)}$$

Initial Conditions & Boundary Conditions

$C(x,y,0)=C_{initial}$

$C(x,+\infty,t)=0$ $\qquad$ $C(x,-\infty,t)=0$

$C(\infty,y,t)=0$ $\qquad$ $C(0,y,t)=0$

In order to estimate the initial concentrations, Equation 3.3.2 was used. Further description of Equation 3.3.2 can be found in Wexler (1992).

Initial Concentration Estimation

$$C(x,y)=\frac{C_{in}Q(\exp\left[\frac{u_x x}{2D_x}\right])}{2n_e\pi\sqrt{D_xD_y}}\exp\left(\frac{u_x x}{2D_x}\right)K_0\{\sqrt{\left(\frac{u_x^2}{4D_x}+\lambda\right)\left[\frac{x^2}{D_x}+\frac{y^2}{D_y}\right]}\} \qquad \text{(Equation 3.3.2)}$$

where:

C_{in}: Input concentration [M/V]
Q: Volumetric flow [V/T]
D_x: x-Direction dispersion [L^2/T]
D_y: y-Direction dispersion [L^2/T]
x: Length [L]
y: Width [L]
u_x: Average linear velocity [L/T]
K_0: Bessel Function
λ: reaction rate [1/T]
n_e: Effective porosity

Equation 3.3.2 is used because it has been assumed that the initial spatial distribution of TCE or PCE has already achieved a steady state condition.

Since a pentadiagonal solution is too complicated and computationally inefficient, the ADI was utilized. Each half of the time step is presented below.

$$AC_{x+1y}^{t+1} + CC_{xy}^{t+1} + DC_{x-1y}^{t+1} = BC_{xy+1}^{t+1} + C_{xy}^{t} + k_{CR}\Delta t C_S + EC_{xy-1}^{t+1} \quad \text{(Equation 3.3.3)}$$

$$BC_{xy+1}^{t+1} + CC_{xy}^{t+1} + EC_{xy-1}^{t+1} = AC_{x+1y}^{t+1} + C_{xy}^{t} + k_{CR}\Delta t C_S + DC_{x-1y}^{t+1} \quad \text{(Equation 3.3.4)}$$

where:

$$A = \frac{-D_x/_R\,\Delta t}{\Delta x^2} \qquad B = \frac{-D_y \Delta t}{R\,\Delta y^2}$$

$$C = 1 + \frac{2D_x/_R\,\Delta t}{\Delta x^2} + \frac{2D_y/_R\,\Delta t}{\Delta y^2} + \frac{u_x/_R\,\Delta t}{\Delta x} + \frac{k_{ox}\Delta t}{R} + \frac{k_{CR}\Delta t}{R} + MF^4$$

$$D = \frac{-D_x/_R\,\Delta t}{\Delta x^2} - \frac{-u_x/_R\,\Delta t}{\Delta x}$$

$$E = \frac{-D_y/_R\,\Delta t}{\Delta y^2}$$

Linear algebra was used to solve each half step tridiagonal matrix for each respective column and row. There does not appear to be any software program intended for groundwater modeling that is sophisticated enough to handle these computations, so MATLAB was used to compute the numerical solution.

3. 4 Method to Assess Mass Conservation

In order to confirm that mass conservation is maintained by this numerical solution, an analytical solution with similar variables was identified. Unfortunately, the

[4] MF is the mass fixer that was added to correct the mass lost during the computations. The mass fixer will be defined later in the mass conservation subsection.

analytical solution (Equation 3.4.1) that is best suited for this purpose is not intended for a continuous source and also requires the use of numerical integration.

$$C(x,y,t) = \frac{C_{in}Q}{4n_e\pi\sqrt{D_xD_y}} \exp\left(\frac{u_x x}{2D_x}\right) \int_0^t \exp\left[-\left(\frac{u_x^2}{4D_x} + k_h\right)t - \frac{x^2}{4D_x t} - \frac{y^2}{4D_y t}\right] dt \qquad \text{(Equation 3.4.1)}$$

t: Time [T]
C_{in}: Input concentration [M/V]
Q: Volumetric flow [V/T]
D_x: x-Direction dispersion [L^2/T]
D_y: y-Direction dispersion [L^2/T]
x: Length [L]
y: Width [L]
u_x: Average linear velocity [L/T]
k_h: Reaction rate
n_e: Effective porosity

Since Equation 3.4.1 requires a numerical integration and is only intended for an instantaneous source, it can't be used to examine whether or not mass is conserved for this numerical solution. Therefore, an alternative method was developed. If it is assumed that D_y is zero and that k_{OX} is also zero, this numerical solution can be compared to the Equation 3.4.2 (Miller, 1990) at a time after the numerical solution has achieved steady state.

$$C(x) = C_S - C_s \exp\left[\left(\frac{x}{2D_x}\right)\left((u_x) - (u_x^2 + 4D_x k_{CR})^{1/2}\right)\right] \qquad \text{(Equation 3.4.2)}$$

where:

C(x): Aqueous concentration at x [M/V]
D_x: Dispersion in the x-direction [L^2/T]
x: Length [L]
u_x: Average linear velocity [L/T]
k_{CR}: Rate of concentration rebound [1/T]
C_s: Concentration at water/solvent interface (assumed to be the solubility) [M/V]

Equation 3.4.2 is plotted in Figure 3.4.1. Figure 3.4.1 is followed by Figure 3.4.2 that presents how this numerical solution plots concentrations with respect to the x-direction when $D_y = 0$ and $k_{OX} = 0$. If Figure 3.4.1 is compared to Figure 3.4.2, it can be

seen that Equation 3.4.2 can compared to this numerical solution regardless of the location on the y-axis.

In Figure 3.4.4, three solutions are plotted. The first solution is the curve generated by Equation 3.4.2. The second curve is the curve generated by this numerical solution. There is a difference between the two curves that indicates that this numerical solution does not conserve mass, so a mass fixer was necessary. To conserve mass, two modifications were made to the numerical solution. The first modification altered Equation 3.1.2 to Equation 3.4.3.

$$D_x = (\alpha_x u_x + D_*) - ((21.7\ \text{ft.})u_x) \qquad \text{(Equation 3.4.3)}$$

where:

D_x: Dispersion in the x-direction [L^2/T]
α_x: x-Dispersivity [L]
u_x: Average linear velocity [L/T]

This modification is to ensure that numerical dispersion is not a problem for this simulation. Twenty-one and seven tenths feet was determined as the numerical dispersion corrector with the ratios published by Ataie-Ashtiani and Hosseini (2005).

The second modification added a mass fixing correction factor (MF) to the C coefficients in used in Equation 3.3.3 and Equation 3.3.4.

$$MF = \left[0.0006 - 0.7889\left(\frac{\text{day}}{\text{ft.}}\right)(u_x)\right](\log(x)) \qquad \text{(Equation 3.4.4)}$$

where:

MF: Mass Fixer
u_x: Average linear velocity [L/T]
$x = \frac{\text{change in length}}{\text{unit change in length}}$

There does not appear to be any published procedure that can be applied to this numerical solution, so an original approach was necessary. The mass fixer should be a constant factor that corrects the mass lost at each spatial change. The C coefficient used in Equations 3.3.3 and Equation 3.3.4 is the only coefficient that affects all locations in both half steps of the ADI and includes all variables, so it was an ideal variable to place a mass fixing correction factor. Figure 3.4.4 also shows that the mass fixer must also decrease as Δx increases. Therefore, a logarithmic relationship (as opposed to a linear relationship) with respect to Δx was the ideal choice based on the shape of the curves.

The mass fixer was estimated by identifying a value that when added to the uncorrected C coefficient would result in a numerical simulation that fit the analytical solution more accurately. The value added to the uncorrected C coefficient will be defined as C_{error}.

$$MF = C_{error} = C_{corrected} - C_{uncorrected} \qquad \text{(Equation 3.4.5)}$$

where:

C_{error}: value added to C coefficient
$C_{corrected}$: value of corrected C coefficient
$C_{uncorrected}$: Value of uncorrected C coefficient
MF: Mass Fixer

The logic is simple. When the C_{error} is added to the $C_{uncorrected}$ the numerical solution will result in a curve that estimates the analytical solution more accurately. However, this relationship is assumed to be logarithmic with respect to the change in x.

$$MF = C_{error} = (\theta)\log(x) \qquad \text{(Equation 3.4.6)}$$

where:

θ: coefficient that alters C_{error} proportionally as hydrogeological parameters vary.
MF: Mass Fixer

$$x = \frac{\text{change in length}}{\text{unit change in length}}$$

C_{error} : Value added to C coefficient

Theta was determined by choosing a set of parameters (average linear velocity, dispersivity, and the rate of concentration rebound) and creating a curve for the analytical solution and curve for the uncorrected numerical solution. C_{error} was varied until an optimal R^2 was determined that resulted in a corrected numerical solution. Afterwards, the average linear velocity was altered and another optimal R^2 was determined by varying C_{error}. This process was completed five times to find a linear relationship between C_{error} and the average linear velocity. This regression analysis (R^2=0.94) is presented in Figure 3.4.3. Afterwards, the slope was substituted for theta thereby arriving at Equation 3.4.4.

$$\mathrm{MF} = \left[0.0006 - 0.7889\left(\frac{\text{day}}{\text{ft.}}\right)(u_x)\right](\log(x))$$

The third curve in Figure 3.4.4 illustrates that the numerical solution after the two modifications were made conserves mass.

3.5 Uncertainty Analysis

This original approach to simulating concentration rebound requires an analysis to estimate the uncertainty of the simulated concentration rebound. In order to accomplish this, a Monte Carlo analysis was completed for each of the nine cells simulated. Each Monte Carlo analysis is cell specific and location specific. That is, the Monte Carlo analysis was completed for each cell at the location of the concentration rebound

calibration (e.g., the Busch cell's Monte Carlo analysis was completed at x= 13 ft. and y = 1 ft.) in order to estimate the error of each particular calibration. Each Monte Carlo analysis generated the particular DNAPL (i.e., TCE or PCE) concentration over the time span of that particular simulation (e.g., the PGDP Monte Carlo Analysis had 100 days of PCE concentration generated) 1000 times (i.e., day 1 has 1000 concentrations, day 2 has 1000 concentrations, etc...). Afterwards, the mean and standard deviation for each day in each cell was computed.

The last aspect to summarize for the nine Monte Carlo analyses completed is how each of the parameters is randomized. MATLAB has a command to generate random numbers over a desired range. For example, this code can randomize longitudinal dispersivity from 1 m to 100 m or hydraulic conductivity from 1×10^{-1} m/s to 1×10^{-11} m/s. The code written that executes the linear algebra necessary to solve this model's numerical solution has an input file that defines the parameters for each simulation. That input file replaced a set parameter with the code for a value from a random range. For example, the retardation factor may have be previously defined with a value (e.g., 13 or 8.2), but was now defined with a value generated randomly from a range (e.g., 8.2 to 13). The following parameters were all defined to be chosen randomly from a range: hydraulic conductivity, porosity, longitudinal dispersivity, dispersivity ratio, fraction organic carbon, solubility, oxidation rate, and concentration rebound rate. The specific range of values used for each Monte Carlo analysis along with their respective source is presented in Table 3.5.1.

3.6 Calibration Algorithm & Parameter Estimation

The data used to simulate each site came from a variety of sources that include published articles, engineering reports, and federal documents. All of these sources were reviewed to see if enough information was available for a simulation. Eleven sites had been collected for this project and five were rejected for insufficient or problematic data. For example, one site that initially appeared to be ideal for this project was rejected because insufficient groundwater samples for VOCs were available. In another case, the NOD calibration was impossible unless unjustifiable assumptions were made. After each site was selected based on whether or not it was feasible to simulate, the site was divided into cells. Each cell division was based on similarities to other cells. In one case, a cell was based on a groundwater divide, but most of the cell divisions were based on vertical changes in the soil profile and proximity to injection wells. Once each site was divided, a total of 9 cells could be simulated

The next step was to choose a well that was not an injection well that could be used for calibration. Calibration wells were chosen based upon two criteria. The first criterion for well selection required that a well had to have an observed permanganate presence. There were many locations that had temporarily decreased DNAPL concentrations, but this could be natural variation or due to decreased upstream concentrations. The second criterion required that no other phenomena other than these in the model occurred in the well. This may be perceived as selecting locations that fit the purposes of the study. However, other phenomena do occur that can be attributed to known factors that this model is not designed to simulate. For example, the following case would be grounds to reject a well for calibration. In some cases, the DNAPL

concentrations increased in wells located slightly downstream from injection wells immediately after injections. This is caused by a displacement of DNAPL by injecting a large volume of a fluid into the source zone and the model was not designed to include this phenomena.

After sites and monitoring wells were selected, each parameter was estimated with the following approaches.

Advection

Equation 3.1.1 was used to estimate the average linear velocity for each site. In order to apply Equation 3.1.1, three variables were estimated. The hydraulic gradient, porosity, and hydraulic conductivity were all determined by information published reports. In some cases, the value was published (e.g., hydraulic conductivity or porosity) and in other cases the information had to be determined with information from a report (e.g., hydraulic gradient). All values were compared to generally accepted values. If a parameter was not available, the mean of a generally accepted range was used.

Dispersion

Equation 3.1.2 and Equation 3.1.3 were used to estimate the dispersion in both directions (i.e., x-direction and y-direction). Each dispersivity coefficient was estimated with the relationship to system length that was described in Schnoor (1996).

Longitudinal/Transverse Dispersivity Ratio

The ratio between dispersivities was estimated with generally accepted values respective to the media of each system.

Solubility

The solubility of PCE and TCE as estimated by Knauss et al. (2000) was used for all of the cells simulated.

Retardation Factor

Equation 3.1.4 was used to estimate the retardation factor. In order to apply Equation 3.1.4, the fraction of organic carbon, octanol/water partition coefficient, density, and porosity were estimated. The octanol/water partition coefficient published in Schnoor (1996) was used in all cases. All other values were found in reports and compared to generally accepted values.

Initial Concentration

Equation 3.3.2 was used to estimate the initial concentrations of each cell simulated. Graphs that present the estimated PCE or TCE spatial distribution for each cell before the permanganate was injected is included at the end of the next chapter.

Rate of Concentration Rebound

The numerical solution presented in section three was used to estimate the rate of concentration rebound. The rate of concentration rebound was identified by varying the k_{cr} until an optimal R^2 was found.

Rate of Oxidation

The oxidation rates published by Huang et al. (2001) were used in this study because it was the only study that published second order reaction kinetics.

Natural Oxidant Demand Rate

Equation 3.1.6 was used to estimate the rate of natural oxidant demand for each site simulated. The end of Chapter 4 presents graphs showing the change in permanganate concentration with respect to time along with an R^2 score to assess how well Equation 3.1.6 predicts the rate of natural oxidant demand for each site.

Unfortunately, a comparison to published NOD rates is difficult. Most values published have units that involve mass (e.g. [(mass of permanganate)/ (mass of soil·unit of time)]), which makes a rate with only units of time (e.g., 1/s) incommensurate.

3.7 Sensitivity Analysis Approach

A sensitivity analysis was run on all variables to examine how each variable influenced the outcome of the simulation. The analysis was a simple approach that kept all variables fixed and varied one over a range that is slightly larger than the generally accepted range for that variable. The variables included average linear velocity, dispersivity, dispersivity ratio, retardation, solubility, rate of concentration rebound, rate of oxidation, and the NOD rate. In addition, one sensitivity analysis was completed with a parameter, hydraulic conductivity, altered after 250 days. This was intended to examine the effect of precipitates changing average linear velocity after the permanganate injection.

3.8 Mass Reduction Analysis

In order to estimate the amount of mass reduced by the permanganate injections, the initial total mass in two phases was compared to the total mass in two phases 100 days after the permanganate injections. One hundred days was not an arbitrary choice.

For comparison, a common time length was necessary and 100 days was chosen because it is the shortest time length of all the simulations completed. So, 100 days is the longest time interval that all simulations have in common. Liquid phase was not estimated, but the total masses of the aqueous phase and the solid phase were estimated.

Aqueous Phase Estimation

$$\sum M_{aq} = \sum Vn\, c_{xy} \qquad \text{(Equation 3.8.1)}$$

and

$$V = \Delta X \cdot \Delta Y \cdot \text{Depth of zone}$$

where:

M_{aq}: Mass in the aqueous phase [M]
V: segment volume [V]
n: porosity
C_{xy}: Aqueous concentration [M/V]

Solid Phase estimation

$$\sum M_s = \sum V(1-n)\,[(K_{oc} foc)\rho]c_{xy} \qquad \text{(Equation 3.8.2)}$$

and:

$$V = \Delta X \cdot \Delta Y \cdot \text{Depth of zone}$$

where:

M_s: Mass in the solid phase [M]
V: segment volume [V]
n: porosity
C_{xy}: Aqueous concentration [M/V]
foc: Fraction of organic carbon
K_{oc}: Octanol-water partition coefficient [V/M]
ρ: soil density [M/V]

3.9 Precipitate Accumulation Analysis

As discussed in the literature review, the accumulation of precipitates can cause substantial problems for an ISCO project. In order to assess whether or not manganese oxides will pose a problem for this study, an assessment was completed. The assessment took a simple approach by asking if the porosity was altered by the accumulation of precipitates.

First the total mass of manganese dioxide was estimated stoichiometrically with Equation 3.9.1. (Mumford et al., 2005)

$$3CH_2O + 4MnO_4^- \rightarrow 3CO_2 + 4MnO_{2(s)} + H_2O + 4OH^- \quad \text{(Equation 3.9.1)}$$

For example, if 100 mol was injected than 100 mol of manganese dioxide form since there is a 1:1 ratio. Afterwards, the volume of the total mass of manganese dioxide was calculated using the molar mass and density of manganese dioxide. The volume of the pore space in the cell simulated was estimated with the porosity (i.e., a 100 liter volume cell with a 20% porosity will have 20 liters of pore space). Finally, the volume of the precipitates was subtracted from the volume of the pore space to assess whether or not the change was greater than negligible.

3.10 Limitations and Assumptions

This model makes the common assumption that variables remain constant over time. This assumption also implies that the concentration rebound can be represented with a single term for the entire volume. This does not allow for concentration rebound by back diffusion to be distinguishable from concentration rebound by dissolution.

Differing driving forces will be distributed spatially (and perhaps temporally as well) and a single term may make calibration difficult because a single term ignores the influence of varying site architecture on concentration rebound. This assumption must be acknowledged, but all estimated variables in contaminant fate and transport modeling share these problems. These assumptions will be addressed by dividing sites into cells of an appropriate size.

Figure 3.2.1: Conceptual Schematic

Figure 3.2.1 shows the instantaneous source permanganate injection moving through the continuous source DNAPL plume. The y-axis shows the width and the x-axis shows the length.

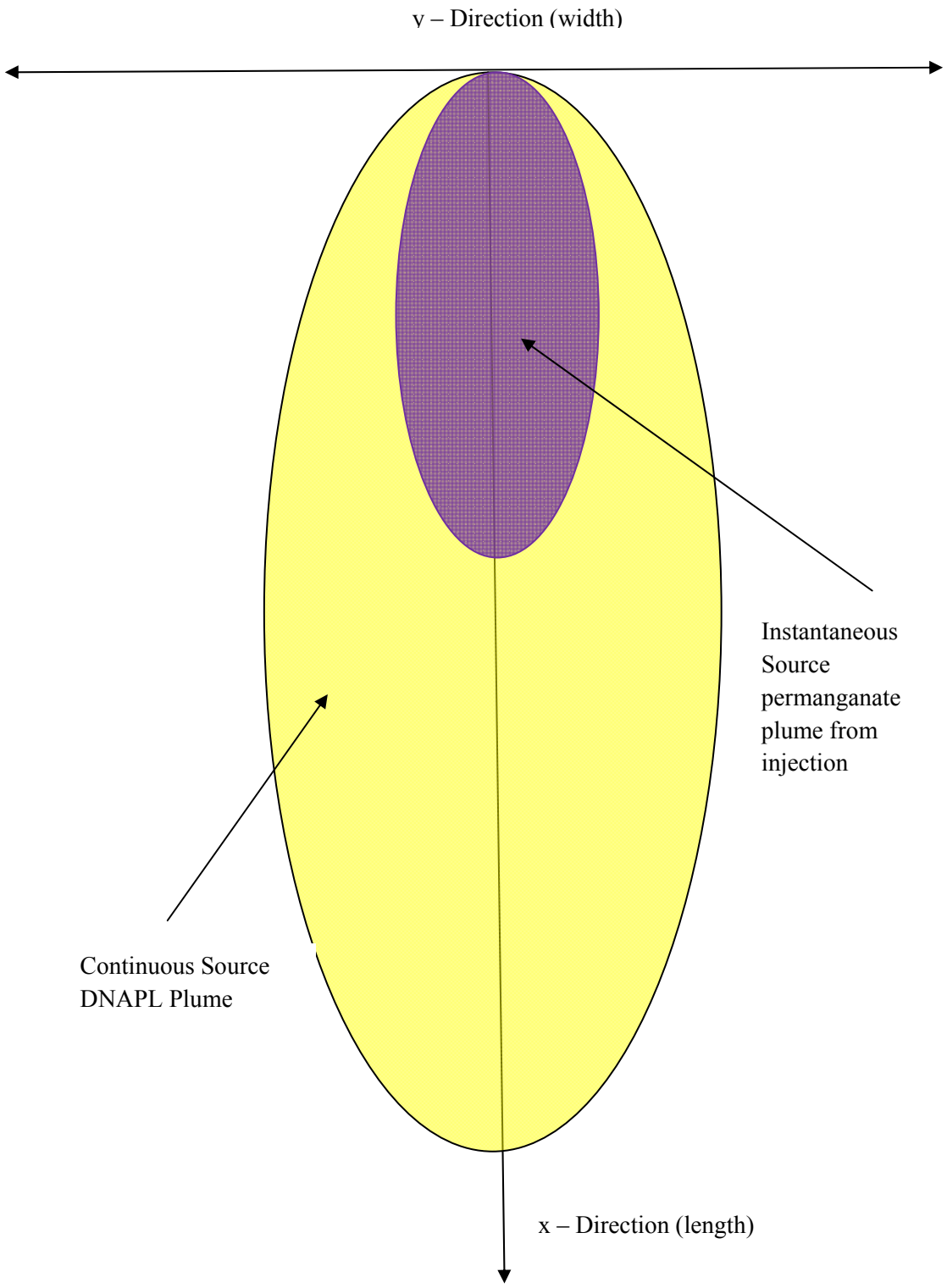

Figure 3.4.1: Curve Generated by 1-Dimensional Analytical Solution

The DNAPL concentration with respect to length is described by Equation 3.4.2. Figure 3.4.1 shows that concentration will approach solubility as it moves in the x-direction

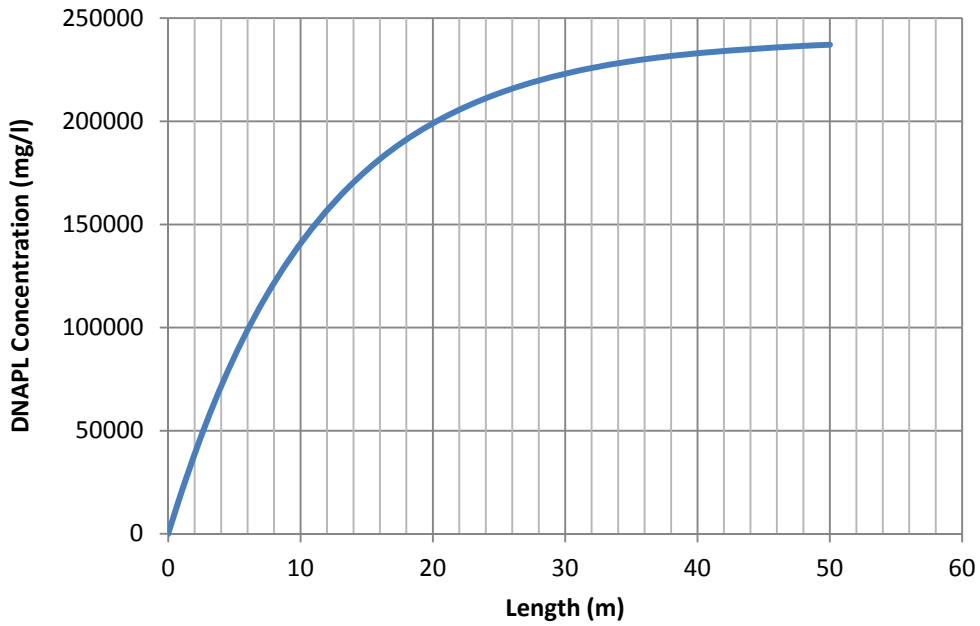

Figure 3.4.2: Two-Dimensional Plot for Comparison to Analytical Plot

Figure 3.4.2 shows the numerical solution plotted when D_y=0 and k_{OX}=0. It shows that Equation 3.4.2 can be applied to any line along the x-direction regardless of the value of y because concentration only changes in the x-direction.

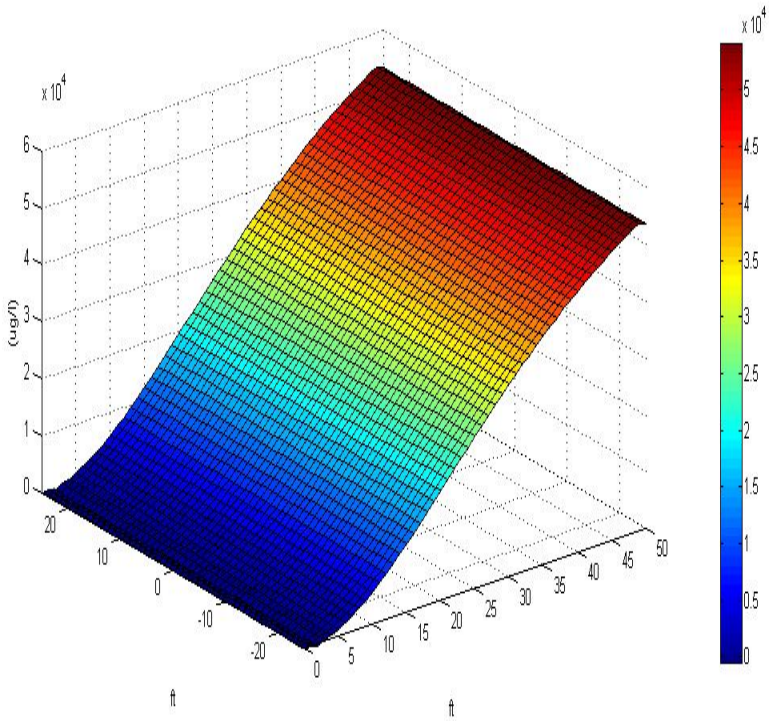

Figure 3.4.3: Regression Analysis for Mass Fixer

Figure 3.4.3 presents the results of the regression analysis used to identify the slope of the mass fixer. (R^2= 0.9443).

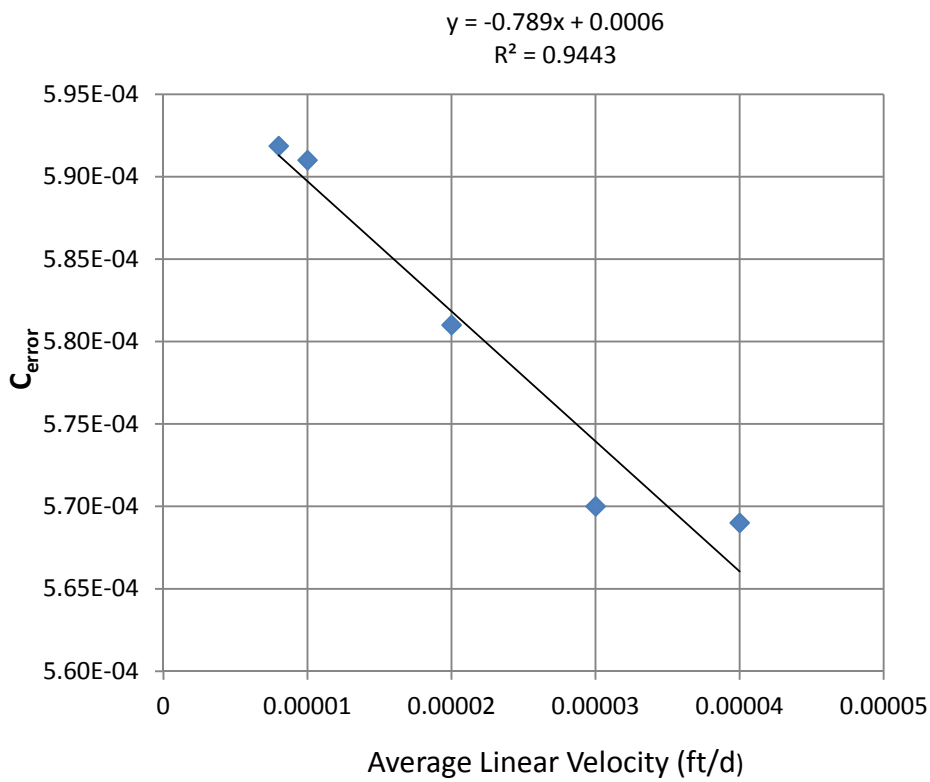

Figure 3.4.4: Comparison of Three Solutions

Figure 3.4.4 compares three solutions. The first curve is generated by Equation 3.4.2 (the analytical solution) and the second curve is generated by the uncorrected numerical solution. It shows that they have a similar curve, but mass is lost by the numerical solution. The third curve presents the numerical solution after a mass fixer has be added to the solution. Curve 3 is a much better approximation of the analytical solution (R^2= 0.9493).

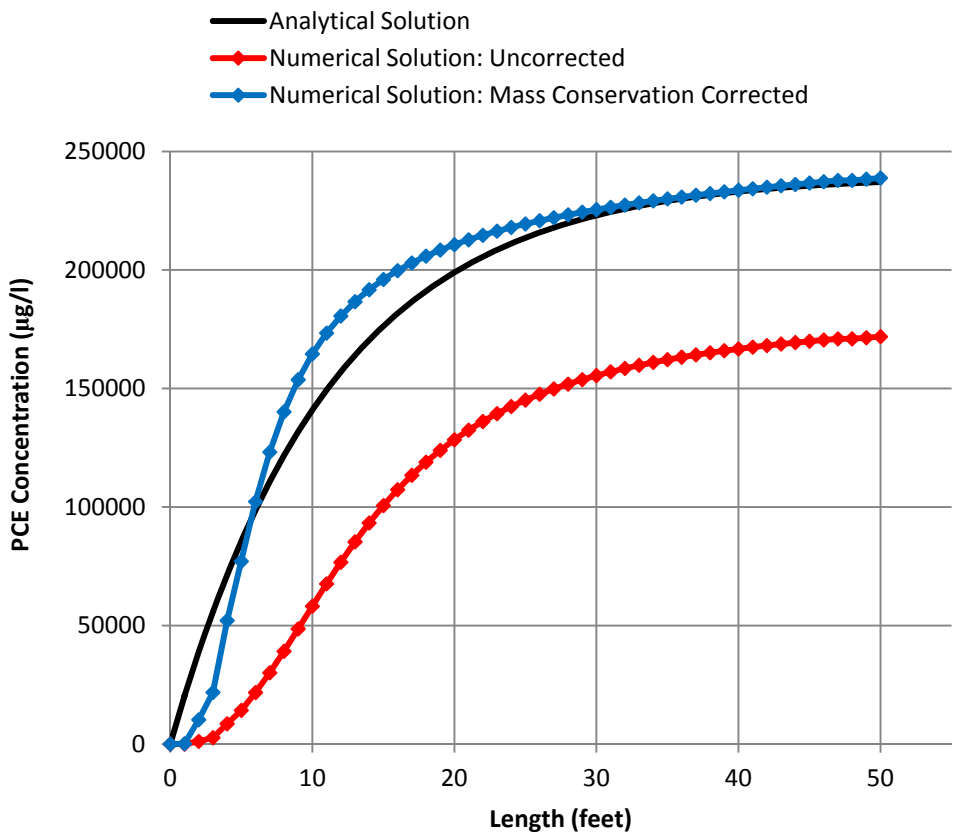

Table 3.5.1: Monte Carlo Analysis Ranges

Table 3.5.1 presents the ranges of each parameter that was randomized in the Monte Carlo analysis.

Cell	Hydraulic Conductivtiy Coefficient of Variance	Porosity Coefficient of Variance	x-dispersivity	Dispersivity Ratio	Fraction Organic Carbon Coeffcient of Variance	Solubility	Oxidation Rate	Concentration Rebound Rate Coefficient of Variance
Source	Warrick & Nielson (1980)	Warrick & Nielson (1980)	Vanderborght & Vereecken (2007)	Delgado (2007)	Warrick & Nielson (1980)	Knauss et al. (2000)	Huang et al. (2001)	Calculated with estimated concentration rebound rates
Units	NA	NA	m	NA	NA	mg/l	1/(Ms)	NA
Busch	200%	20%	± 15	5:1 to 100:1	± 0.0001	240-252	0.031-0.039	167%
Cape Canaveral 2S	200%	20%	± 15	5:1 to 100:1	± 0.0001	1280-1476	1.47 - 1.57	20%
Cape Canaveral 5S	200%	20%	± 15	5:1 to 100:1	± 0.0001	1280-1476	1.47 - 1.57	20%
Chemplex	200%	20%	± 15	5:1 to 100:1	± 0.0001	240-252	0.031-0.039	167%
PGDP	200%	20%	± 15	5:1 to 100:1	± 0.0001	1280-1476	1.47 - 1.57	20%
Valmont EW1	200%	20%	± 15	5:1 to 100:1	± 0.0001	1280-1476	1.47 - 1.57	20%
Valmont EW5	200%	20%	± 15	5:1 to 100:1	± 0.0001	1280-1476	1.47 - 1.57	20%
Watervliet IW1	200%	20%	± 15	5:1 to 100:1	± 0.0001	240-252	0.031-0.039	167%
Watervliet IW4	200%	20%	±15	5:1 to 100:1	±0.0001	240-252	0.031-0.039	167%

Chapter 4: Results

This chapter has several subsections. The first presents a brief description of all the sites simulated in this study, their respective estimated concentration rebound rates, and the limitations of that particular simulation. Afterwards, the results of the uncertainty analysis and the sensitivity analysis are summarized. Subsection four compares the estimates of the total mass in the aqueous and solid phases before the permanganate injection to both total masses after the permanganate injections. The fifth presents the results of the precipitate accumulation examination. Lastly, a correlation between the rate of concentration rebound and the diffusion coefficients in pure water will be presented.

4.1 Site Descriptions & Concentration Rebound Rates

The end of this chapter presents the specific values for each site along with the source (e.g., reports, commonly accepted values, equations, assumptions, or other publications) of that particular value. This subsection presents a brief description of each site along with a review of each site simulation's specific limitations.

Busch Campus Garage Cell

The Busch Campus Garage is located on the Busch Campus of Rutgers University in Piscataway, NJ. This 50' by 50' cell with the origin at the injection well ISCO-1 was based on the pilot study performed by Langan Engineering (2011). The cell modeled is predominantly made up of weathered brunswick shale and the direction of the groundwater flow is roughly a southwestern direction from ISCO-1. ISCO-3 was the

well used to perform all calibrations. This simulation employed the injections that occurred on weekdays between 8/25/09 and 9/10/09. ISCO-1 had 9702 liters of a 10% sodium permanganate solution injected within that time period. All estimated parameters are presented in Table 4.1.1 and the initial concentrations along with well locations are presented in Figure 4.1.1. The rate of NOD and rate of concentration rebound calibrations are presented respectively in Figure 4.1.2 and Figure 4.1.3. The rate of concentration rebound was estimated to be 8.68×10^{-12} 1/s.

There are several limitations to this simulation. The first limitation is permanganate monitoring was only performed with visually check for shades of purple. Since permanganate was not quantitatively measured, the NOD calibration was completed by modeling manganese concentrations. The manganese concentration was the sum of the dissolved and solid manganese with an estimated background subtracted. It was also assumed that for every one mole of permanganate consumed, one mole of manganese was released. Estimating NOD with manganese concentrations offers an advantage of seeing reaction rates, but unknown background manganese concentrations add uncertainty to the estimation. Second, the simulation is based on limited data. Several rounds of groundwater samples were collected, but the concentration rebound is only observable in the most recent round. Another round or two of groundwater samples would make a more confident estimation of rebound rate.

Cape Caneveral Cells

Both Cape Canaveral cells are at Launch Pad 34 which is located in Cape Canaveral, FL. This site allowed two 50' by 50' cells to be simulated. Both cells are comprised of sand and the direction of the groundwater flow is approximately

northeastern. Both sites have three vertical layers and each layer had its own injection. However, estimating the permanganate migration is too complicated for the lower two levels due to the difficulty in knowing which injection migrated to which locations. The data for this calibration was found in a report that presented three pilot studies for three separate remediation technologies. The two other concurrent pilot projects do not appear to have an impact on the ISCO pilot. Both calibrations used the injections that occurred in the shallow zone from 08/08/99 to 08/27/99. A total of 13,330 kg of sodium permanganate were injected into this zone.

The parameters for both the Cape Canaveral 2S cell and Cape Canaveral 5S cell are presented in Table 4.1.2. The initial concentrations and well locations for the Cape Canaveral 2S cell are presented in Figure 4.1.4 and the initial concentrations and well locations for the Cape Canaveral 5S cell are presented in Figure 4.1.5. The NOD was assumed to be the same for both sites because they are nearly identical so the NOD rate calibration for both sites is presented in Figure 4.1.6. However, the rate of concentration rebounds were calibrated independently and can be found in Figure 4.1.7 for Cape Canaveral 2S and Figure 4.1.8 for Cape Canaveral 5S. Cape Canaveral 2S has a concentration rebound rate of 1.39×10^{-8} 1/s and Cape Canaveral 5S has a concentration rebound rate of 2.31×10^{-8} 1/s.

This simulation has two problems that add uncertainty to the simulation. First, the mass of potassium permanganate appears to fit the NOD estimation well. However, the influence of potassium permanganate injected into the lower zones on the shallow zone wells cannot be estimated. Second, the influence of the other pilot projects may have an influence beyond their expected zones.

Chemplex Cell

The Chemplex site is a Superfund site owned by Equistar Chemicals, LP, in Clinton, Iowa, and was previously used for polyethylene manufacturing. This site had several pilot studies completed on its many sources of contamination. A few included pilot studies for vegetable oil injections and others included permanganate injections. Only one monitoring well was available for the calibration of concentration rebound rate despite the large 300' by 300' cell simulated, so all calibrations used well MW-112A for its calibration. The geology of this large cell is a mixture of silt and clay and the direction of the groundwater flow is approximately south. This simulation is based upon the 1289 liters of 10% sodium permanganate that was injected into monitoring well 108B on July 15th, 2009. The estimated parameters are presented in Table 4.1.3 and the initial concentrations along with well locations are presented in Figure 4.1.9. The rate of NOD and rate of concentration rebound calibrations are presented respectively in Figure 4.1.10 and Figure 4.1.11. The rate of concentration rebound was estimated to be 4.05×10^{-10} 1/s.

One problem with this simulation is that estimating NOD rate with the reported total manganese concentrations that are not specifically defined adds uncertainty to the NOD calibration. Of course, using total manganese concentrations has all of the limitations discussed previously in the Busch Campus Garage subsection.

Portsmouth Gaseous Diffusion Plant Cell

The Portsmouth Gaseous Diffusion Plant is located in Piketon, OH, and like many of the sites used for this project it has several contaminated zones. This simulation examines only the X-701B TCE plume. The permanganate injection was introduced into

the treatment zone with a horizontal well injection and one vertical well injection. The treatment zone is sand and gravel and the direction of the groundwater flow moves from the east to the west. The source of the plume is believed to be a retention pond where large volumes of solvents where dumped before regulations prohibited this practice. This simulation employed the potassium permanganate injections that occurred between 8/20/97 and 8/21/97 when 1960 kg were injected into injection well 74G. The 50' by 50' cell that simulated MW-74G used MW-89G for the rebound calibration. However, MW-88G was used for the NOD calibration. The estimated parameters are presented in Table 4.1.4 and the initial concentrations along with well locations are presented in Figure 4.1.12. The rate of NOD and rate of concentration rebound calibrations are presented respectively in Figure 4.1.13 and Figure 4.1.14. The rate of concentration rebound was estimated to be 1.16×10^{-6} 1/s.

There are two limitations for this simulation. The ISCO project at the location used a horizontal well to inject the potassium permanganate. To avoid the complications of trying to estimate parameters for a re-circulated horizontal well, MW-74G was used for the simulations because it was the only vertical well with a permanganate injection. Oxidant injections from the horizontal well may have added more potassium permanganate to the cell than this simulation estimated. The second limitation is that this simulation was the only simulation that used two different wells for calibration. One well was used for the calibration of the NOD (MW-88G) and another well (MW-89G) was used for the calibration of the rebound. MW-89G was rejected as a location for the NOD calibration because the groundwater samples for the permanganate indicated permanganate may have arrived from the nearby horizontal well injections. One likely

explanation for the unexpected arrival of permanganate is unpredictable preferential flow. If this explanation is correct, the affect preferential flow has on the rest of the simulation cannot be determined.

Valmont Cells

The Valmont TCE cells are located in Hazleton, PA. The source is believed to be from a previous owner's upholstery manufacturing. This site allowed two large cells to be simulated. The first cell (EW-1) is 500' by 500' and the other cell (EW-5) is 200' by 200'. Both cells are comprised of sandstone and siltstone and the direction of the groundwater flow splits at a groundwater divide. On side of the split it flows north and the other side it flows to the southwest. Both simulations used the injections that occurred between mid-August 2009 and early September 2009. Injection well 1 (EW-1) had 9240 kg of sodium permanganate injected and injection well 5 (EW-5) had 4312 kg of sodium permanganate injected.

The parameters for both the Valmont EW-1 cell and the Valmont EW-5 cell are presented in Table 4.1.5. The initial concentrations and well locations for the Valmont EW-1 cell are presented in Figure 4.1.16 and the initial concentrations and well locations for the Valmont EW-5 cell are presented in Figure 4.1.17. The NOD rate was assumed to be the same for both sites because they are nearly identical so the NOD rate calibration for both sites is presented in Figure 4.1.18. However, the rate of concentration rebounds were calibrated independently and can be found in Figure 4.1.19 for Valmont EW-1 cell and Figure 4.1.20 for Valmont EW-5 cell. The Valmont EW-1 cell has a concentration rebound rate of 1.74×10^{-8} 1/s and the Valmont EW-5 cell has a concentration rebound rate of 1.56×10^{-8} 1/s.

The Valmont cells have a unique limitation. Figure 4.1.19 and Figure 4.1.20 show a temporary increase in the concentration immediately after the permanganate injection. The stability of the Monte Carlo analysis reveals that this is not artificial oscillation which can sometimes occur in advection dominant ADI approaches. The spike after the injection results from dissolution occurring until the permanganate reaches the location of the monitoring wells used for the calibrations. The monitoring wells used for the Valmont cells are much more distant from the injection wells than the monitoring wells used in other cells, so more time will pass before the permanganate reaches the monitoring wells. Slight concentration growth can be expected, but this spike is undoubtedly too high. However, this does not pose a problem for the other large cell (i.e., the Chemplex cell). This may suggest distant locations of this cell are modeled inaccurately during the early time steps of this simulation.

Watervliet

The Watervliet Arsenal is located in Watervliet, NY and has been listed as a national historic landmark. This site had a pilot study with one injection location and four injection locations for the full scale project. Only two injection locations (IW-1 and IW-4) will be simulated and each cell is 50' by 50'. Both cells modeled were in the intermediary zone of the site that ranges from 51 feet below the ground surface (fbg) to 100 fbg. Both cells are comprised of black, medium-hard laminated shale (Goldstein et al., 2004). The direction of the groundwater flow for both cells is approximately southeast towards the Hudson River. The source of the plume is believed to be a degreasing unit located in Building 40 and it is also believed to have started over 30 years ago. This simulation used the injections that occurred between 4/3/06 and 4/7/06.

Injection well 1 (IW-1) had 6557 liters of a 5% sodium permanganate solution injected and injection well 4 (IW-4) had 3676 liters of a 5% sodium permanganate solution injected. The 50' by 50' cell that simulated IW-1 injection used monitoring well 87 for its calibrations. The 50' by 50' cell that simulated IW-4 injection used monitoring well 86 for its calibrations.

The parameters for both the Watervliet IW-1 cell and the Watervliet IW-4 cell are presented in Table 4.1.6. The initial concentrations and well locations for the Watervliet IW-1 cell are presented in Figure 4.1.21 and the initial concentrations and well locations for the Watervliet IW-4 cell are presented in Figure 4.1.22. The NOD rate was assumed to be the same for both sites because they are nearly identical so the NOD rate calibration for both sites is presented in Figure 4.1.23. However, the rate of concentration rebounds were calibrated independently and can be found in Figure 4.1.24 for the Watervliet IW-1 cell and Figure 4.1.25 for the Watervliet IW-4 cell. The Watervliet IW-1 cell has a concentration rebound rate of 1.16×10^{-12} 1/s and the Watervliet IW-4 cell has a concentration rebound rate of 2.89×10^{-12} 1/s.

4.2 Uncertainty Analysis Results

Unfortunately, the range of concentrations generated by these simulations is wide enough that presenting the uncertainty with error bars is inconvenient. In short, the uncertainty will be almost impossible to interpret in with error bars. Therefore, Table 4.2.1 through Table 4.2.9 presents the mean and standard deviation for each day.

4.3 Results of Sensitivity Analysis

The following subsection presents the results for each of the parameters examined in the sensitivity analysis.

Average linear velocity (u_x)

Average linear velocity is influential as illustrated by Figure 4.3.1. This is expected and the general pattern in clear. As average linear velocity decreased, other variables (such as rebound) become much more influential. For example, an average linear velocity of 0.01 $^m/_s$ will overcome a rebound rate of 0.000001/s and keep rebound very low. However, an average linear velocity of 0.0000001 $^m/_s$ allows a rebound rate of 0.000001/s to be much more influential. The physical phenomenon represented by this mathematical output is that faster average linear velocities will transport rebounded DNAPLs away before they accumulate, whereas slower average linear velocities make transport less influential.

Dispersivity & Longitudinal/Transverse Dispersivity Ratio (α_x,α_y, & α_x/α_y)

Dispersivity was examined in two steps. First, α_x and α_y were changed. This demonstrates how dispersivity alters the outputs of the numerical simulation. The second step changed the ratio, α_x/α_y, to examine how unequal dispersivities influence the outputs. The results of this sensitivity analysis are presented in Figure 4.3.2 and Figure 4.3.3. As dispersivity increases, it lowers the concentration of the DNAPL because transport becomes more influential. However, Figure 4.3.2 and Figure 4.3.3 show that dispersivity is not as influential as average linear velocity.

Retardation Factor (R)

Figure 4.3.4 illustrates the influence that R has on the concentrations predicted by this numerical simulation. A comparison of the five curves in Figure 4.3.4 shows that R has substantial influence on the model outputs. The first curve is a curve where there is no retardation (R=1) and each curve after that illustrates the output as R is increased. The pattern shows that an increase in R decreases the slope of the curve (i.e., concentration rebound decreases).

Solubility (C_s)

In Figure 4.3.5 five curves are plotted to show how increasing solubility alters the output of this numerical solution. Figure 4.3.5 also shows that solubility also has a substantial influence. As solubility increases, more DNAPL will be found in the aqueous phase (i.e., concentration rebound increases) and Figure 4.3.5 demonstrates that this physical phenomenon is captured by this numerical solution.

Rate of Natural Oxidant Demand (k_{NOD})

As the rate of natural oxidant demand increases, more permanganate is consumed by naturally occurring organic materials. This implies that less permanganate is available to treat the target contaminant and this phenomenon is reflected in Figure 4.3.6. As the rate of natural oxidant demand increases, the concentration rebound increases. Figure 4.3.6 also shows that the k_{NOD} is very influential. One order of magnitude change in k_{NOD} results in several orders of magnitude change in the concentration rebound simulated. Since the scale of concentration changes makes the curves in the lower concentration range difficult to distinguish, the y-axis was presented with a logarithmic scale.

Rate of Oxidation (k_{OX})

Figure 4.3.7 reflects the expected phenomenon for this variable. As the oxidation rate between the permanganate and DNAPL increases, more contaminant mass is oxidized. Therefore, as the rate of oxidation increases the concentration rebound decreases because more contaminant mass has been destroyed. Figure 4.3.7 also shows that the oxidation rate is influential on the output.

Rate of Concentration Rebound (k_{CR})

The final variable that was examined during the sensitivity analysis was the rate of concentration rebound. Figure 4.3.8 shows that as the concentration rebound rate increases, the concentration curve also increases. Concentration rebound has a substantial impact on the outputs of this numerical solution.

Reduced Hydraulic Conductivity (k)

In order to investigate how precipitate accumulation may alter the concentration rebound, one simulation was completed that reduced the hydraulic conductivity. Figure 4.3.9 demonstrates that as average linear velocity is reduced that the amount of mass transported away is also reduced and the rebound increases. This result may have troubling implications. If precipitates are not transported away, the estimated rate of concentration rebound may be artificially high. It also may indicate that sites with a lasting accumulation of precipitates will have more concentration rebound.

4.4 Mass Reduction Analysis Results

Table 4.4.1 presents a table that compares the total mass in the aqueous phase and the total mass adsorbed to the soil within the area modeled. All of the cells show the expected substantial reduction in both phases at 100 days except two sites. Valmont EW-5 and Chemplex only show small decreases in total mass in both phases. The two cells that have small decreases in total mass probably result from the size of the cell. Both cells that have small total mass reduced are both very large cells, so the permanganate probably did not treat the entire area. This may result from a design flaw by the professional who performed the ISCO project. For example, an insufficient amount of permanganate was injected to treat the entire area or it may result from a flawed estimation of hydrogeological parameters. A flawed estimation of hydrogeological parameters may result a residence time that is too short or sections that are not treated. For example, if only enough permanganate is injected to treat a 75' x 75' area and the source zone is an 80' x 80' area, there will be untreated sections and much less mass reduced.

To determine whether or not the percentage of mass reduced is related to the concentration rebound rate, a regression analysis was completed[e]. Figure 4.6.2 shows that the rate of concentration rebound and the percentage of mass reduced are not correlated (R^2=0.0151).

[e] One outlier (PGDP) was not used for the regression analysis. Table 4.6.1 presents the Dixon Q-test.

4.5 Precipitate Accumulation Analysis Results

Table 4.5.1 presents the results of the precipitate accumulation analysis. The pore volume of the total cell volume was altered, but the alterations are negligible. In one case, the pore volume remained at 100% of the original pore volume. The case with the greatest reduction in pore volume still retained 99.52% of the original pore volume. These pore volume reductions indicate that there is a negligible impact on the average linear velocity.

4.6 Molecular Diffusion/Rate of Concentration Rebound Correlation Results

In the literature review, it has already been established that diffusivity influences the spatial and temporal distribution of DNAPLs in groundwater. The relationship between the diffusion coefficient in pure water and the rate of concentration rebound is demonstrated in Figure 4.6.1. Using a regression analysis, a R^2 of 0.9257 was found between the diffusion coefficient in pure water and the rate of concentration rebound. The diffusion coefficients in pure water ($D_{PCE} = 1.02 \times 10^{-9}$ m^2/s and $D_{TCE} = 1.04 \times 10^{-9}$ m^2/s) were estimated in EPA (2004a and b). This result indicates that the diffusion coefficient in water is a reliable predictor of the rate of concentration rebound. This result also concurs with the stagnant film model of dissolution because diffusion is the process that drives the phase change from the liquid phase to the aqueous phase.

The regression analysis was completed with one of the concentration rebound rates removed because it was an outlier. Table 4.6.1 shows the results of Q-tests. The rate of concentration rebound for the Portsmouth Gaseous Diffusion Plant (1.16×10^{-6} 1/s) was rejected. The reason why this concentration rebound rate is much higher than

the rest of the rates estimated is unclear. However, the most likely reason for the outlier is the small amount of data available for that site. Only three rounds of groundwater samples were available for the calibration process and only one indicated observable concentration rebound. If more data was available, the rate estimated for the Portsmouth Gaseous Diffusion plant may be lower and more reliable. Another possible explanation for the outlier is can be found in the speculation about preferential flow that complicated the rate of NOD calibration.

Table 4.1.1: Estimated Parameters for the Busch Campus Site

Table 4.1.1 summarizes all of the estimated parameters used to simulate the concentration rebound at the Busch Campus site.

Parameter	Unit	ISCO3	Source
Media	NA	Weathered Brunswick Shale	Langan, 2011
Solubility (C_s)	mg/l	240	Knauss; 2000
Longitudinal Dispersivity (α_x)	m	100	Schnoor; 1996
Dispersivity Ratio (α_x/α_y)	unitless	1	McKay et al.; 1997
Hydraulic Gradient (dh/dl)	unitless	0.85	Langan, 2011
Fraction of Organic Carbon (*foc*)	unitless	0.002	EPA Guidance, 2008
Hydraulic Conductivity (k)	m/s	2.35×10^{-11}	Domenico & Schwartz, 1990
Concentration Rebound Rate (k_{cr})	1/s	8.68×10^{-12}	Calibration presented in Appendix 8
Natural Oxidant Demand Rate (k_{nod})	1/s	1.53×10^{-6}	Calibration presented in Appendix 7
Oxidation Rate (k_{ox})	1/(M s)	0.035 ± 0.004	Huang et al.; 2001
Porosity (n)	unitless	20%	Langan, 2011
Density (ρ)	g/ml	1.586	http://www.simetric.co.uk/si_materials.htm
K_{oc}	l/g	759	Schnoor; 1996
Retardation Factor (R)	unitless	13.04	Equation 3.1.4
ALV (u_x)	m/s	1.55×10^{-11}	Equation 3.1.1
ΔX	ft.	1	NA
ΔY	ft.	1	NA

Figure 4.1.1: Busch Campus Garage Well Locations & Initial Concentration Distribution

Figure 4.1.1 presents the PCE concentrations before the permanganate was injected. It also shows the locations of the well used for injection and the well used for calibrations. The direction of groundwater flow is the x-direction. The injection well's location is at the origin (0,0) and the well used to calibrate k_{NOD} and k_{CR} is ISCO-3 located at (13,1). (R^2=0.99)

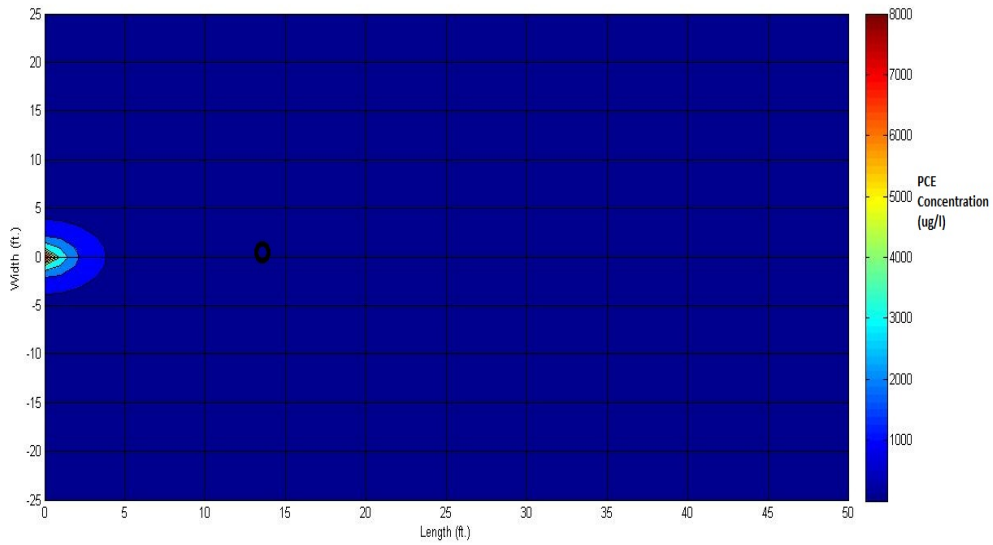

Figure 4.1.2: Busch Campus Garage Natural Oxidant Demand Calibration

Figure 4.1.2 presents the rate of natural oxidant demand calibration that employs the sum of least squares (R^2=0.99). The permanganate injection was at t=0 d.

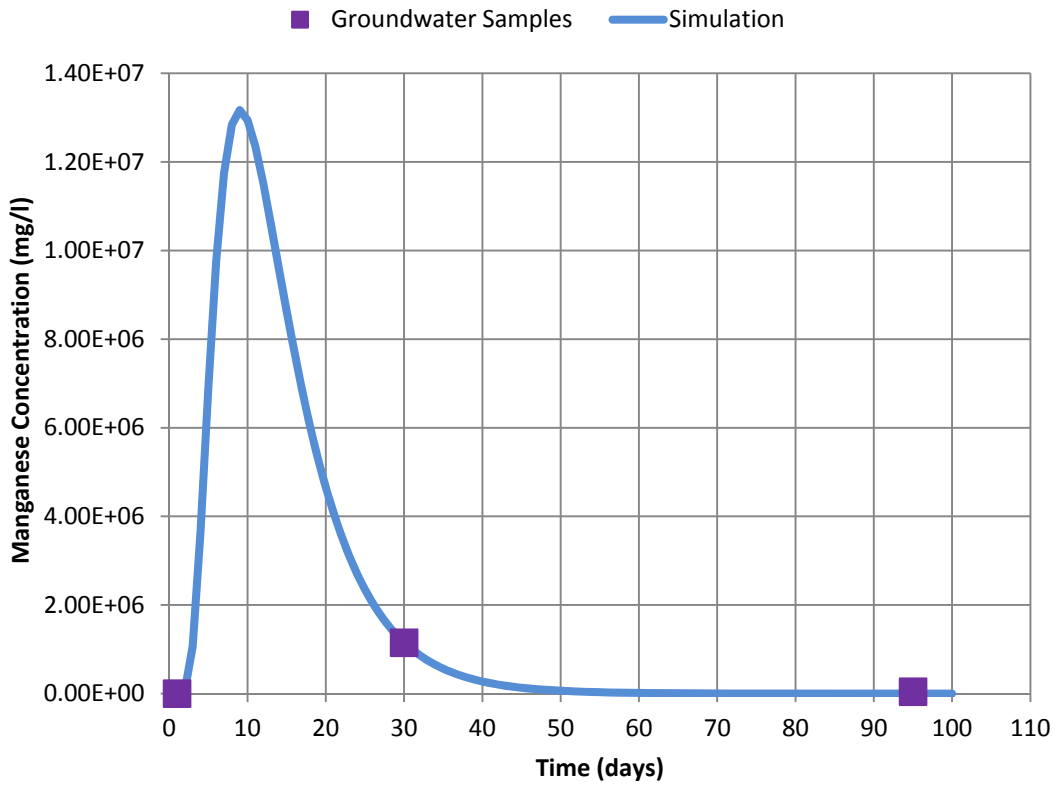

Figure 4.1.3: Busch Campus Garage Concentration Rebound Rate Calibration

Figure 4.1.3 presents the rate of concentration rebound calibration that employs the sum of least squares (R^2=0.81). The permanganate injection was at t=0 d.

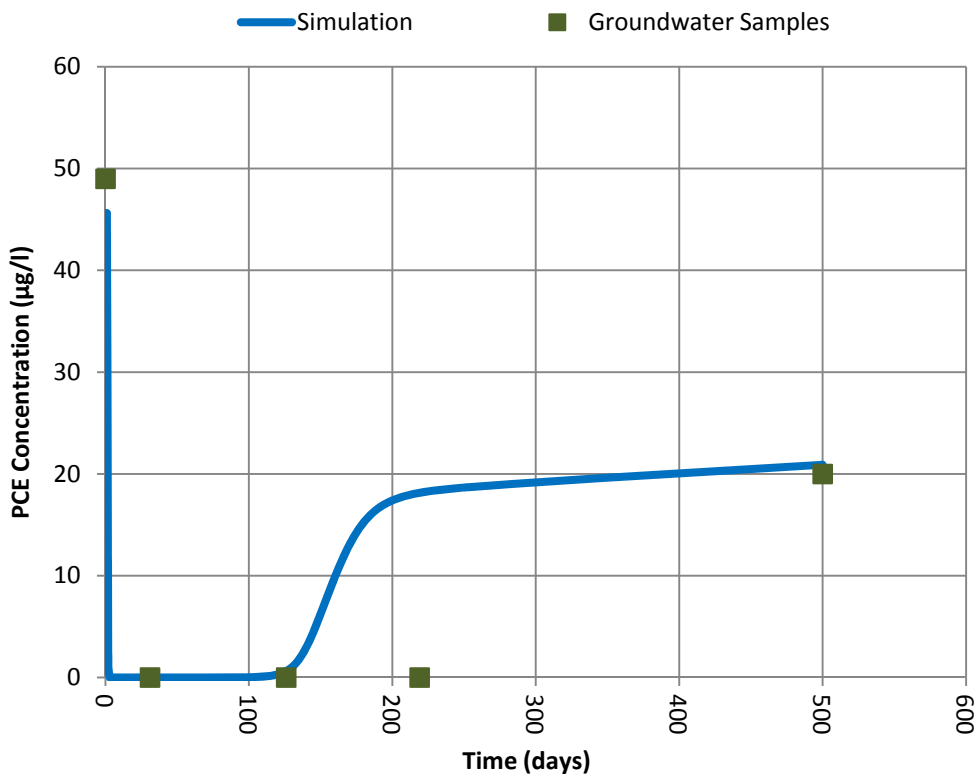

Table 4.1.2: Estimated Parameters for the Cape Canaveral Sites

Table 4.1.2 summarizes all of the estimated parameters used to simulate the concentration rebound at the Cape Canaveral cells.

Parameter	Unit	2S	5S	Source
Media	NA	Sand	Sand	Batelle; 2002
Solubility (C_s)	mg/l	1280	1280	Knauss; 2000
Longitudinal Dispersivity (α_x)	m	100	100	Schnoor; 1996
Dispersivity Ratio (α_x/α_y)	unitless	10	10	Schnoor; 1996
Hydraulic Gradient (dh/dl)	unitless	9.00×10^{-5}	9.00×10^{-5}	Batelle; 2002
Fraction of Organic Carbon (*foc*)	unitless	0.002	0.002	EPA Guidance, 2008
Hydraulic Conductivity (k)	m/s	1.59×10^{-5}	1.59×10^{-5}	Batelle; 2002
Concentration Rebound Rate (k_{cr})	1/s	1.39×10^{-8}	2.31×10^{-8}	Calibration presented in Appendix 8
Natural Oxidant Demand Rate (k_{nod})	1/s	3.07×10^{-7}	3.07×10^{-7}	Calibration presented in Appendix 7
Oxidation Rate (k_{ox})	1/M s	1.52 ± 0.05	1.52 ± 0.05	Huang et al.; 2001
Porosity (n)	unitless	26%	26%	Batelle; 2002
Density (ρ)	g/ml	1.59	1.59	Batelle; 2002
K_{oc}	l/g	141.3	141.3	Schnoor; 1996
Retardation Factor (R)	unitless	2.73	2.73	Equation 3.1.4
ALV (u_x)	m/s	8.53×10^{-10}	8.53×10^{-10}	Equation 3.1.1
ΔX	ft.	1	1	NA
ΔY	ft.	1	1	NA

Figure 4.1.4: Cape Canaveral Well Locations & Initial Concentration Distribution (MW-2S)

Figure 4.1.4 presents the TCE concentrations before the permanganate was injected. It also shows the locations of the well used for injection and the well used for calibrations. The direction of groundwater flow is the x-direction. The injection well's location is at the origin (0,0) and the well used to calibrate k_{NOD} and k_{CR} is MW-2S located at (6,1). (R^2=0.46)

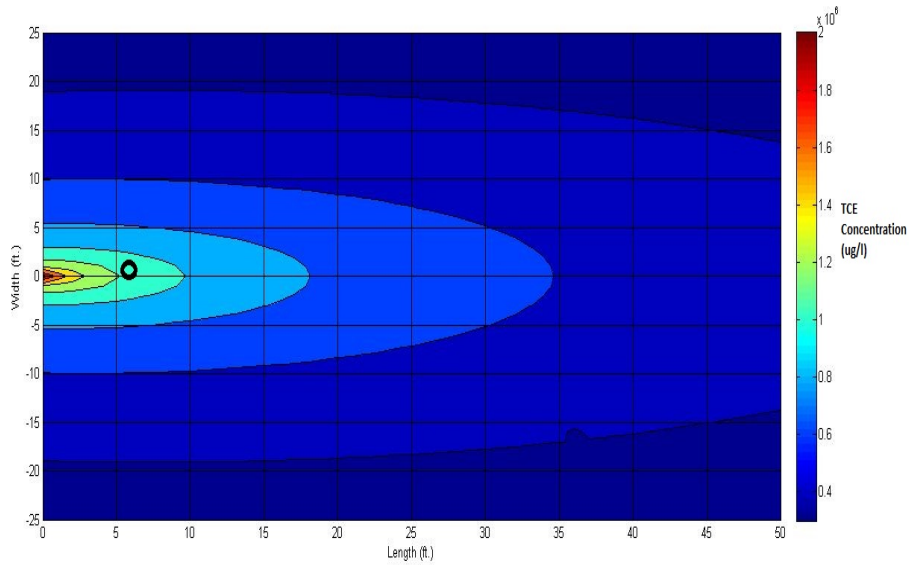

Figure 4.1.5: Cape Canaveral Well Locations & Initial Concentration Distribution (MW-5S)

Figure 4.1.5 presents the TCE concentrations before the permanganate was injected. It also shows the locations of the well used for injection and the well used for calibrations. The direction of groundwater flow is the x-direction. The injection well's location is at the origin (0,0) and the well used to calibrate k_{NOD} and k_{CR} is MW-5S located at (3,15). (R^2=0.82)

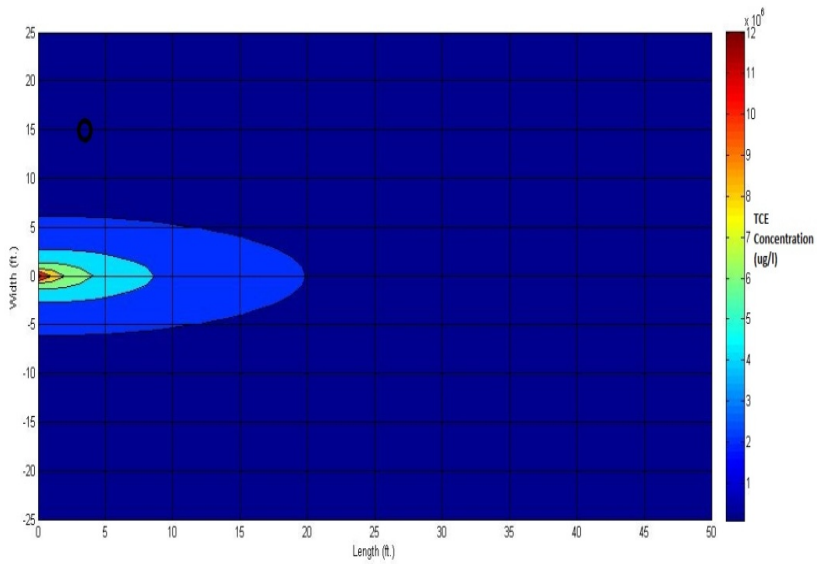

Figure 4.1.6: Cape Canaveral Natural Oxidant Demand Calibration

Figure 4.1.6 presents the rate of natural oxidant demand calibration that employs the sum of least squares (R^2=0.78). The permanganate injection was at t=0 d.

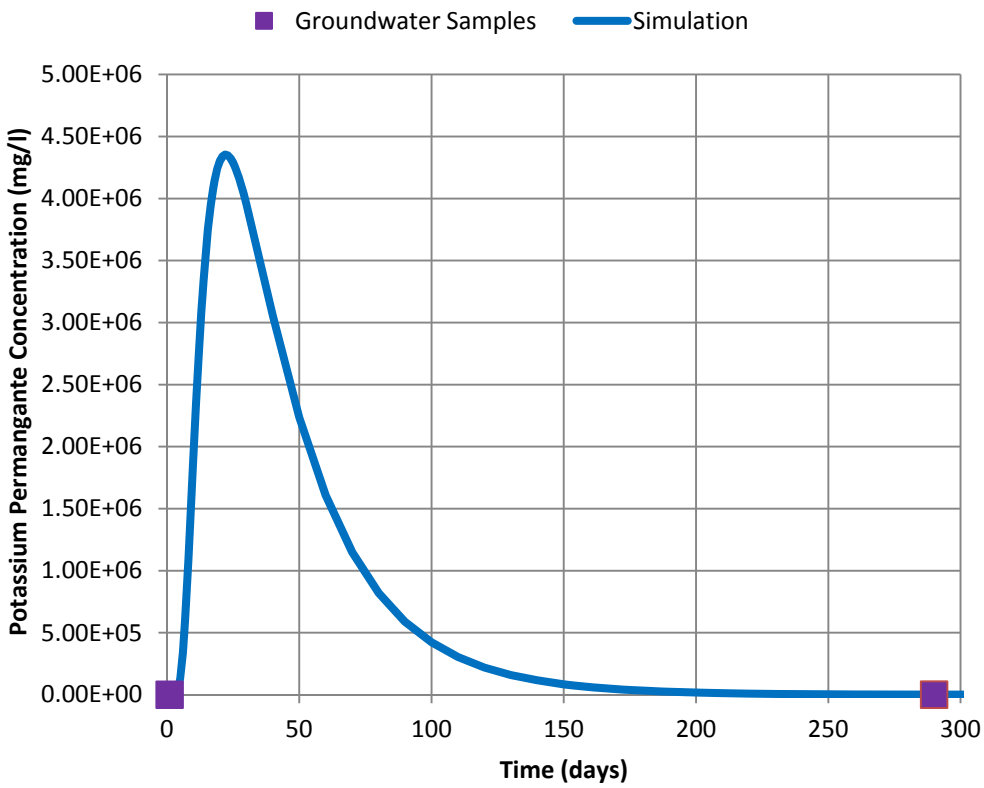

Figure 4.1.7: Cape Canaveral (2S) Concentration Rebound Rate Calibration

Figure 4.1.7 presents the rate of concentration rebound calibration that employs the sum of least squares (R^2=1.00). The permanganate injection was at t=0 d.

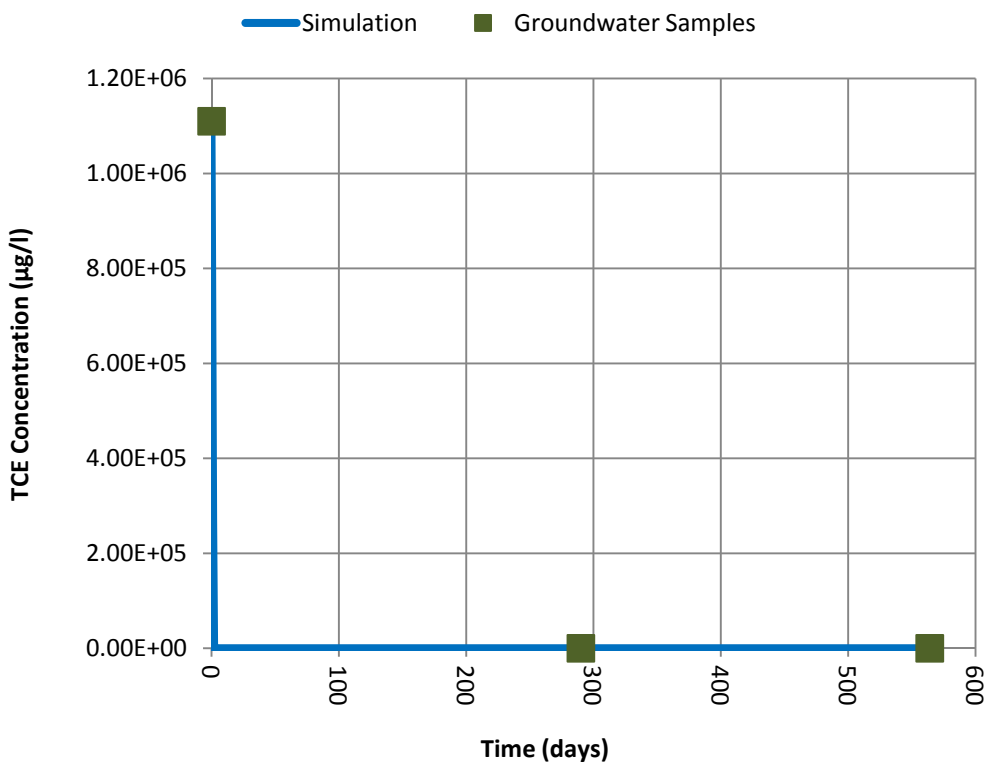

Figure 4.1.8: Cape Canaveral (5S) Concentration Rebound Rate Calibration

Figure 4.1.8 presents the rate of concentration rebound calibration that employs the sum of least squares (R^2=1.00). The permanganate injection was at t=0 d.

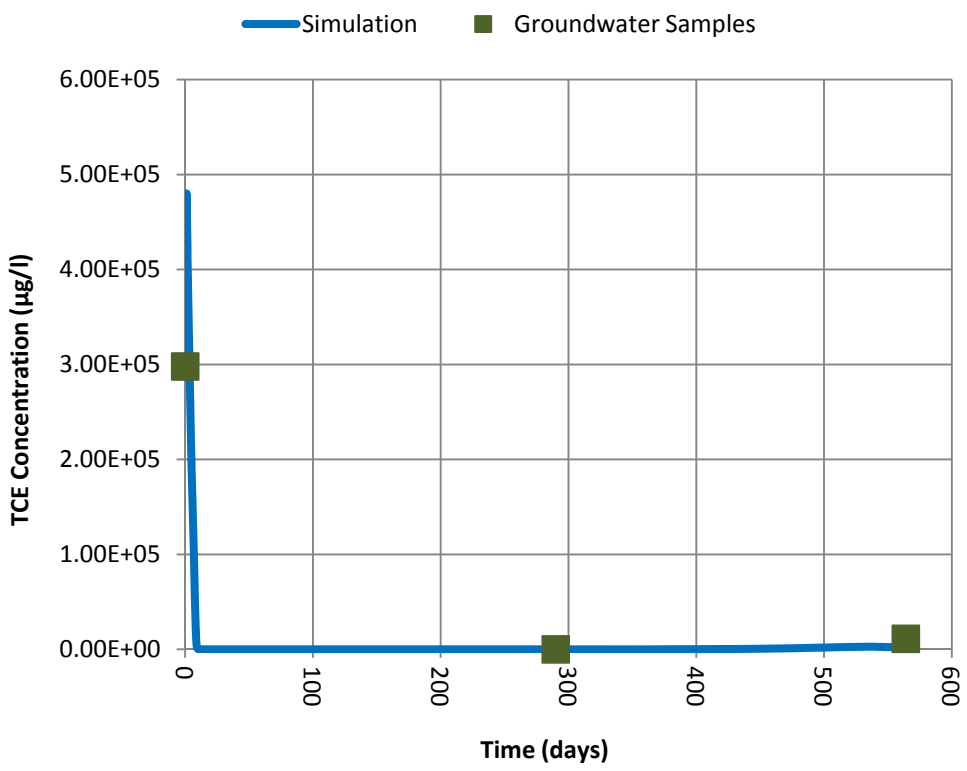

Table 4.1.3: Estimated Parameters for the Chemplex Site

Table 4.1.3 summarizes all of the estimated parameters used to simulate the concentration rebound at the Chemplex cell.

Parameter	Unit	MW112	Source
Media	NA	Silt and Clay	MWH; 2010
Solubility (C_s)	mg/l	240	Knauss; 2000
Longitudinal Dispersivity (α_x)	m	100	Schnoor; 1996
Dispersivity Ratio (α_x/α_y)	unitless	10	Schnoor; 1996
Hydraulic Gradient (dh/dl)	unitless	1.24×10^{-2}	EPA; 2009
Fraction of Organic Carbon (*foc*)	unitless	0.002	EPA Guidance, 2008
Hydraulic Conductivity (k)	m/s	7.17×10^{-9}	Domenico & Schwartz, 1990
Concentration Rebound Rate (k_{cr})	1/s	4.05×10^{-10}	Calibration presented in Appendix 8
Natural Oxidant Demand Rate (k_{nod})	1/s	1.16×10^{-8}	Calibration presented in Appendix 7
Oxidation Rate (k_{ox})	1/M s	0.035 ± 0.004	Huang et al.; 2001
Porosity (n)	unitless	36 %	Domenico & Schwartz, 1990
Density (ρ)	g/ml	1.826	http://www.simetric.co.uk/si_materials.htm
K_{oc}	l/g	759	Schnoor; 1996
Retardation Factor (R)	unitless	121.5	Equation 3.1.4
ALV (u_x)	m/s	3.83×10^{-10}	Equation 3.1.1
ΔX	ft.	6	NA
ΔY	ft.	6	NA

Figure 4.1.9: Chemplex Site Well Locations & Initial Concentration Distribution

Figure 4.1.9 presents the PCE concentrations before the permanganate was injected. It also shows the locations of the well used for injection and the well used for calibrations. The direction of groundwater flow is the x-direction. The injection well's location is at the origin (0,0) and the well used to calibrate k_{NOD} and k_{CR} is MW-112 located at (222, 6). (R^2=0.99)

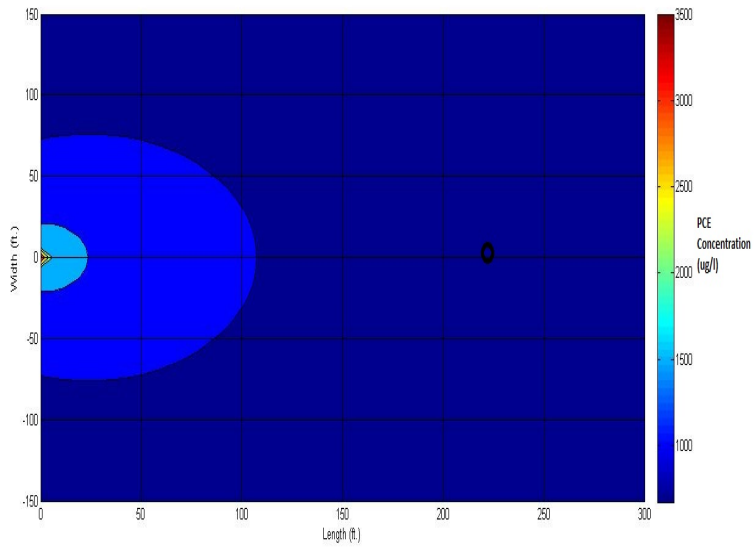

Figure 4.1.10: Chemplex Natural Oxidant Demand Calibration

Figure 4.1.10 presents the rate of natural oxidant demand calibration that employs the sum of least squares (R^2=0.78). The permanganate injection was at t=0 d.

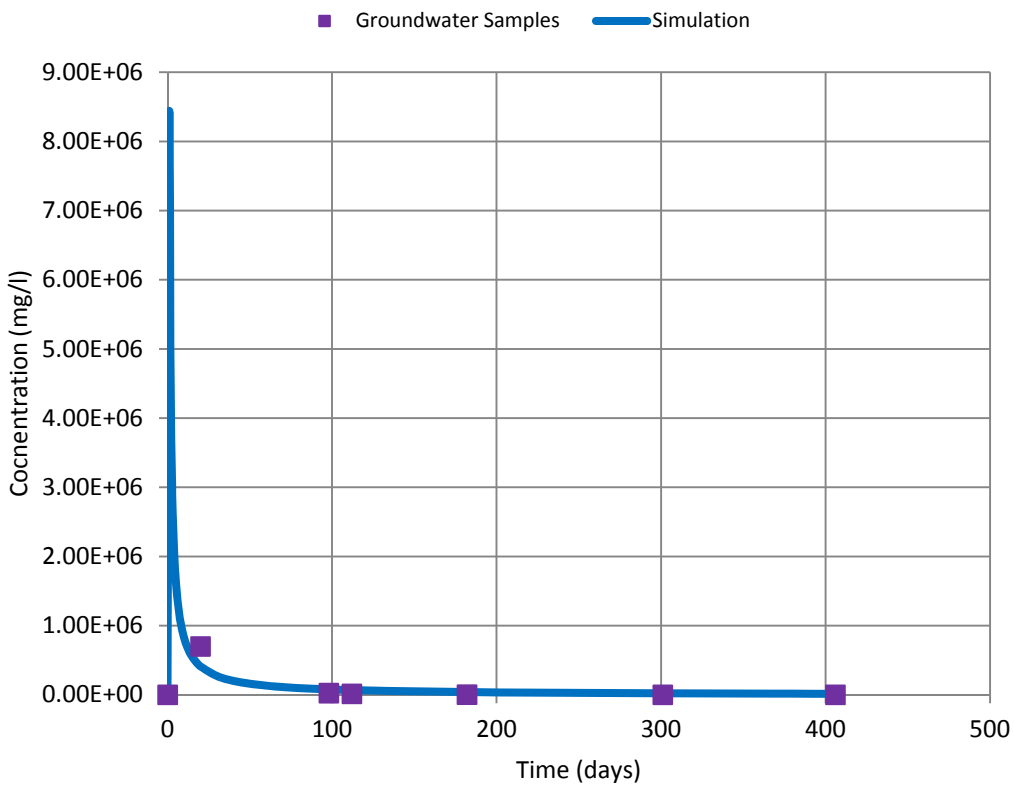

Figure 4.1.11: Chemplex Site Concentration Rebound Rate Calibration

Figure 4.1.11 presents the rate of concentration rebound calibration that employs the sum of least squares (R^2=0.57). The permanganate injection was at t=0 d.

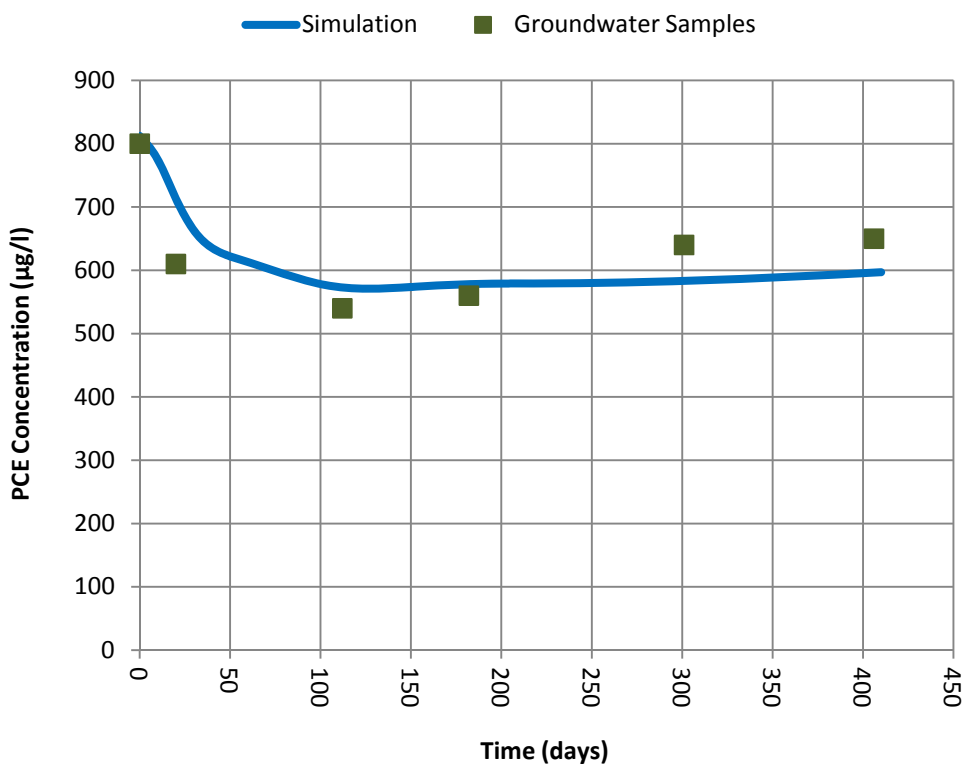

Table 4.1.4: Estimated Parameters for the Portsmouth Gaseous Diffusion Plant Site

Table 4.1.4 summarizes all of the estimated parameters used to simulate the concentration rebound at the Portsmouth Gaseous Diffusion Plant cell.

Parameter	Unit	MW89G	Source
Media	NA	Sand & gravel	West et al.; 1997
Solubility (C_s)	mg/l	1280	Knauss; 2000
Longitudinal Dispersivity (α_x)	m	100	Schnoor; 1996
Dispersivity Ratio (α_x/α_y)	unitless	10	Schnoor; 1996
Hydraulic Gradient (dh/dl)	unitless	2.84×10^{-2}	RWMA; 2002
Fraction of Organic Carbon (*foc*)	unitless	0.002	EPA Guidance, 2008
Hydraulic Conductivity (k)	m/s	1.42×10^{-7}	Domenico & Schwartz, 1990
Concentration Rebound Rate (k_{cr})	1/s	1.16×10^{-6}	Calibration presented in Appendix 8
Natural Oxidant Demand Rate (k_{nod})	1/s	2.31×10^{-7}	Calibration presented in Appendix 7
Oxidation Rate (k_{ox})	1/M s	1.52 ± 0.05	Huang et al.; 2001
Porosity (n)	unitless	30%	West et al.; 1997
Density (ρ)	g/ml	2.02	http://www.simetric.co.uk/si_materials.htm
K_{oc}	l/g	141.3	Schnoor; 1996
Retardation Factor (R)	unitless	2.90	Equation 3.1.4
ALV (u_x)	m/s	3.13×10^{-9}	Equation 3.1.1
ΔX	ft.	1	NA
ΔY	ft.	1	NA

Figure 4.1.12:Portsmouth Gaseous Diffusion Plant Well Locations and nitial Concentration Distribution

Figure 4.1.12 presents the TCE concentrations before the permanganate was injected. It also shows the locations of the well used for injection and the well used for calibrations. The direction of groundwater flow is the x-direction. The injection well's location is at the origin (0,0) and the well used to calibrate k_{NOD} and k_{CR} is MW-89G located at (38,1). (R^2=0.94)

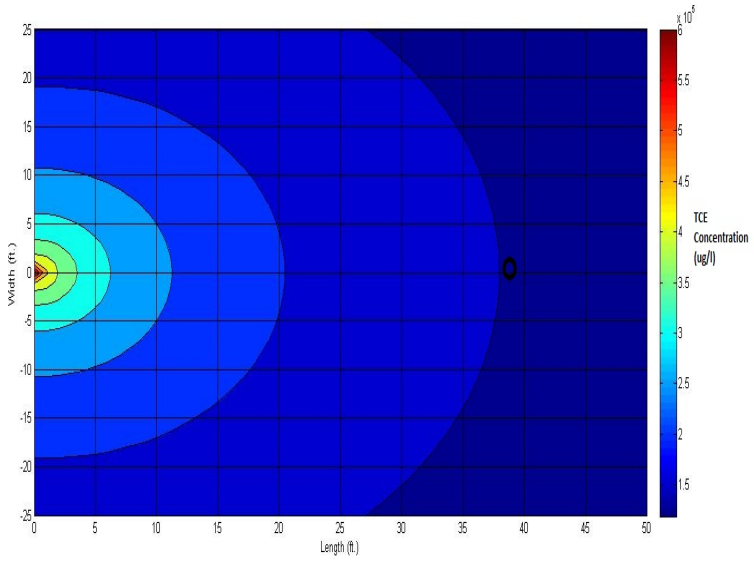

Figure 4.1.13: Portsmouth Gaseous Diffusion Plant Natural Oxidant Demand Calibration

Figure 4.1.13 presents the rate of natural oxidant demand calibration that employs the sum of least squares (R^2=0.77). The permanganate injection was at t=0 d.

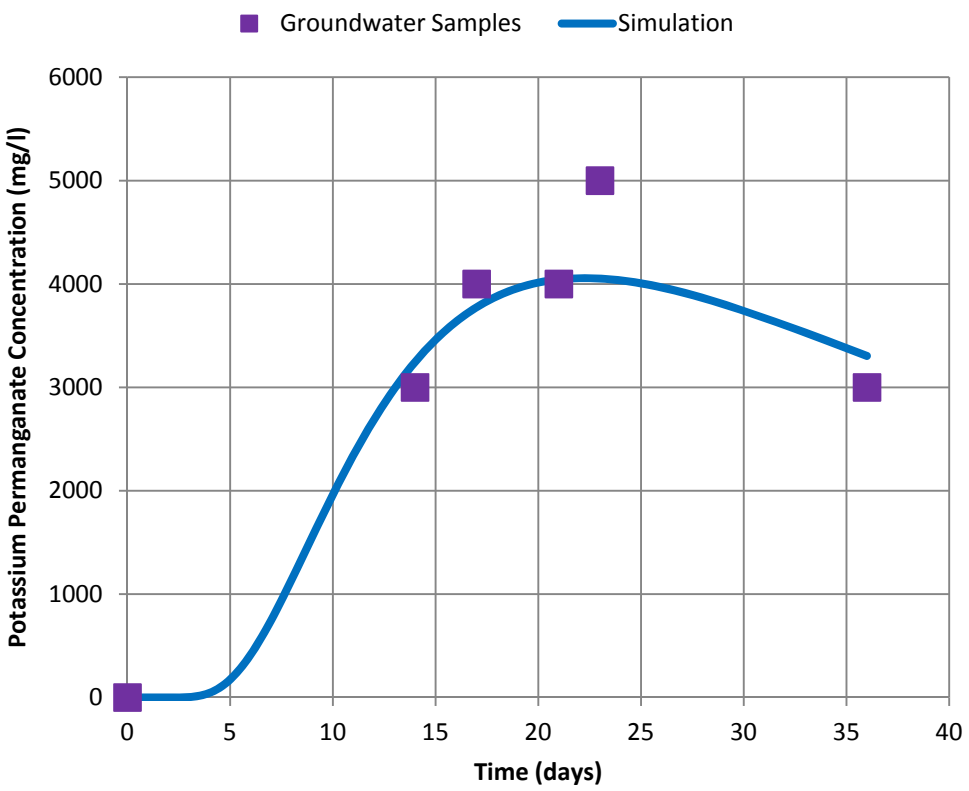

Figure 4.1.14: Portsmouth Gaseous Diffusion Plant Concentration Rebound Rate Calibration

Figure 4.1.14 presents the rate of concentration rebound calibration that employs the sum of least squares (R^2=1.00). The permanganate injection was at t=0 d.

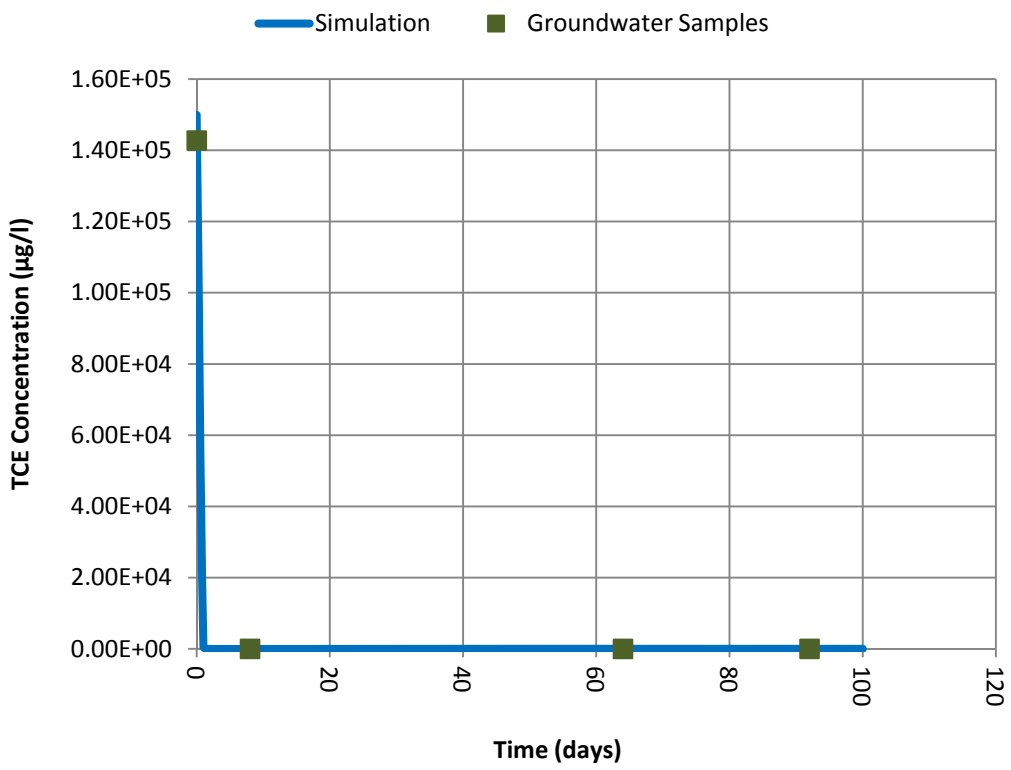

Table 4.1.5: Estimated Parameters for the Valmont Site

Table 4.1.5 summarizes all of the estimated parameters used to simulate the concentration rebound at the Valmont cells.

Parameter	Unit	EW1	EW5	Source
Media	NA	Sandstone & Siltstone	Sandstone & Siltstone	Tetratech; 2010
Solubility (C_s)	mg/l	1280	1280	Knauss; 2000
Longitudinal Dispersivity (α_x)	m	100	100	Schnoor; 1996
Dispersivity Ratio (α_x/α_y)	unitless	10	10	Schnoor; 1996
Hydraulic Gradient (dh/dl)	unitless	8.18×10^{-3}	2.19×10^{-3}	Tetratech; 2010
Fraction of Organic Carbon (*foc*)	unitless	0.002	0.002	EPA Guidance, 2008
Hydraulic Conductivity (k)	m/s	9.07×10^{-10}	9.07×10^{-10}	Domenico & Schwartz, 1990
Concentration Rebound Rate (k_{cr})	1/s	1.74×10^{-8}	1.56×10^{-8}	Calibration presented in Appendix 8
Natural Oxidant Demand Rate (k_{nod})	1/s	1.16×10^{-8}	1.16×10^{-8}	Calibration presented in Appendix 7
Oxidation Rate (k_{ox})	1/M s	1.52 ± 0.05	1.52 ± 0.05	Huang et al.; 2001
Porosity (n)	unitless	12%	12&	Tetratech; 2010
Density (ρ)	g/ml	2.58	2.58	Tetratech; 2010
K_{oc}	l/g	141.3	141.3	Schnoor; 1996
Retardation Factor (R)	unitless	7.08	7.08	Equation 3.1.4
ALV (u_x)	m/s	9.57×10^{-12}	1.66×10^{-11}	Equation 3.1.1
ΔX	ft.	10	4	NA
ΔY	ft.	10	4	NA

Figure 4.1.16: Valmont Site Well Locations & Initial Concentration Distribution (EW-1)

Figure 4.1.16 presents the TCE concentrations before the permanganate was injected. It also shows the locations of the well used for injection and the well used for calibrations. The direction of groundwater flow is the x-direction. The injection well's location is at the origin (0,0) and the well used to calibrate k_{NOD} and k_{CR} is MW-10C located at (170,200). (R^2=0.96)

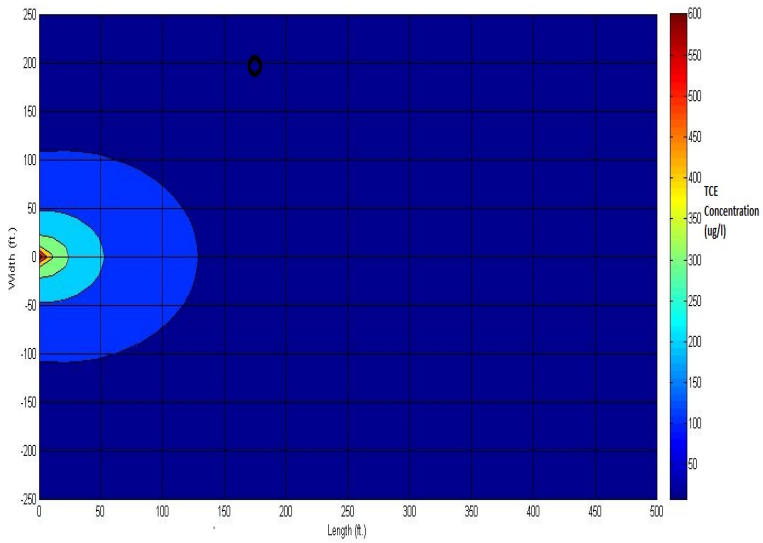

Figure 4.1.17: Valmont Site Well Locations & Initial Concentration Distribution (EW-5)

Figure 4.1.17 presents the TCE concentrations before the permanganate was injected. It also shows the locations of the well used for injection and the well used for calibrations. The direction of groundwater flow is the x-direction. The injection well's location is at the origin (0,0,) and the well used to calibrate k_{NOD} and k_{CR} is MW-2I located at (144,80). (R^2=0.60)

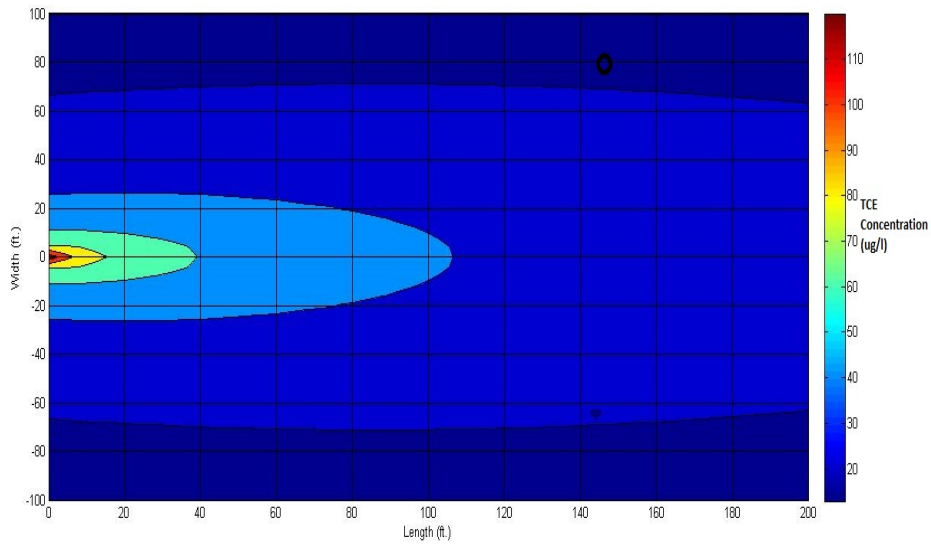

Figure 4.1.18: Valmont Natural Oxidant Demand Calibration

Figure 4.1.18 presents the rate of natural oxidant demand calibration that employs the sum of least squares (R^2=0.99). The permanganate injection was at t=0 d.

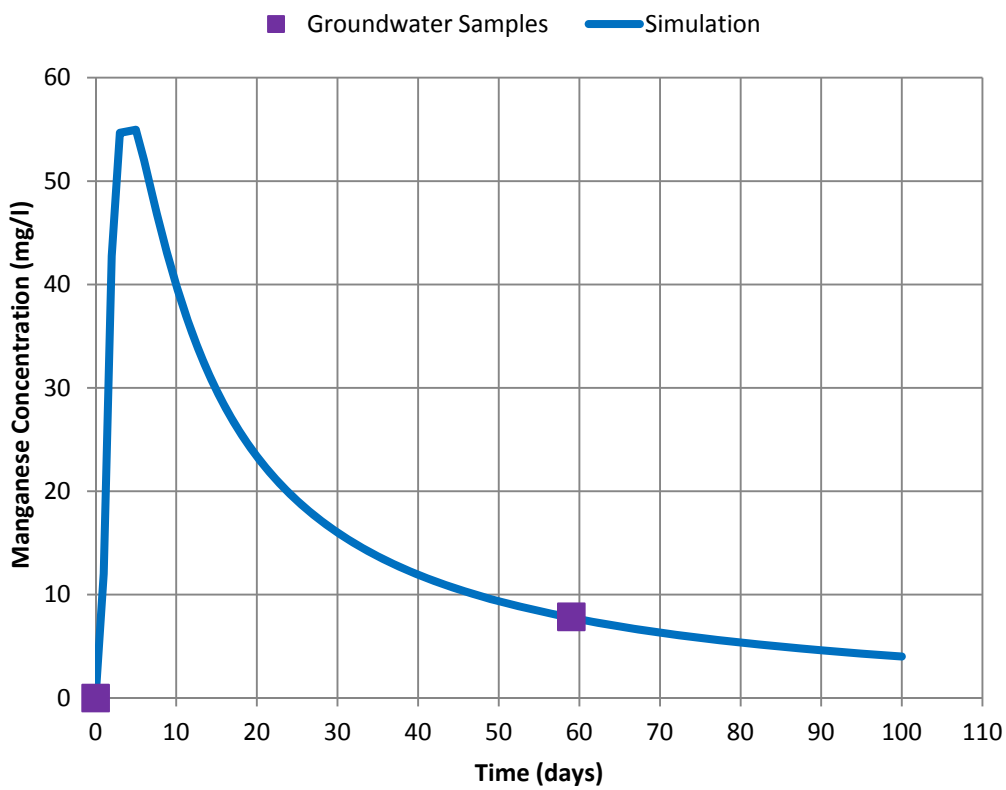

Figure 4.1.19: Valmont Site (EW-1) Concentration Rebound Rate Calibration

Figure 4.1.19 presents the rate of concentration rebound calibration that employs the sum of least squares (R^2=0.99). The permanganate injection was at t=0 d.

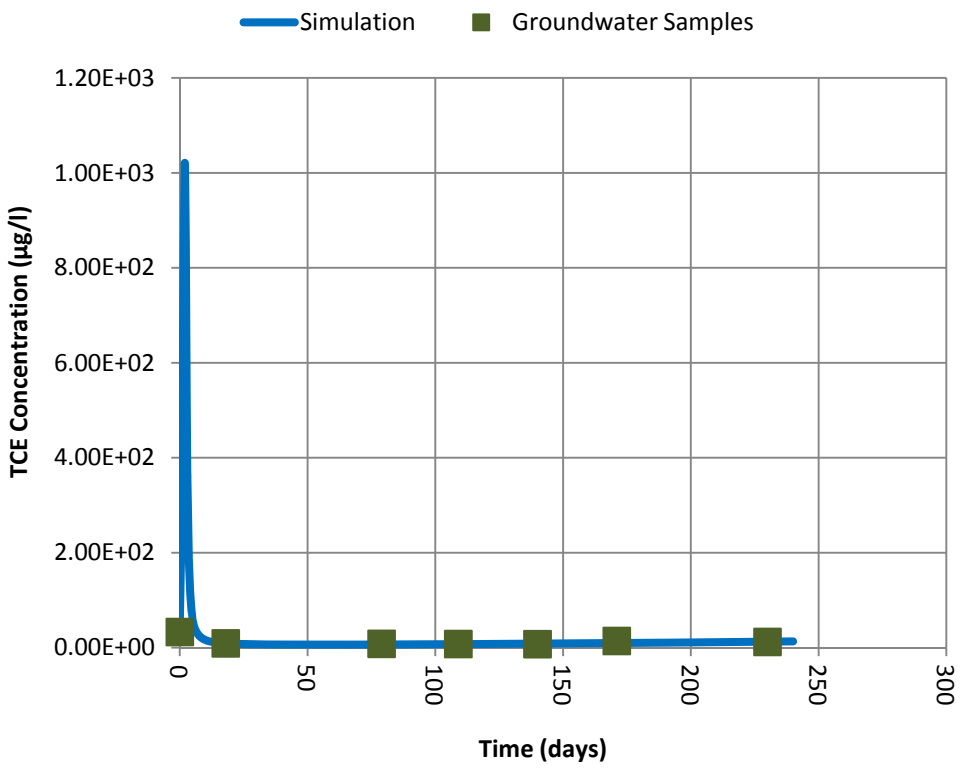

Figure 4.1.20: Valmont Site (EW-5) Concentration Rebound Rate Calibration

Figure 4.1.20 presents the rate of concentration rebound calibration that employs the sum of least squares (R^2=0.66). The permanganate injection was at t=0 d.

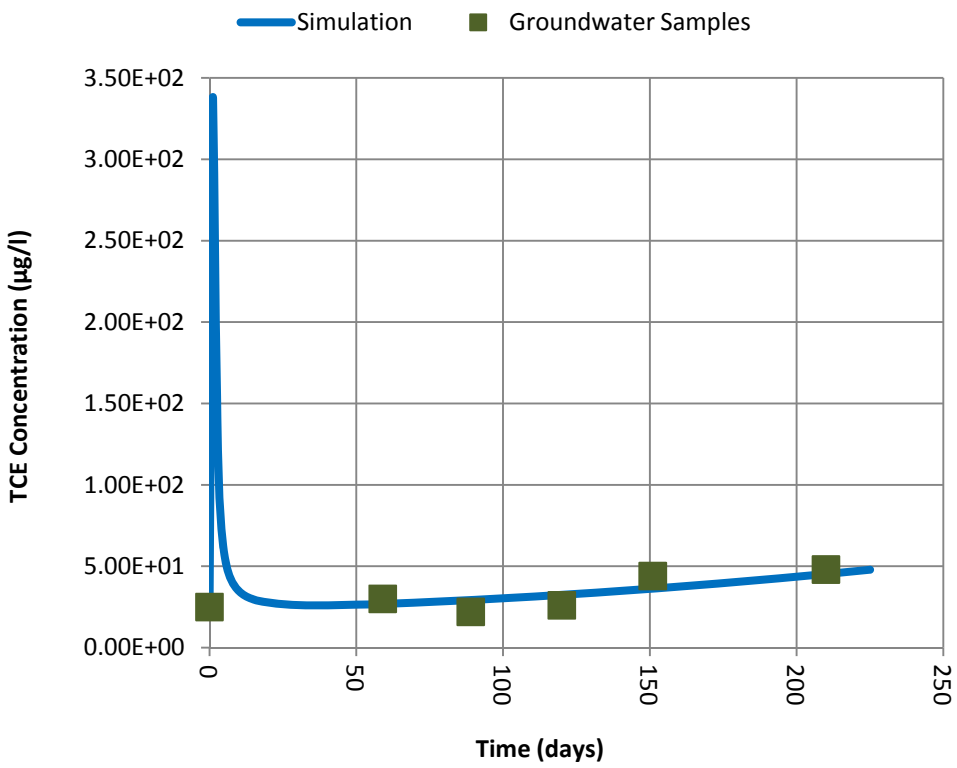

Table 4.1.6: Estimated Parameters for the Watervliet Site

Table 4.1.6 summarizes all of the estimated parameters used to simulate the concentration rebound at the Watervliet cells.

Parameter	Unit	IW1	IW4	Source
Media	NA	Black, laminated shale	Black, laminated shale	Goldstein; 2004
Solubility (C_s)	mg/l	240	240	Knauss; 2000
Longitudinal Dispersivity (α_x)	m	100	100	Schnoor; 1996
Dispersivity Ratio (α_x/α_y)	unitless	1	1	McKay et al.; 1997
Hydraulic Gradient (dh/dl)	unitless	4.4×10^{-3}	3.5×10^{-3}	Williams & Paillet; 2002
Fraction of Organic Carbon (*foc*)	unitless	0.0031	0.0031	Goldstein; 2004
Hydraulic Conductivity (k)	m/s	1.69×10^{-12}	1.69×10^{-12}	Domenico & Schwartz, 1990
Concentration Rebound Rate (k_{cr})	1/s	1.16×10^{-12}	2.89×10^{-12}	Calibration presented in Appendix 8
Natural Oxidant Demand Rate (k_{nod})	1/s	1.5×10^{-6}	1.5×10^{-6}	Calibration presented in Appendix 7
Oxidation Rate (k_{ox})	1/M s	0.035 ± 0.004	0.035 ± 0.004	Huang et al.; 2001
Porosity (n)	unitless	2.3%	2.3%	Goldstein; 2004
Density (ρ)	g/ml	2.66	2.66	Goldstein; 2004
K_{oc}	l/g	759	759	Goldstein; 2004
Retardation Factor (R)	unitless	136	136	Equation 3.1.4
ALV(u_x)	m/s	5.47×10^{-14}	1.31×10^{-13}	Equation 3.1.1
ΔX	ft.	1	1	NA
ΔY	ft.	1	1	NA

Figure 4.1.21: Watervliet Site Well Locations & Initial Concentration Distribution (IW-1)

Figure 4.1.21 presents the PCE concentrations before the permanganate was injected. It also shows the locations of the well used for injection and the well used for calibrations. The direction of groundwater flow is the x-direction. The injection well's location is at the origin (0,0) and the well used to calibrate k_{NOD} and k_{CR} is MW-87 located at (20,20). (R^2=0.70)

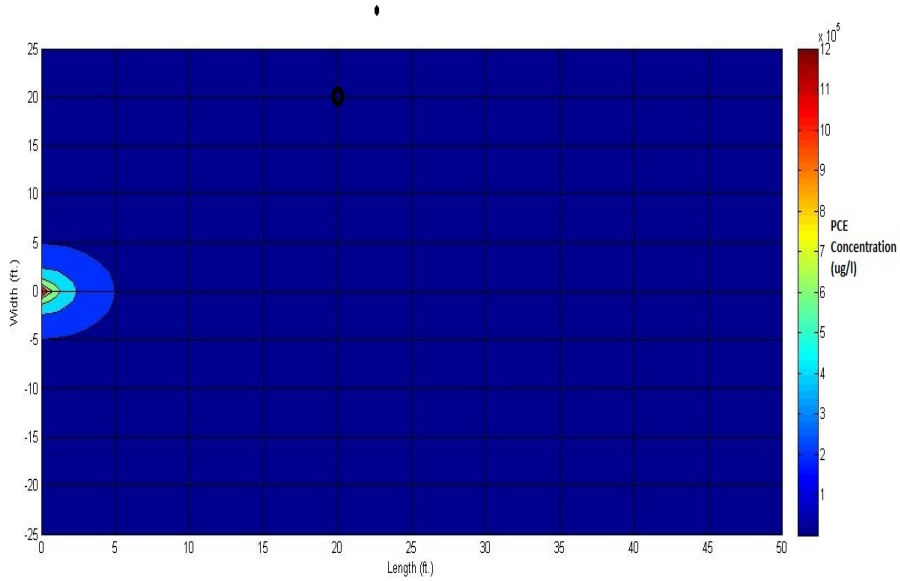

Figure 4.1.22: Watervliet Site Well Locations & Initial Concentration Distribution (IW-4)

Figure 4.1.22 presents the PCE concentrations before the permanganate was injected. It also shows the locations of the well used for injection and the well used for calibrations. The direction of groundwater flow is the x-direction. The injection well's location is at the origin (0,0) and the well used to calibrate k_{NOD} and k_{CR} is MW-86 located at (33,15). (R^2=0.70)

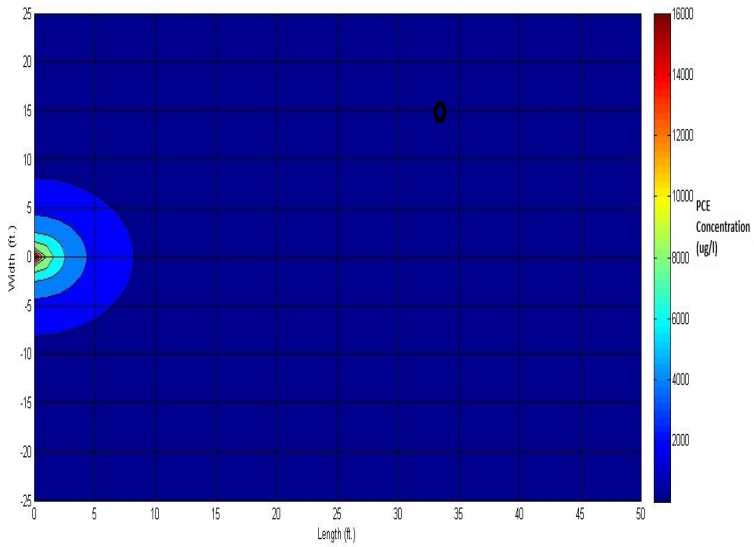

Figure 4.1.23: Watervliet Natural Oxidant Demand Calibration

Figure 4.1.23 presents the rate of natural oxidant demand calibration that employs the sum of least squares (R^2=0.75). The permanganate injection was at t=0 d.

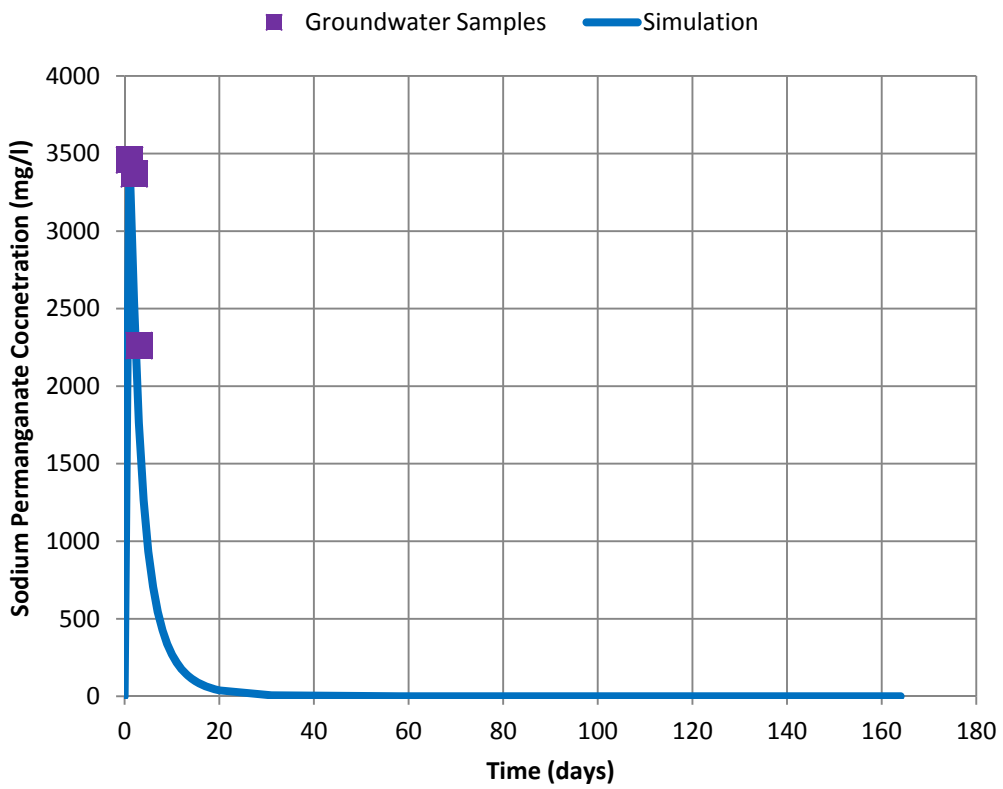

Figure 4.1.24: Watervliet Site (IW-1) Concentration Rebound Rate Calibration

Figure 4.1.24 presents the rate of concentration rebound calibration that employs the sum of least squares (R^2=0.92). The permanganate injection was at t=0 d.

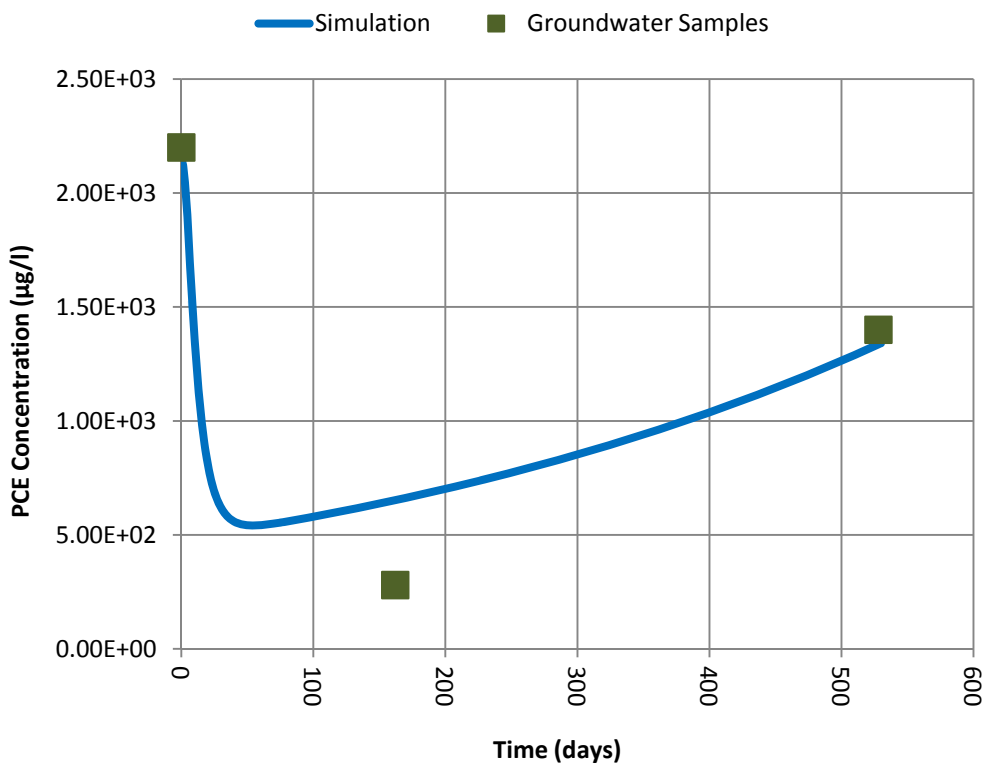

Figure 4.1.25: Watervliet Site (IW-4) Concentration Rebound Rate Calibration

Figure 4.1.25 presents the rate of concentration rebound calibration that employs the sum of least squares (R^2=0.80). The permanganate injection was at t=0 d.

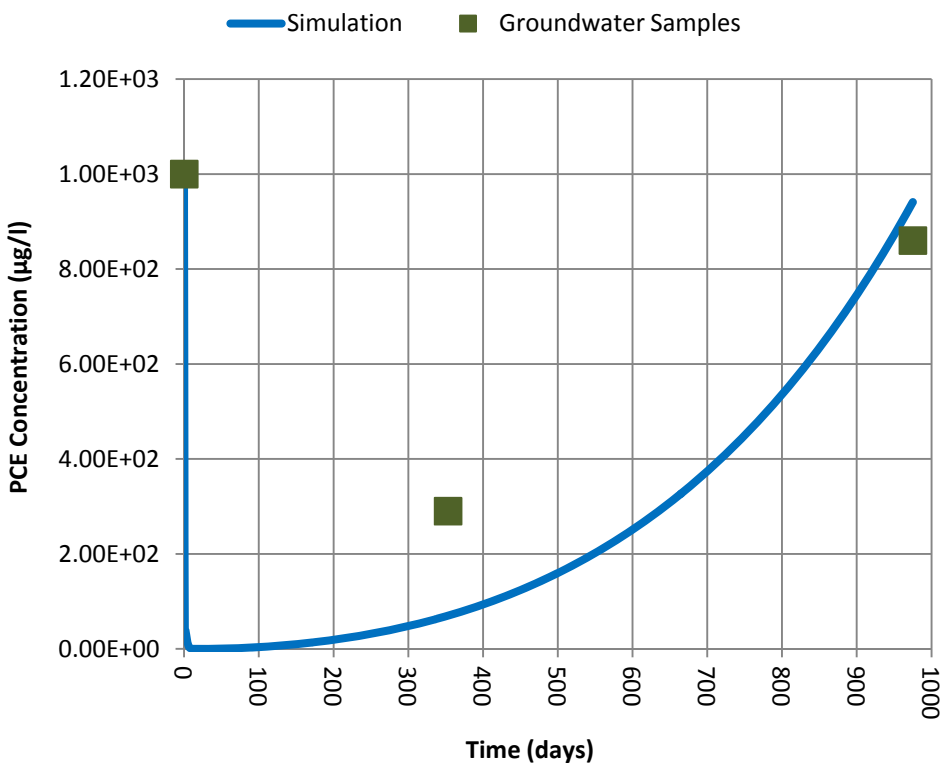

Table 4.1.7: Summary Estimated Parameters

Table 4.1.7 summarizes all of the estimated parameters used to simulate the concentration rebound at each site.

Parameter	Unit	Busch	Cape Canaveral (2S)	Cape Canaveral (5S)	Chemplex	PGDP	Valmont (EW1)	Valmont (EW5)	Watervliet (IW1)	Watervliet (IW4)
Media	NA	Weathered Brunswick Shale	Sand	Sand	Silt and Clay	Sand & gravel	Sandstone & Siltstone	Sandstone & Siltstone	Black, laminated shale	Black, laminated shale
Contaminant	NA	PCE	TCE	TCE	PCE	TCE	TCE	TCE	PCE	PCE
Solubility (C_s)	kg/l	240	1280	1280	240	1280	1280	1280	240	240
Longitudinal Dispersivity (α_x)	m	100	100	100	100	100	100	100	100	100
Dispersivity Ratio (α_x/α_y)	unitless	1	10	10	10	10	10	10	1	1
Hydraulic Gradient (dh/dl)	unitless	0.85	9.00×10^{-5}	9.00×10^{-5}	1.24×10^{-2}	2.84×10^{-2}	8.18×10^{-3}	0.00219	0.0044	0.0035
Fraction of Organic Carbon (*foc*)	unitless	0.002	0.002	0.002	0.002	0.002	0.002	0.002	0.0031	0.0031
Hydraulic Conductivity (k)	m/s	2.35×10^{-11}	1.59×10^{-6}	1.59×10^{-6}	7.17×10^{-9}	1.42×10^{-7}	9.07×10^{-10}	9.07×10^{-10}	1.69×10^{-12}	1.69×10^{-12}
Concentration Reboud Rate (k_{cr})	1/s	8.68×10^{-12}	1.39×10^{-8}	2.31×10^{-8}	4.05×10^{-10}	1.16×10^{-6}	1.74×10^{-8}	1.56×10^{-8}	1.16×10^{-12}	2.89×10^{-12}
Natural Oxidant Demand Rate (k_{nod})	1/s	1.53×10^{-6}	3.07×10^{-7}	3.07×10^{-7}	1.16×10^{-8}	2.31×10^{-7}	1.16×10^{-8}	1.16×10^{-8}	1.5×10^{-6}	1.5×10^{-6}
Oxidation Rate (k_{ox})	1/M s	0.035 ± 0.004	1.52 ± 0.05	1.52 ± 0.05	0.035 ± 0.004	1.52 ± 0.05	1.52 ± 0.05	1.52 ± 0.05	0.035 ± 0.004	0.035 ± 0.004
Porosity (n)	unitless	20%	26%	26%	36%	30%	12%	12%	2.3%	2.3%
Density (P)	kg/l	1.586	1.59	1.59	1.826	2.02	2.58	2.58	2.66	2.66
K_{oc}	l/g	759	141.3	141.3	759	141.3	141.3	141.3	759	759
Retardation Factor (R)	unitless	13.04	2.73	2.73	121.5	2.90	7.08	7.08	136	136
ALV (u_x)	m/s	1.55×10^{-11}	8.53×10^{-10}	8.53×10^{-10}	3.83×10^{-10}	3.13×10^{-9}	9.57×10^{-12}	1.66×10^{-11}	5.47×10^{-14}	1.31×10^{-13}
ΔX	ft.	1	1	1	6	1	10	4	1	1
ΔY	ft.	1	1	1	6	1	10	4	1	1

Table 4.2.1: Standard Deviations for the Busch Campus Garage Cell

Table 4.2.1 presents the concentrations estimated by the numerical solution along with their respective standard deviations.

Time (day)	Mean (µg/l)	Standard Deviation (µg/l)	Time (day)	Mean (µg/l)	Standard Deviation (µg/l)
1	4.56E+01	3.77E-02	51	3.39E-05	3.96E-06
2	1.02E+00	1.26E-01	52	3.84E-05	4.48E-06
3	4.00E-05	5.48E-06	53	4.35E-05	5.08E-06
4	6.80E-06	7.90E-07	54	4.93E-05	5.75E-06
5	2.86E-06	3.32E-07	55	5.59E-05	6.52E-06
6	1.68E-06	1.95E-07	56	6.34E-05	7.39E-06
7	1.19E-06	1.39E-07	57	7.19E-05	8.38E-06
8	9.51E-07	1.11E-07	58	8.15E-05	9.51E-06
9	8.22E-07	9.58E-08	59	9.25E-05	1.08E-05
10	7.52E-07	8.76E-08	60	1.05E-04	1.22E-05
11	7.16E-07	8.34E-08	61	1.19E-04	1.39E-05
12	7.02E-07	8.19E-08	62	1.35E-04	1.58E-05
13	7.05E-07	8.22E-08	63	1.54E-04	1.79E-05
14	7.21E-07	8.41E-08	64	1.74E-04	2.03E-05
15	7.48E-07	8.73E-08	65	1.98E-04	2.31E-05
16	7.86E-07	9.16E-08	66	2.25E-04	2.62E-05
17	8.33E-07	9.72E-08	67	2.55E-04	2.98E-05
18	8.91E-07	1.04E-07	68	2.90E-04	3.38E-05
19	9.59E-07	1.12E-07	69	3.30E-04	3.84E-05
20	1.04E-06	1.21E-07	70	3.75E-04	4.37E-05
21	1.13E-06	1.32E-07	71	4.26E-04	4.97E-05
22	1.24E-06	1.44E-07	72	4.84E-04	5.64E-05
23	1.35E-06	1.58E-07	73	5.50E-04	6.42E-05
24	1.49E-06	1.74E-07	74	6.26E-04	7.29E-05
25	1.65E-06	1.92E-07	75	7.11E-04	8.29E-05
26	1.82E-06	2.12E-07	76	8.08E-04	9.27E-05
27	2.02E-06	2.36E-07	77	9.18E-04	1.06E-04
28	2.25E-06	2.62E-07	78	1.05E-03	1.23E-04
29	2.50E-06	2.92E-07	79	1.18E-03	1.37E-04
30	2.79E-06	3.25E-07	80	1.36E-03	1.54E-04
31	3.11E-06	3.63E-07	81	1.54E-03	1.80E-04
32	3.48E-06	4.06E-07	82	1.75E-03	2.16E-04
33	3.90E-06	4.55E-07	83	2.00E-03	2.34E-04
34	4.37E-06	5.10E-07	84	2.28E-03	2.67E-04
35	4.91E-06	5.72E-07	85	2.58E-03	2.99E-04
36	5.51E-06	6.43E-07	86	2.94E-03	3.39E-04
37	6.20E-06	7.23E-07	87	3.34E-03	3.91E-04
38	6.97E-06	8.13E-07	88	3.82E-03	4.36E-04
39	7.85E-06	9.15E-07	89	4.33E-03	5.13E-04
40	8.84E-06	1.03E-06	90	4.94E-03	5.69E-04
41	9.97E-06	1.16E-06	91	5.63E-03	6.48E-04
42	1.12E-05	1.31E-06	92	6.39E-03	7.51E-04
43	1.27E-05	1.48E-06	93	7.27E-03	8.60E-04
44	1.43E-05	1.67E-06	94	8.29E-03	9.60E-04
45	1.62E-05	1.89E-06	95	9.43E-03	1.10E-03
46	1.83E-05	2.13E-06	96	1.07E-02	1.25E-03
47	2.07E-05	2.41E-06	97	1.22E-02	1.42E-03
48	2.34E-05	2.73E-06	98	1.39E-02	1.61E-03
49	2.65E-05	3.09E-06	99	1.59E-02	1.85E-03
50	3.00E-05	3.49E-06	100	1.81E-02	2.10E-03

Table 4.2.1: Standard Deviations for the Busch Campus Garage Cell Continued

Time (day)	Mean (µg/l)	Standard Deviation (µg/l)	Time (day)	Mean (µg/l)	Standard Deviation (µg/l)
101	2.06E-02	2.39E-03	151	6.80E+00	2.30E+00
102	2.34E-02	2.73E-03	152	7.29E+00	2.62E+00
103	2.67E-02	3.11E-03	153	7.80E+00	2.96E+00
104	3.04E-02	3.53E-03	154	8.33E+00	3.33E+00
105	3.46E-02	4.04E-03	155	8.87E+00	3.73E+00
106	3.94E-02	4.59E-03	156	9.43E+00	4.17E+00
107	4.49E-02	5.22E-03	157	1.00E+01	4.63E+00
108	5.12E-02	5.95E-03	158	1.06E+01	5.14E+00
109	5.83E-02	6.78E-03	159	1.12E+01	5.67E+00
110	6.64E-02	7.73E-03	160	1.18E+01	6.24E+00
111	7.57E-02	8.79E-03	161	1.24E+01	6.84E+00
112	8.62E-02	1.00E-02	162	1.30E+01	7.48E+00
113	9.82E-02	1.14E-02	163	1.37E+01	8.15E+00
114	1.12E-01	1.30E-02	164	1.43E+01	8.86E+00
115	1.28E-01	1.48E-02	165	1.50E+01	9.60E+00
116	1.45E-01	1.68E-02	166	1.56E+01	1.04E+01
117	1.65E-01	1.92E-02	167	1.63E+01	1.12E+01
118	1.88E-01	2.18E-02	168	1.69E+01	1.20E+01
119	2.15E-01	2.48E-02	169	1.76E+01	1.29E+01
120	2.44E-01	2.83E-02	170	1.82E+01	1.38E+01
121	2.78E-01	3.22E-02	171	1.89E+01	1.47E+01
122	3.16E-01	3.66E-02	172	1.95E+01	1.56E+01
123	3.60E-01	4.17E-02	173	2.02E+01	1.66E+01
124	4.09E-01	4.74E-02	174	2.08E+01	1.76E+01
125	4.64E-01	5.39E-02	175	2.15E+01	1.87E+01
126	5.27E-01	6.14E-02	176	2.21E+01	1.97E+01
127	5.97E-01	6.98E-02	177	2.28E+01	2.08E+01
128	6.77E-01	7.95E-02	178	2.34E+01	2.19E+01
129	7.66E-01	9.06E-02	179	2.41E+01	2.30E+01
130	8.65E-01	1.03E-01	180	2.47E+01	2.41E+01
131	9.76E-01	1.18E-01	181	2.53E+01	2.53E+01
132	1.10E+00	1.35E-01	182	2.60E+01	2.64E+01
133	1.24E+00	1.55E-01	183	2.66E+01	2.76E+01
134	1.39E+00	1.79E-01	184	2.72E+01	2.88E+01
135	1.56E+00	2.07E-01	185	2.78E+01	3.00E+01
136	1.74E+00	2.40E-01	186	2.84E+01	3.13E+01
137	1.94E+00	2.80E-01	187	2.90E+01	3.25E+01
138	2.16E+00	3.27E-01	188	2.96E+01	3.37E+01
139	2.40E+00	3.83E-01	189	3.02E+01	3.50E+01
140	2.65E+00	4.49E-01	190	3.08E+01	3.63E+01
141	2.93E+00	5.27E-01	191	3.14E+01	3.76E+01
142	3.22E+00	6.18E-01	192	3.20E+01	3.88E+01
143	3.54E+00	7.24E-01	193	3.26E+01	4.01E+01
144	3.88E+00	8.47E-01	194	3.31E+01	4.15E+01
145	4.23E+00	9.88E-01	195	3.37E+01	4.28E+01
146	4.61E+00	1.15E+00	196	3.43E+01	4.41E+01
147	5.01E+00	1.33E+00	197	3.48E+01	4.54E+01
148	5.43E+00	1.54E+00	198	3.54E+01	4.67E+01
149	5.87E+00	1.77E+00	199	3.59E+01	4.81E+01
150	6.32E+00	2.02E+00	200	3.65E+01	4.94E+01

Table 4.2.1: Standard Deviations for the Busch Campus Garage Cell Continued

Time (day)	Mean (µg/l)	Standard Deviation (µg/l)	Time (day)	Mean (µg/l)	Standard Deviation (µg/l)
201	3.70E+01	5.08E+01	251	6.12E+01	1.21E+02
202	3.75E+01	5.21E+01	252	6.16E+01	1.22E+02
203	3.81E+01	5.35E+01	253	6.21E+01	1.24E+02
204	3.86E+01	5.48E+01	254	6.25E+01	1.25E+02
205	3.91E+01	5.62E+01	255	6.30E+01	1.26E+02
206	3.97E+01	5.76E+01	256	6.34E+01	1.28E+02
207	4.02E+01	5.89E+01	257	6.38E+01	1.29E+02
208	4.07E+01	6.03E+01	258	6.43E+01	1.31E+02
209	4.12E+01	6.17E+01	259	6.47E+01	1.32E+02
210	4.17E+01	6.31E+01	260	6.52E+01	1.33E+02
211	4.22E+01	6.44E+01	261	6.56E+01	1.35E+02
212	4.27E+01	6.58E+01	262	6.61E+01	1.36E+02
213	4.33E+01	6.72E+01	263	6.65E+01	1.38E+02
214	4.38E+01	6.86E+01	264	6.69E+01	1.39E+02
215	4.43E+01	7.00E+01	265	6.74E+01	1.41E+02
216	4.48E+01	7.14E+01	266	6.78E+01	1.42E+02
217	4.52E+01	7.28E+01	267	6.82E+01	1.43E+02
218	4.57E+01	7.42E+01	268	6.87E+01	1.45E+02
219	4.62E+01	7.56E+01	269	6.91E+01	1.46E+02
220	4.67E+01	7.70E+01	270	6.95E+01	1.48E+02
221	4.72E+01	7.84E+01	271	7.00E+01	1.49E+02
222	4.77E+01	7.98E+01	272	7.04E+01	1.50E+02
223	4.82E+01	8.12E+01	273	7.08E+01	1.52E+02
224	4.87E+01	8.26E+01	274	7.13E+01	1.53E+02
225	4.91E+01	8.40E+01	275	7.17E+01	1.55E+02
226	4.96E+01	8.54E+01	276	7.21E+01	1.56E+02
227	5.01E+01	8.68E+01	277	7.25E+01	1.57E+02
228	5.06E+01	8.82E+01	278	7.30E+01	1.59E+02
229	5.10E+01	8.96E+01	279	7.34E+01	1.60E+02
230	5.15E+01	9.10E+01	280	7.38E+01	1.62E+02
231	5.20E+01	9.24E+01	281	7.42E+01	1.63E+02
232	5.25E+01	9.38E+01	282	7.47E+01	1.64E+02
233	5.29E+01	9.53E+01	283	7.51E+01	1.66E+02
234	5.34E+01	9.67E+01	284	7.55E+01	1.67E+02
235	5.39E+01	9.81E+01	285	7.59E+01	1.68E+02
236	5.43E+01	9.95E+01	286	7.63E+01	1.70E+02
237	5.48E+01	1.01E+02	287	7.67E+01	1.71E+02
238	5.53E+01	1.02E+02	288	7.72E+01	1.73E+02
239	5.57E+01	1.04E+02	289	7.76E+01	1.74E+02
240	5.62E+01	1.05E+02	290	7.80E+01	1.75E+02
241	5.66E+01	1.07E+02	291	7.84E+01	1.77E+02
242	5.71E+01	1.08E+02	292	7.88E+01	1.78E+02
243	5.76E+01	1.09E+02	293	7.92E+01	1.79E+02
244	5.80E+01	1.11E+02	294	7.97E+01	1.81E+02
245	5.85E+01	1.12E+02	295	8.01E+01	1.82E+02
246	5.89E+01	1.14E+02	296	8.05E+01	1.84E+02
247	5.94E+01	1.15E+02	297	8.09E+01	1.85E+02
248	5.98E+01	1.16E+02	298	8.13E+01	1.86E+02
249	6.03E+01	1.18E+02	299	8.17E+01	1.88E+02
250	6.07E+01	1.19E+02	300	8.21E+01	1.89E+02

Table 4.2.1: Standard Deviations for the Busch Campus Garage Cell Continued

Time (day)	Mean (µg/l)	Standard Deviation (µg/l)	Time (day)	Mean (µg/l)	Standard Deviation (µg/l)
301	8.25E+01	1.90E+02	351	1.02E+02	2.56E+02
302	8.29E+01	1.92E+02	352	1.02E+02	2.57E+02
303	8.33E+01	1.93E+02	353	1.02E+02	2.58E+02
304	8.37E+01	1.94E+02	354	1.03E+02	2.60E+02
305	8.41E+01	1.96E+02	355	1.03E+02	2.61E+02
306	8.45E+01	1.97E+02	356	1.04E+02	2.62E+02
307	8.49E+01	1.99E+02	357	1.04E+02	2.63E+02
308	8.53E+01	2.00E+02	358	1.04E+02	2.65E+02
309	8.57E+01	2.01E+02	359	1.05E+02	2.66E+02
310	8.61E+01	2.03E+02	360	1.05E+02	2.67E+02
311	8.65E+01	2.04E+02	361	1.05E+02	2.68E+02
312	8.69E+01	2.05E+02	362	1.06E+02	2.70E+02
313	8.73E+01	2.07E+02	363	1.06E+02	2.71E+02
314	8.77E+01	2.08E+02	364	1.06E+02	2.72E+02
315	8.81E+01	2.09E+02	365	1.07E+02	2.73E+02
316	8.85E+01	2.11E+02	366	1.07E+02	2.75E+02
317	8.89E+01	2.12E+02	367	1.07E+02	2.76E+02
318	8.93E+01	2.13E+02	368	1.08E+02	2.77E+02
319	8.97E+01	2.15E+02	369	1.08E+02	2.78E+02
320	9.01E+01	2.16E+02	370	1.08E+02	2.79E+02
321	9.04E+01	2.17E+02	371	1.09E+02	2.81E+02
322	9.08E+01	2.19E+02	372	1.09E+02	2.82E+02
323	9.12E+01	2.20E+02	373	1.10E+02	2.83E+02
324	9.16E+01	2.21E+02	374	1.10E+02	2.84E+02
325	9.20E+01	2.22E+02	375	1.10E+02	2.86E+02
326	9.24E+01	2.24E+02	376	1.11E+02	2.87E+02
327	9.28E+01	2.25E+02	377	1.11E+02	2.88E+02
328	9.31E+01	2.26E+02	378	1.11E+02	2.89E+02
329	9.35E+01	2.28E+02	379	1.12E+02	2.90E+02
330	9.39E+01	2.29E+02	380	1.12E+02	2.92E+02
331	9.43E+01	2.30E+02	381	1.12E+02	2.93E+02
332	9.47E+01	2.32E+02	382	1.13E+02	2.94E+02
333	9.50E+01	2.33E+02	383	1.13E+02	2.95E+02
334	9.54E+01	2.34E+02	384	1.13E+02	2.96E+02
335	9.58E+01	2.36E+02	385	1.14E+02	2.98E+02
336	9.62E+01	2.37E+02	386	1.14E+02	2.99E+02
337	9.66E+01	2.38E+02	387	1.14E+02	3.00E+02
338	9.69E+01	2.39E+02	388	1.15E+02	3.01E+02
339	9.73E+01	2.41E+02	389	1.15E+02	3.02E+02
340	9.77E+01	2.42E+02	390	1.15E+02	3.03E+02
341	9.80E+01	2.43E+02	391	1.16E+02	3.05E+02
342	9.84E+01	2.45E+02	392	1.16E+02	3.06E+02
343	9.88E+01	2.46E+02	393	1.16E+02	3.07E+02
344	9.92E+01	2.47E+02	394	1.17E+02	3.08E+02
345	9.95E+01	2.48E+02	395	1.17E+02	3.09E+02
346	9.99E+01	2.50E+02	396	1.17E+02	3.11E+02
347	1.00E+02	2.51E+02	397	1.18E+02	3.12E+02
348	1.01E+02	2.52E+02	398	1.18E+02	3.13E+02
349	1.01E+02	2.53E+02	399	1.18E+02	3.14E+02
350	1.01E+02	2.55E+02	400	1.19E+02	3.15E+02

Table 4.2.1: Standard Deviations for the Busch Campus Garage Cell Continued

Time (day)	Mean (µg/l)	Standard Deviation (µg/l)	Time (day)	Mean (µg/l)	Standard Deviation (µg/l)
401	1.19E+02	3.16E+02	451	1.34E+02	3.72E+02
402	1.19E+02	3.17E+02	452	1.35E+02	3.73E+02
403	1.20E+02	3.19E+02	453	1.35E+02	3.74E+02
404	1.20E+02	3.20E+02	454	1.35E+02	3.75E+02
405	1.20E+02	3.21E+02	455	1.36E+02	3.76E+02
406	1.21E+02	3.22E+02	456	1.36E+02	3.78E+02
407	1.21E+02	3.23E+02	457	1.36E+02	3.78E+02
408	1.21E+02	3.24E+02	458	1.36E+02	3.79E+02
409	1.21E+02	3.26E+02	459	1.37E+02	3.81E+02
410	1.22E+02	3.27E+02	460	1.37E+02	3.82E+02
411	1.22E+02	3.28E+02	461	1.37E+02	3.83E+02
412	1.22E+02	3.29E+02	462	1.38E+02	3.84E+02
413	1.23E+02	3.30E+02	463	1.38E+02	3.85E+02
414	1.23E+02	3.31E+02	464	1.38E+02	3.86E+02
415	1.23E+02	3.32E+02	465	1.38E+02	3.87E+02
416	1.24E+02	3.33E+02	466	1.39E+02	3.88E+02
417	1.24E+02	3.35E+02	467	1.39E+02	3.89E+02
418	1.24E+02	3.36E+02	468	1.39E+02	3.90E+02
419	1.25E+02	3.37E+02	469	1.40E+02	3.91E+02
420	1.25E+02	3.38E+02	470	1.40E+02	3.92E+02
421	1.25E+02	3.39E+02	471	1.40E+02	3.93E+02
422	1.26E+02	3.40E+02	472	1.40E+02	3.94E+02
423	1.26E+02	3.41E+02	473	1.41E+02	3.95E+02
424	1.26E+02	3.42E+02	474	1.41E+02	3.96E+02
425	1.27E+02	3.44E+02	475	1.41E+02	3.97E+02
426	1.27E+02	3.45E+02	476	1.42E+02	3.98E+02
427	1.27E+02	3.46E+02	477	1.42E+02	3.99E+02
428	1.27E+02	3.47E+02	478	1.42E+02	4.00E+02
429	1.28E+02	3.48E+02	479	1.42E+02	4.01E+02
430	1.28E+02	3.49E+02	480	1.43E+02	4.03E+02
431	1.28E+02	3.50E+02	481	1.43E+02	4.04E+02
432	1.29E+02	3.51E+02	482	1.43E+02	4.05E+02
433	1.29E+02	3.52E+02	483	1.44E+02	4.06E+02
434	1.29E+02	3.54E+02	484	1.44E+02	4.07E+02
435	1.30E+02	3.55E+02	485	1.44E+02	4.08E+02
436	1.30E+02	3.56E+02	486	1.44E+02	4.09E+02
437	1.30E+02	3.57E+02	487	1.45E+02	4.10E+02
438	1.30E+02	3.58E+02	488	1.45E+02	4.11E+02
439	1.31E+02	3.59E+02	489	1.45E+02	4.12E+02
440	1.31E+02	3.60E+02	490	1.45E+02	4.13E+02
441	1.31E+02	3.61E+02	491	1.46E+02	4.14E+02
442	1.32E+02	3.62E+02	492	1.46E+02	4.15E+02
443	1.32E+02	3.63E+02	493	1.46E+02	4.16E+02
444	1.32E+02	3.63E+02	494	1.47E+02	4.17E+02
445	1.32E+02	3.64E+02	495	1.47E+02	4.18E+02
446	1.33E+02	3.67E+02	496	1.47E+02	4.19E+02
447	1.33E+02	3.68E+02	497	1.47E+02	4.20E+02
448	1.33E+02	3.69E+02	498	1.48E+02	4.21E+02
449	1.34E+02	3.70E+02	499	1.48E+02	4.22E+02
450	1.34E+02	3.71E+02	500	1.48E+02	4.23E+02

Table 4.2.2: Standard Deviations for the Cape Canaveral 2S Cell

Table 4.2.2 presents the concentrations estimated by the numerical solution along with their respective standard deviations.

Time (day)	Mean (µg/l)	Standard Deviation (µg/l)	Time (day)	Mean (µg/l)	Standard Deviation (µg/l)
1	1.26E+06	1.09E+05	51	6.34E-06	2.33E-06
2	4.99E+05	2.56E+05	52	6.24E-06	2.28E-06
3	1.90E+04	1.56E+04	53	6.14E-06	2.24E-06
4	8.25E+02	1.05E+03	54	6.06E-06	2.20E-06
5	3.04E+01	4.56E+01	55	5.98E-06	2.17E-06
6	8.67E-01	1.69E+00	56	5.92E-06	2.14E-06
7	3.36E-02	7.71E-02	57	5.86E-06	2.11E-06
8	1.41E-03	2.72E-03	58	5.80E-06	2.09E-06
9	3.70E-04	2.19E-04	59	5.75E-06	2.07E-06
10	2.74E-04	1.45E-04	60	5.70E-06	2.05E-06
11	2.32E-04	1.23E-04	61	5.66E-06	2.03E-06
12	2.02E-04	1.07E-04	62	5.62E-06	2.02E-06
13	1.80E-04	9.56E-05	63	5.58E-06	2.00E-06
14	1.63E-04	8.66E-05	64	5.54E-06	1.99E-06
15	1.50E-04	7.95E-05	65	5.51E-06	1.98E-06
16	1.39E-04	7.37E-05	66	5.48E-06	1.96E-06
17	1.30E-04	6.89E-05	67	5.45E-06	1.95E-06
18	1.22E-04	6.49E-05	68	5.42E-06	1.94E-06
19	1.16E-04	6.14E-05	69	5.39E-06	1.93E-06
20	1.10E-04	5.83E-05	70	5.37E-06	1.92E-06
21	1.04E-04	5.54E-05	71	5.34E-06	1.91E-06
22	9.87E-05	5.25E-05	72	5.32E-06	1.91E-06
23	9.28E-05	4.97E-05	73	5.30E-06	1.90E-06
24	8.65E-05	4.69E-05	74	5.27E-06	1.89E-06
25	7.96E-05	4.41E-05	75	5.25E-06	1.88E-06
26	7.21E-05	4.10E-05	76	5.23E-06	1.87E-06
27	6.43E-05	3.77E-05	77	5.21E-06	1.87E-06
28	5.64E-05	3.40E-05	78	5.20E-06	1.86E-06
29	4.87E-05	3.01E-05	79	5.18E-06	1.85E-06
30	4.14E-05	2.61E-05	80	5.16E-06	1.85E-06
31	3.49E-05	2.22E-05	81	5.15E-06	1.84E-06
32	2.93E-05	1.85E-05	82	5.13E-06	1.84E-06
33	2.46E-05	1.53E-05	83	5.11E-06	1.83E-06
34	2.08E-05	1.26E-05	84	5.10E-06	1.83E-06
35	1.77E-05	1.04E-05	85	5.09E-06	1.82E-06
36	1.53E-05	8.61E-06	86	5.07E-06	1.82E-06
37	1.35E-05	7.19E-06	87	5.06E-06	1.81E-06
38	1.20E-05	6.08E-06	88	5.04E-06	1.81E-06
39	1.08E-05	5.22E-06	89	5.03E-06	1.80E-06
40	9.90E-06	4.55E-06	90	5.02E-06	1.80E-06
41	9.18E-06	4.04E-06	91	5.01E-06	1.79E-06
42	8.59E-06	3.64E-06	92	5.00E-06	1.79E-06
43	8.12E-06	3.33E-06	93	4.98E-06	1.78E-06
44	7.74E-06	3.09E-06	94	4.97E-06	1.78E-06
45	7.43E-06	2.90E-06	95	4.96E-06	1.78E-06
46	7.17E-06	2.75E-06	96	4.95E-06	1.77E-06
47	6.94E-06	2.63E-06	97	4.94E-06	1.77E-06
48	6.76E-06	2.53E-06	98	4.93E-06	1.76E-06
49	6.60E-06	2.45E-06	99	4.92E-06	1.76E-06
50	6.46E-06	2.38E-06	100	4.91E-06	1.76E-06

Table 4.2.2: Standard Deviations for the Cape Canaveral 2S Cell Continued

Time (day)	Mean (µg/l)	Standard Deviation (µg/l)	Time (day)	Mean (µg/l)	Standard Deviation (µg/l)
101	4.90E-06	1.75E-06	151	4.61E-06	1.65E-06
102	4.89E-06	1.75E-06	152	4.61E-06	1.65E-06
103	4.89E-06	1.75E-06	153	4.61E-06	1.65E-06
104	4.88E-06	1.74E-06	154	4.60E-06	1.65E-06
105	4.87E-06	1.74E-06	155	4.60E-06	1.64E-06
106	4.86E-06	1.74E-06	156	4.60E-06	1.64E-06
107	4.85E-06	1.74E-06	157	4.59E-06	1.64E-06
108	4.84E-06	1.73E-06	158	4.59E-06	1.64E-06
109	4.84E-06	1.73E-06	159	4.58E-06	1.64E-06
110	4.83E-06	1.73E-06	160	4.58E-06	1.64E-06
111	4.82E-06	1.72E-06	161	4.58E-06	1.64E-06
112	4.81E-06	1.72E-06	162	4.58E-06	1.64E-06
113	4.81E-06	1.72E-06	163	4.57E-06	1.63E-06
114	4.80E-06	1.72E-06	164	4.57E-06	1.63E-06
115	4.79E-06	1.71E-06	165	4.57E-06	1.63E-06
116	4.79E-06	1.71E-06	166	4.56E-06	1.63E-06
117	4.78E-06	1.71E-06	167	4.56E-06	1.63E-06
118	4.77E-06	1.71E-06	168	4.56E-06	1.63E-06
119	4.77E-06	1.70E-06	169	4.55E-06	1.63E-06
120	4.76E-06	1.70E-06	170	4.55E-06	1.63E-06
121	4.75E-06	1.70E-06	171	4.55E-06	1.63E-06
122	4.75E-06	1.70E-06	172	4.55E-06	1.62E-06
123	4.74E-06	1.70E-06	173	4.54E-06	1.62E-06
124	4.74E-06	1.69E-06	174	4.54E-06	1.62E-06
125	4.73E-06	1.69E-06	175	4.54E-06	1.62E-06
126	4.73E-06	1.69E-06	176	4.53E-06	1.62E-06
127	4.72E-06	1.69E-06	177	4.53E-06	1.62E-06
128	4.72E-06	1.69E-06	178	4.53E-06	1.62E-06
129	4.71E-06	1.68E-06	179	4.53E-06	1.62E-06
130	4.70E-06	1.68E-06	180	4.52E-06	1.62E-06
131	4.70E-06	1.68E-06	181	4.52E-06	1.62E-06
132	4.69E-06	1.68E-06	182	4.52E-06	1.62E-06
133	4.69E-06	1.68E-06	183	4.52E-06	1.61E-06
134	4.68E-06	1.68E-06	184	4.51E-06	1.61E-06
135	4.68E-06	1.67E-06	185	4.51E-06	1.61E-06
136	4.68E-06	1.67E-06	186	4.51E-06	1.61E-06
137	4.67E-06	1.67E-06	187	4.51E-06	1.61E-06
138	4.67E-06	1.67E-06	188	4.50E-06	1.61E-06
139	4.66E-06	1.67E-06	189	4.50E-06	1.61E-06
140	4.66E-06	1.67E-06	190	4.50E-06	1.61E-06
141	4.65E-06	1.66E-06	191	4.50E-06	1.61E-06
142	4.65E-06	1.66E-06	192	4.50E-06	1.61E-06
143	4.64E-06	1.66E-06	193	4.49E-06	1.61E-06
144	4.64E-06	1.66E-06	194	4.49E-06	1.61E-06
145	4.64E-06	1.66E-06	195	4.49E-06	1.60E-06
146	4.63E-06	1.66E-06	196	4.49E-06	1.60E-06
147	4.63E-06	1.65E-06	197	4.48E-06	1.60E-06
148	4.62E-06	1.65E-06	198	4.48E-06	1.60E-06
149	4.62E-06	1.65E-06	199	4.48E-06	1.60E-06
150	4.62E-06	1.65E-06	200	4.48E-06	1.60E-06

Table 4.2.2: Standard Deviations for the Cape Canaveral 2S Cell Continued

Time (day)	Mean (µg/l)	Standard Deviation (µg/l)	Time (day)	Mean (µg/l)	Standard Deviation (µg/l)
201	4.48E-06	1.60E-06	251	4.39E-06	1.58E-06
202	4.47E-06	1.60E-06	252	4.39E-06	1.58E-06
203	4.47E-06	1.60E-06	253	4.39E-06	1.58E-06
204	4.47E-06	1.60E-06	254	4.39E-06	1.58E-06
205	4.47E-06	1.60E-06	255	4.39E-06	1.58E-06
206	4.47E-06	1.60E-06	256	4.38E-06	1.57E-06
207	4.46E-06	1.60E-06	257	4.38E-06	1.57E-06
208	4.46E-06	1.60E-06	258	4.38E-06	1.57E-06
209	4.46E-06	1.59E-06	259	4.38E-06	1.57E-06
210	4.46E-06	1.59E-06	260	4.38E-06	1.57E-06
211	4.46E-06	1.59E-06	261	4.38E-06	1.57E-06
212	4.45E-06	1.59E-06	262	4.38E-06	1.57E-06
213	4.45E-06	1.60E-06	263	4.38E-06	1.57E-06
214	4.45E-06	1.60E-06	264	4.38E-06	1.57E-06
215	4.44E-06	1.60E-06	265	4.37E-06	1.57E-06
216	4.44E-06	1.60E-06	266	4.37E-06	1.57E-06
217	4.44E-06	1.60E-06	267	4.37E-06	1.57E-06
218	4.44E-06	1.59E-06	268	4.37E-06	1.57E-06
219	4.44E-06	1.59E-06	269	4.37E-06	1.57E-06
220	4.44E-06	1.59E-06	270	4.37E-06	1.57E-06
221	4.43E-06	1.59E-06	271	4.37E-06	1.57E-06
222	4.43E-06	1.59E-06	272	4.37E-06	1.57E-06
223	4.43E-06	1.59E-06	273	4.37E-06	1.57E-06
224	4.43E-06	1.59E-06	274	4.36E-06	1.57E-06
225	4.43E-06	1.59E-06	275	4.36E-06	1.57E-06
226	4.43E-06	1.59E-06	276	4.36E-06	1.57E-06
227	4.42E-06	1.59E-06	277	4.36E-06	1.57E-06
228	4.42E-06	1.59E-06	278	4.36E-06	1.57E-06
229	4.42E-06	1.59E-06	279	4.36E-06	1.57E-06
230	4.42E-06	1.59E-06	280	4.36E-06	1.57E-06
231	4.42E-06	1.59E-06	281	4.36E-06	1.57E-06
232	4.42E-06	1.59E-06	282	4.36E-06	1.56E-06
233	4.42E-06	1.59E-06	283	4.36E-06	1.56E-06
234	4.41E-06	1.59E-06	284	4.35E-06	1.56E-06
235	4.41E-06	1.59E-06	285	4.35E-06	1.56E-06
236	4.41E-06	1.58E-06	286	4.35E-06	1.56E-06
237	4.41E-06	1.58E-06	287	4.35E-06	1.56E-06
238	4.41E-06	1.58E-06	288	4.35E-06	1.56E-06
239	4.41E-06	1.58E-06	289	4.35E-06	1.56E-06
240	4.41E-06	1.58E-06	290	4.35E-06	1.56E-06
241	4.40E-06	1.58E-06	291	4.35E-06	1.56E-06
242	4.40E-06	1.58E-06	292	4.35E-06	1.56E-06
243	4.40E-06	1.58E-06	293	4.35E-06	1.56E-06
244	4.40E-06	1.58E-06	294	4.35E-06	1.56E-06
245	4.40E-06	1.58E-06	295	4.34E-06	1.56E-06
246	4.40E-06	1.58E-06	296	4.34E-06	1.57E-06
247	4.40E-06	1.58E-06	297	4.34E-06	1.57E-06
248	4.39E-06	1.58E-06	298	4.34E-06	1.57E-06
249	4.39E-06	1.58E-06	299	4.34E-06	1.56E-06
250	4.39E-06	1.58E-06	300	4.34E-06	1.56E-06

Table 4.2.2: Standard Deviations for the Cape Canaveral 2S Cell Continued

Time (day)	Mean (µg/l)	Standard Deviation (µg/l)	Time (day)	Mean (µg/l)	Standard Deviation (µg/l)
301	4.33E-06	1.56E-06	351	4.30E-06	1.55E-06
302	4.33E-06	1.56E-06	352	4.30E-06	1.55E-06
303	4.33E-06	1.56E-06	353	4.30E-06	1.55E-06
304	4.33E-06	1.56E-06	354	4.30E-06	1.55E-06
305	4.33E-06	1.56E-06	355	4.30E-06	1.55E-06
306	4.33E-06	1.56E-06	356	4.30E-06	1.55E-06
307	4.33E-06	1.56E-06	357	4.29E-06	1.55E-06
308	4.33E-06	1.56E-06	358	4.29E-06	1.55E-06
309	4.33E-06	1.56E-06	359	4.29E-06	1.55E-06
310	4.33E-06	1.56E-06	360	4.29E-06	1.55E-06
311	4.33E-06	1.56E-06	361	4.29E-06	1.55E-06
312	4.33E-06	1.56E-06	362	4.29E-06	1.55E-06
313	4.33E-06	1.56E-06	363	4.29E-06	1.55E-06
314	4.32E-06	1.56E-06	364	4.29E-06	1.55E-06
315	4.32E-06	1.56E-06	365	4.29E-06	1.55E-06
316	4.32E-06	1.56E-06	366	4.29E-06	1.55E-06
317	4.32E-06	1.56E-06	367	4.29E-06	1.55E-06
318	4.32E-06	1.56E-06	368	4.29E-06	1.55E-06
319	4.32E-06	1.56E-06	369	4.29E-06	1.55E-06
320	4.32E-06	1.56E-06	370	4.29E-06	1.55E-06
321	4.32E-06	1.56E-06	371	4.29E-06	1.55E-06
322	4.32E-06	1.56E-06	372	4.29E-06	1.55E-06
323	4.32E-06	1.56E-06	373	4.29E-06	1.55E-06
324	4.32E-06	1.56E-06	374	4.28E-06	1.55E-06
325	4.32E-06	1.56E-06	375	4.28E-06	1.55E-06
326	4.32E-06	1.56E-06	376	4.28E-06	1.55E-06
327	4.31E-06	1.56E-06	377	4.28E-06	1.55E-06
328	4.31E-06	1.56E-06	378	4.28E-06	1.55E-06
329	4.31E-06	1.56E-06	379	4.28E-06	1.55E-06
330	4.31E-06	1.56E-06	380	4.28E-06	1.54E-06
331	4.31E-06	1.56E-06	381	4.28E-06	1.54E-06
332	4.31E-06	1.56E-06	382	4.28E-06	1.54E-06
333	4.31E-06	1.56E-06	383	4.28E-06	1.54E-06
334	4.31E-06	1.56E-06	384	4.28E-06	1.54E-06
335	4.31E-06	1.55E-06	385	4.28E-06	1.54E-06
336	4.31E-06	1.55E-06	386	4.28E-06	1.54E-06
337	4.31E-06	1.55E-06	387	4.28E-06	1.54E-06
338	4.31E-06	1.55E-06	388	4.28E-06	1.54E-06
339	4.31E-06	1.55E-06	389	4.28E-06	1.54E-06
340	4.31E-06	1.55E-06	390	4.28E-06	1.54E-06
341	4.30E-06	1.55E-06	391	4.28E-06	1.54E-06
342	4.30E-06	1.55E-06	392	4.28E-06	1.54E-06
343	4.30E-06	1.55E-06	393	4.27E-06	1.54E-06
344	4.30E-06	1.55E-06	394	4.27E-06	1.54E-06
345	4.30E-06	1.55E-06	395	4.27E-06	1.54E-06
346	4.30E-06	1.55E-06	396	4.27E-06	1.54E-06
347	4.30E-06	1.55E-06	397	4.27E-06	1.54E-06
348	4.30E-06	1.55E-06	398	4.27E-06	1.54E-06
349	4.30E-06	1.55E-06	399	4.27E-06	1.54E-06
350	4.30E-06	1.55E-06	400	4.27E-06	1.54E-06

Table 4.2.2: Standard Deviations for the Cape Canaveral 2S Cell Continued

Time (day)	Mean (µg/l)	Standard Deviation (µg/l)	Time (day)	Mean (µg/l)	Standard Deviation (µg/l)
401	4.27E-06	1.54E-06	451	5.37E-06	1.65E-05
402	4.27E-06	1.54E-06	452	5.16E-06	1.34E-05
403	4.27E-06	1.54E-06	453	5.04E-06	1.17E-05
404	4.27E-06	1.54E-06	454	4.95E-06	1.04E-05
405	4.27E-06	1.54E-06	455	4.88E-06	9.40E-06
406	4.27E-06	1.54E-06	456	4.83E-06	8.62E-06
407	4.27E-06	1.54E-06	457	4.78E-06	7.99E-06
408	4.27E-06	1.54E-06	458	4.75E-06	7.48E-06
409	4.27E-06	1.54E-06	459	4.72E-06	7.04E-06
410	4.27E-06	1.54E-06	460	4.69E-06	6.66E-06
411	4.27E-06	1.54E-06	461	4.66E-06	6.30E-06
412	4.27E-06	1.54E-06	462	4.64E-06	5.94E-06
413	4.27E-06	1.54E-06	463	4.61E-06	5.54E-06
414	4.26E-06	1.54E-06	464	4.55E-06	4.66E-06
415	4.26E-06	1.54E-06	465	4.55E-06	4.66E-06
416	4.26E-06	1.54E-06	466	4.51E-06	4.24E-06
417	4.26E-06	1.54E-06	467	4.48E-06	3.86E-06
418	4.26E-06	1.54E-06	468	4.45E-06	3.52E-06
419	4.26E-06	1.54E-06	469	4.42E-06	3.21E-06
420	4.26E-06	1.54E-06	470	4.40E-06	2.91E-06
421	4.26E-06	1.54E-06	471	4.37E-06	2.63E-06
422	4.26E-06	1.54E-06	472	4.35E-06	2.38E-06
423	4.26E-06	1.54E-06	473	4.33E-06	2.17E-06
424	4.26E-06	1.54E-06	474	4.32E-06	1.99E-06
425	4.26E-06	1.54E-06	475	4.30E-06	1.85E-06
426	4.26E-06	1.54E-06	476	4.29E-06	1.75E-06
427	4.26E-06	1.54E-06	477	4.28E-06	1.68E-06
428	4.26E-06	1.54E-06	478	4.28E-06	1.63E-06
429	4.26E-06	1.54E-06	479	4.27E-06	1.60E-06
430	4.26E-06	1.54E-06	480	4.27E-06	1.58E-06
431	4.26E-06	1.54E-06	481	4.26E-06	1.56E-06
432	4.26E-06	1.54E-06	482	4.26E-06	1.55E-06
433	4.26E-06	1.54E-06	483	4.26E-06	1.55E-06
434	4.26E-06	1.54E-06	484	4.25E-06	1.54E-06
435	4.26E-06	1.54E-06	485	4.25E-06	1.54E-06
436	4.26E-06	1.54E-06	486	4.25E-06	1.54E-06
437	4.26E-06	1.54E-06	487	4.25E-06	1.53E-06
438	4.25E-06	1.54E-06	488	4.25E-06	1.53E-06
439	4.25E-06	1.54E-06	489	4.25E-06	1.53E-06
440	4.25E-06	1.54E-06	490	4.25E-06	1.53E-06
441	4.25E-06	1.53E-06	491	4.24E-06	1.53E-06
442	6.34E+03	8.95E+04	492	4.24E-06	1.53E-06
443	2.42E+03	4.28E+04	493	4.24E-06	1.53E-06
444	1.21E+02	2.56E+03	494	4.24E-06	1.53E-06
445	7.39E+00	1.87E+02	495	4.24E-06	1.53E-06
446	3.30E-01	8.89E+00	496	4.24E-06	1.53E-06
447	1.31E-02	3.81E-01	497	4.24E-06	1.53E-06
448	6.40E-04	1.91E-02	498	4.24E-06	1.53E-06
449	2.94E-05	7.34E-04	499	4.24E-06	1.53E-06
450	6.68E-06	4.73E-05	500	4.24E-06	1.53E-06

Table 4.2.2: Standard Deviations for the Cape Canaveral 2S Cell Continued

Time (day)	Mean (µg/l)	Standard Deviation (µg/l)	Time (day)	Mean (µg/l)	Standard Deviation (µg/l)
501	4.24E-06	1.53E-06	551	4.22E-06	1.52E-06
502	4.24E-06	1.53E-06	552	4.22E-06	1.52E-06
503	4.24E-06	1.53E-06	553	4.22E-06	1.52E-06
504	4.24E-06	1.53E-06	554	4.22E-06	1.52E-06
505	4.24E-06	1.53E-06	555	4.22E-06	1.52E-06
506	4.24E-06	1.53E-06	556	4.22E-06	1.52E-06
507	4.24E-06	1.53E-06	557	4.22E-06	1.52E-06
508	4.23E-06	1.53E-06	558	4.22E-06	1.52E-06
509	4.23E-06	1.53E-06	559	4.22E-06	1.52E-06
510	4.23E-06	1.53E-06	560	4.22E-06	1.52E-06
511	4.23E-06	1.53E-06	561	4.22E-06	1.52E-06
512	4.23E-06	1.53E-06	562	4.22E-06	1.52E-06
513	4.23E-06	1.53E-06	563	4.22E-06	1.52E-06
514	4.23E-06	1.53E-06	564	4.22E-06	1.52E-06
515	4.23E-06	1.53E-06	565	4.22E-06	1.52E-06
516	4.23E-06	1.53E-06	566	4.22E-06	1.52E-06
517	4.23E-06	1.53E-06	567	4.22E-06	1.52E-06
518	4.23E-06	1.53E-06	568	4.22E-06	1.52E-06
519	4.23E-06	1.53E-06	569	4.22E-06	1.52E-06
520	4.23E-06	1.53E-06	570	4.22E-06	1.52E-06
521	4.23E-06	1.53E-06			
522	4.23E-06	1.53E-06			
523	4.23E-06	1.53E-06			
524	4.23E-06	1.53E-06			
525	4.23E-06	1.53E-06			
526	4.23E-06	1.53E-06			
527	4.23E-06	1.53E-06			
528	4.23E-06	1.52E-06			
529	4.23E-06	1.52E-06			
530	4.23E-06	1.52E-06			
531	4.23E-06	1.52E-06			
532	4.23E-06	1.52E-06			
533	4.23E-06	1.52E-06			
534	4.23E-06	1.52E-06			
535	4.23E-06	1.52E-06			
536	4.23E-06	1.52E-06			
537	4.22E-06	1.52E-06			
538	4.22E-06	1.52E-06			
539	4.22E-06	1.52E-06			
540	4.22E-06	1.52E-06			
541	4.22E-06	1.52E-06			
542	4.22E-06	1.52E-06			
543	4.22E-06	1.52E-06			
544	4.22E-06	1.52E-06			
545	4.22E-06	1.52E-06			
546	4.22E-06	1.52E-06			
547	4.22E-06	1.52E-06			
548	4.22E-06	1.52E-06			
549	4.22E-06	1.52E-06			
550	4.22E-06	1.52E-06			

Table 4.2.3: Standard Deviations for the Cape Canaveral 5S Cell

Table 4.2.3 presents the concentrations estimated by the numerical solution along with their respective standard deviations.

Time (day)	Mean (µg/l)	Standard Deviation (µg/l)	Time (day)	Mean (µg/l)	Standard Deviation (µg/l)
1	9.57E+04	7.04E+04	51	4.86E-05	3.42E-05
2	4.50E+04	4.34E+04	52	4.66E-05	3.28E-05
3	2.67E+04	3.11E+04	53	4.47E-05	3.15E-05
4	1.83E+04	2.45E+04	54	4.30E-05	3.02E-05
5	1.39E+04	2.05E+04	55	4.13E-05	2.91E-05
6	1.12E+04	1.78E+04	56	3.98E-05	2.80E-05
7	9.24E+03	1.57E+04	57	3.84E-05	2.71E-05
8	6.90E+03	1.28E+04	58	3.71E-05	2.61E-05
9	3.52E+03	7.75E+03	59	3.59E-05	2.53E-05
10	9.71E+02	2.76E+03	60	3.48E-05	2.45E-05
11	1.52E+02	5.58E+02	61	3.37E-05	2.37E-05
12	1.46E+01	6.73E+01	62	3.27E-05	2.30E-05
13	9.46E-01	5.17E+00	63	3.17E-05	2.23E-05
14	5.36E-02	2.68E-01	64	3.09E-05	2.17E-05
15	9.67E-03	1.14E-02	65	3.00E-05	2.11E-05
16	5.70E-03	4.03E-03	66	2.92E-05	2.06E-05
17	3.93E-03	2.78E-03	67	2.85E-05	2.01E-05
18	2.78E-03	1.96E-03	68	2.78E-05	1.96E-05
19	2.03E-03	1.43E-03	69	2.71E-05	1.91E-05
20	1.52E-03	1.07E-03	70	2.65E-05	1.86E-05
21	1.17E-03	8.23E-04	71	2.59E-05	1.82E-05
22	9.19E-04	6.48E-04	72	2.53E-05	1.78E-05
23	7.34E-04	5.17E-04	73	2.48E-05	1.74E-05
24	6.00E-04	4.23E-04	74	2.42E-05	1.71E-05
25	4.96E-04	3.48E-04	75	2.38E-05	1.67E-05
26	4.16E-04	2.93E-04	76	2.33E-05	1.64E-05
27	3.55E-04	2.50E-04	77	2.28E-05	1.61E-05
28	3.05E-04	2.15E-04	78	2.24E-05	1.58E-05
29	2.65E-04	1.87E-04	79	2.20E-05	1.55E-05
30	2.33E-04	1.64E-04	80	2.16E-05	1.52E-05
31	2.06E-04	1.45E-04	81	2.12E-05	1.49E-05
32	1.84E-04	1.29E-04	82	2.09E-05	1.47E-05
33	1.65E-04	1.16E-04	83	2.05E-05	1.44E-05
34	1.49E-04	1.05E-04	84	2.02E-05	1.42E-05
35	1.35E-04	9.53E-05	85	1.99E-05	1.40E-05
36	1.24E-04	8.70E-05	86	1.95E-05	1.38E-05
37	1.13E-04	7.99E-05	87	1.92E-05	1.36E-05
38	1.05E-04	7.36E-05	88	1.90E-05	1.34E-05
39	9.69E-05	6.82E-05	89	1.87E-05	1.32E-05
40	9.00E-05	6.34E-05	90	1.84E-05	1.30E-05
41	8.40E-05	5.91E-05	91	1.82E-05	1.28E-05
42	7.86E-05	5.53E-05	92	1.79E-05	1.26E-05
43	7.38E-05	5.19E-05	93	1.77E-05	1.24E-05
44	6.95E-05	4.89E-05	94	1.75E-05	1.23E-05
45	6.56E-05	4.62E-05	95	1.72E-05	1.21E-05
46	6.21E-05	4.37E-05	96	1.70E-05	1.20E-05
47	5.89E-05	4.14E-05	97	1.68E-05	1.18E-05
48	5.60E-05	3.94E-05	98	1.66E-05	1.17E-05
49	5.33E-05	3.75E-05	99	1.64E-05	1.16E-05
50	5.09E-05	3.58E-05	100	1.62E-05	1.14E-05

Table 4.2.3: Standard Deviations for the Cape Canaveral 5S Cell Continued

Time (day)	Mean (µg/l)	Standard Deviation (µg/l)	Time (day)	Mean (µg/l)	Standard Deviation (µg/l)
101	1.60E-05	1.13E-05	151	1.10E-05	7.77E-06
102	1.59E-05	1.12E-05	152	1.10E-05	7.73E-06
103	1.57E-05	1.10E-05	153	1.09E-05	7.69E-06
104	1.55E-05	1.09E-05	154	1.09E-05	7.65E-06
105	1.54E-05	1.08E-05	155	1.08E-05	7.62E-06
106	1.52E-05	1.07E-05	156	1.08E-05	7.58E-06
107	1.51E-05	1.06E-05	157	1.07E-05	7.54E-06
108	1.49E-05	1.05E-05	158	1.07E-05	7.51E-06
109	1.48E-05	1.04E-05	159	1.06E-05	7.48E-06
110	1.46E-05	1.03E-05	160	1.06E-05	7.44E-06
111	1.45E-05	1.02E-05	161	1.05E-05	7.41E-06
112	1.44E-05	1.01E-05	162	1.05E-05	7.38E-06
113	1.42E-05	1.00E-05	163	1.04E-05	7.34E-06
114	1.41E-05	9.93E-06	164	1.04E-05	7.31E-06
115	1.40E-05	9.84E-06	165	1.03E-05	7.28E-06
116	1.39E-05	9.76E-06	166	1.03E-05	7.25E-06
117	1.37E-05	9.68E-06	167	1.03E-05	7.22E-06
118	1.36E-05	9.60E-06	168	1.02E-05	7.19E-06
119	1.35E-05	9.52E-06	169	1.02E-05	7.16E-06
120	1.34E-05	9.44E-06	170	1.01E-05	7.14E-06
121	1.33E-05	9.37E-06	171	1.01E-05	7.11E-06
122	1.32E-05	9.30E-06	172	1.01E-05	7.08E-06
123	1.31E-05	9.23E-06	173	1.00E-05	7.05E-06
124	1.30E-05	9.16E-06	174	9.98E-06	7.03E-06
125	1.29E-05	9.09E-06	175	9.94E-06	7.00E-06
126	1.28E-05	9.02E-06	176	9.91E-06	6.97E-06
127	1.27E-05	8.96E-06	177	9.87E-06	6.95E-06
128	1.26E-05	8.90E-06	178	9.84E-06	6.92E-06
129	1.26E-05	8.84E-06	179	9.80E-06	6.90E-06
130	1.25E-05	8.78E-06	180	9.77E-06	6.87E-06
131	1.24E-05	8.72E-06	181	9.73E-06	6.85E-06
132	1.23E-05	8.66E-06	182	9.70E-06	6.83E-06
133	1.22E-05	8.60E-06	183	9.66E-06	6.80E-06
134	1.21E-05	8.55E-06	184	9.63E-06	6.78E-06
135	1.21E-05	8.49E-06	185	9.60E-06	6.76E-06
136	1.20E-05	8.44E-06	186	9.57E-06	6.73E-06
137	1.19E-05	8.39E-06	187	9.54E-06	6.71E-06
138	1.18E-05	8.34E-06	188	9.51E-06	6.69E-06
139	1.18E-05	8.29E-06	189	9.47E-06	6.67E-06
140	1.17E-05	8.24E-06	190	9.44E-06	6.65E-06
141	1.16E-05	8.19E-06	191	9.41E-06	6.63E-06
142	1.16E-05	8.15E-06	192	9.39E-06	6.61E-06
143	1.15E-05	8.10E-06	193	9.36E-06	6.59E-06
144	1.14E-05	8.06E-06	194	9.33E-06	6.57E-06
145	1.14E-05	8.01E-06	195	9.30E-06	6.55E-06
146	1.13E-05	7.97E-06	196	9.27E-06	6.53E-06
147	1.13E-05	7.93E-06	197	9.24E-06	6.51E-06
148	1.12E-05	7.89E-06	198	9.22E-06	6.49E-06
149	1.11E-05	7.84E-06	199	9.19E-06	6.47E-06
150	1.11E-05	7.80E-06	200	9.16E-06	6.45E-06

Table 4.2.3: Standard Deviations for the Cape Canaveral 5S Cell Continued

Time (day)	Mean (µg/l)	Standard Deviation (µg/l)	Time (day)	Mean (µg/l)	Standard Deviation (µg/l)
201	9.14E-06	6.43E-06	251	8.16E-06	5.74E-06
202	9.11E-06	6.42E-06	252	8.15E-06	5.73E-06
203	9.09E-06	6.40E-06	253	8.13E-06	5.72E-06
204	9.06E-06	6.38E-06	254	8.12E-06	5.71E-06
205	9.04E-06	6.36E-06	255	8.10E-06	5.70E-06
206	9.01E-06	6.34E-06	256	8.09E-06	5.69E-06
207	8.99E-06	6.33E-06	257	8.07E-06	5.68E-06
208	8.97E-06	6.31E-06	258	8.06E-06	5.67E-06
209	8.94E-06	6.29E-06	259	8.05E-06	5.66E-06
210	8.92E-06	6.28E-06	260	8.03E-06	5.65E-06
211	8.90E-06	6.26E-06	261	8.02E-06	5.65E-06
212	8.87E-06	6.25E-06	262	8.01E-06	5.64E-06
213	8.85E-06	6.23E-06	263	7.99E-06	5.63E-06
214	8.83E-06	6.21E-06	264	7.98E-06	5.62E-06
215	8.81E-06	6.20E-06	265	7.97E-06	5.61E-06
216	8.78E-06	6.18E-06	266	7.95E-06	5.60E-06
217	8.76E-06	6.17E-06	267	7.94E-06	5.59E-06
218	8.74E-06	6.15E-06	268	7.93E-06	5.58E-06
219	8.72E-06	6.14E-06	269	7.92E-06	5.57E-06
220	8.70E-06	6.12E-06	270	7.90E-06	5.56E-06
221	8.68E-06	6.11E-06	271	7.89E-06	5.55E-06
222	8.66E-06	6.10E-06	272	7.88E-06	5.55E-06
223	8.64E-06	6.08E-06	273	7.87E-06	5.54E-06
224	8.62E-06	6.07E-06	274	7.85E-06	5.53E-06
225	8.60E-06	6.05E-06	275	7.84E-06	5.52E-06
226	8.58E-06	6.04E-06	276	7.83E-06	5.51E-06
227	8.56E-06	6.03E-06	277	7.82E-06	5.50E-06
228	8.54E-06	6.01E-06	278	7.81E-06	5.50E-06
229	8.53E-06	6.00E-06	279	7.80E-06	5.49E-06
230	8.51E-06	5.99E-06	280	7.78E-06	5.48E-06
231	8.49E-06	5.98E-06	281	7.77E-06	5.47E-06
232	8.47E-06	5.96E-06	282	7.76E-06	5.46E-06
233	8.45E-06	5.95E-06	283	7.75E-06	5.46E-06
234	8.43E-06	5.94E-06	284	7.74E-06	5.45E-06
235	8.42E-06	5.93E-06	285	7.73E-06	5.44E-06
236	8.40E-06	5.91E-06	286	7.72E-06	5.43E-06
237	8.38E-06	5.90E-06	287	7.71E-06	5.43E-06
238	8.37E-06	5.89E-06	288	7.70E-06	5.42E-06
239	8.35E-06	5.88E-06	289	7.69E-06	5.41E-06
240	8.33E-06	5.87E-06	290	7.68E-06	5.40E-06
241	8.32E-06	5.85E-06	291	7.67E-06	5.40E-06
242	8.30E-06	5.84E-06	292	7.66E-06	5.39E-06
243	8.28E-06	5.83E-06	293	7.65E-06	5.38E-06
244	8.27E-06	5.82E-06	294	7.63E-06	5.37E-06
245	8.25E-06	5.81E-06	295	7.62E-06	5.37E-06
246	8.24E-06	5.80E-06	296	7.61E-06	5.36E-06
247	8.22E-06	5.79E-06	297	7.61E-06	5.35E-06
248	8.21E-06	5.78E-06	298	7.60E-06	5.35E-06
249	8.19E-06	5.77E-06	299	7.59E-06	5.34E-06
250	8.18E-06	5.75E-06	300	7.58E-06	5.33E-06

Table 4.2.3: Standard Deviations for the Cape Canaveral 5S Cell Continued

Time (day)	Mean (µg/l)	Standard Deviation (µg/l)	Time (day)	Mean (µg/l)	Standard Deviation (µg/l)
301	7.57E-06	5.33E-06	351	7.17E-06	5.05E-06
302	7.56E-06	5.32E-06	352	7.16E-06	5.04E-06
303	7.55E-06	5.31E-06	353	7.16E-06	5.04E-06
304	7.54E-06	5.31E-06	354	7.15E-06	5.03E-06
305	7.53E-06	5.30E-06	355	7.14E-06	5.03E-06
306	7.52E-06	5.29E-06	356	7.14E-06	5.02E-06
307	7.51E-06	5.29E-06	357	7.13E-06	5.02E-06
308	7.50E-06	5.28E-06	358	7.12E-06	5.01E-06
309	7.49E-06	5.27E-06	359	7.12E-06	5.01E-06
310	7.48E-06	5.27E-06	360	7.11E-06	5.01E-06
311	7.47E-06	5.26E-06	361	7.10E-06	5.00E-06
312	7.47E-06	5.26E-06	362	7.10E-06	5.00E-06
313	7.46E-06	5.25E-06	363	7.09E-06	4.99E-06
314	7.45E-06	5.24E-06	364	7.09E-06	4.99E-06
315	7.44E-06	5.24E-06	365	7.08E-06	4.98E-06
316	7.43E-06	5.23E-06	366	7.07E-06	4.98E-06
317	7.42E-06	5.23E-06	367	7.07E-06	4.98E-06
318	7.41E-06	5.22E-06	368	7.06E-06	4.97E-06
319	7.41E-06	5.21E-06	369	7.06E-06	4.97E-06
320	7.40E-06	5.21E-06	370	7.05E-06	4.96E-06
321	7.39E-06	5.20E-06	371	7.04E-06	4.96E-06
322	7.38E-06	5.20E-06	372	7.04E-06	4.95E-06
323	7.37E-06	5.19E-06	373	7.03E-06	4.95E-06
324	7.37E-06	5.18E-06	374	7.03E-06	4.95E-06
325	7.36E-06	5.18E-06	375	7.02E-06	4.94E-06
326	7.35E-06	5.17E-06	376	7.01E-06	4.94E-06
327	7.34E-06	5.17E-06	377	7.01E-06	4.93E-06
328	7.33E-06	5.16E-06	378	7.00E-06	4.93E-06
329	7.33E-06	5.16E-06	379	7.00E-06	4.93E-06
330	7.32E-06	5.15E-06	380	6.99E-06	4.92E-06
331	7.31E-06	5.15E-06	381	6.99E-06	4.92E-06
332	7.30E-06	5.14E-06	382	6.98E-06	4.91E-06
333	7.30E-06	5.14E-06	383	6.98E-06	4.91E-06
334	7.29E-06	5.13E-06	384	6.97E-06	4.91E-06
335	7.28E-06	5.13E-06	385	6.97E-06	4.90E-06
336	7.27E-06	5.12E-06	386	6.96E-06	4.90E-06
337	7.27E-06	5.11E-06	387	6.95E-06	4.90E-06
338	7.26E-06	5.11E-06	388	6.95E-06	4.89E-06
339	7.25E-06	5.10E-06	389	6.94E-06	4.89E-06
340	7.24E-06	5.10E-06	390	6.94E-06	4.88E-06
341	7.24E-06	5.09E-06	391	6.93E-06	4.88E-06
342	7.23E-06	5.09E-06	392	6.93E-06	4.88E-06
343	7.22E-06	5.08E-06	393	6.92E-06	4.87E-06
344	7.22E-06	5.08E-06	394	6.92E-06	4.87E-06
345	7.21E-06	5.07E-06	395	6.91E-06	4.87E-06
346	7.20E-06	5.07E-06	396	6.91E-06	4.86E-06
347	7.20E-06	5.07E-06	397	6.90E-06	4.86E-06
348	7.19E-06	5.06E-06	398	6.90E-06	4.86E-06
349	7.18E-06	5.06E-06	399	6.89E-06	4.85E-06
350	7.17E-06	5.05E-06	400	6.89E-06	4.85E-06

Table 4.2.3: Standard Deviations for the Cape Canaveral 5S Cell Continued

Time (day)	Mean (µg/l)	Standard Deviation (µg/l)	Time (day)	Mean (µg/l)	Standard Deviation (µg/l)
401	6.88E-06	4.85E-06	451	6.67E-06	4.70E-06
402	6.88E-06	4.84E-06	452	6.67E-06	4.69E-06
403	6.87E-06	4.84E-06	453	6.66E-06	4.69E-06
404	6.87E-06	4.84E-06	454	6.66E-06	4.69E-06
405	6.86E-06	4.83E-06	455	6.65E-06	4.68E-06
406	6.86E-06	4.83E-06	456	6.65E-06	4.68E-06
407	6.85E-06	4.83E-06	457	6.65E-06	4.68E-06
408	6.85E-06	4.82E-06	458	6.64E-06	4.68E-06
409	6.85E-06	4.82E-06	459	6.64E-06	4.67E-06
410	6.84E-06	4.82E-06	460	6.64E-06	4.67E-06
411	6.84E-06	4.81E-06	461	6.63E-06	4.67E-06
412	6.83E-06	4.81E-06	462	6.63E-06	4.67E-06
413	6.83E-06	4.81E-06	463	6.63E-06	4.66E-06
414	6.82E-06	4.80E-06	464	6.62E-06	4.66E-06
415	6.82E-06	4.80E-06	465	6.62E-06	4.66E-06
416	6.81E-06	4.80E-06	466	6.62E-06	4.66E-06
417	6.81E-06	4.79E-06	467	6.61E-06	4.65E-06
418	6.80E-06	4.79E-06	468	6.61E-06	4.65E-06
419	6.80E-06	4.79E-06	469	6.61E-06	4.65E-06
420	6.80E-06	4.78E-06	470	6.60E-06	4.65E-06
421	6.79E-06	4.78E-06	471	6.60E-06	4.65E-06
422	6.79E-06	4.78E-06	472	6.60E-06	4.64E-06
423	6.78E-06	4.77E-06	473	6.59E-06	4.64E-06
424	6.78E-06	4.77E-06	474	6.59E-06	4.64E-06
425	6.77E-06	4.77E-06	475	6.59E-06	4.64E-06
426	6.77E-06	4.77E-06	476	6.58E-06	4.63E-06
427	6.77E-06	4.76E-06	477	6.58E-06	4.63E-06
428	6.76E-06	4.76E-06	478	6.58E-06	4.63E-06
429	6.76E-06	4.76E-06	479	6.57E-06	4.63E-06
430	6.75E-06	4.75E-06	480	6.57E-06	4.62E-06
431	6.75E-06	4.75E-06	481	6.57E-06	4.62E-06
432	6.74E-06	4.75E-06	482	6.56E-06	4.62E-06
433	6.74E-06	4.74E-06	483	6.56E-06	4.62E-06
434	6.74E-06	4.74E-06	484	6.56E-06	4.61E-06
435	6.73E-06	4.74E-06	485	6.55E-06	4.61E-06
436	6.73E-06	4.74E-06	486	6.55E-06	4.61E-06
437	6.72E-06	4.73E-06	487	6.55E-06	4.61E-06
438	6.72E-06	4.73E-06	488	6.54E-06	4.61E-06
439	6.72E-06	4.73E-06	489	6.54E-06	4.60E-06
440	6.71E-06	4.72E-06	490	6.54E-06	4.60E-06
441	6.71E-06	4.72E-06	491	6.53E-06	4.60E-06
442	6.70E-06	4.72E-06	492	6.53E-06	4.60E-06
443	6.70E-06	4.72E-06	493	6.53E-06	4.60E-06
444	6.70E-06	4.71E-06	494	6.52E-06	4.59E-06
445	6.69E-06	4.71E-06	495	6.52E-06	4.59E-06
446	6.69E-06	4.71E-06	496	6.52E-06	4.59E-06
447	6.68E-06	4.71E-06	497	6.52E-06	4.59E-06
448	6.68E-06	4.70E-06	498	6.51E-06	4.58E-06
449	6.68E-06	4.70E-06	499	6.51E-06	4.58E-06
450	6.67E-06	4.70E-06	500	6.51E-06	4.58E-06

Table 4.2.3: Standard Deviations for the Cape Canaveral 5S Cell Continued

Time (day)	Mean (µg/l)	Standard Deviation (µg/l)	Time (day)	Mean (µg/l)	Standard Deviation (µg/l)
501	6.50E-06	4.58E-06	551	6.37E-06	4.48E-06
502	6.50E-06	4.58E-06	552	6.37E-06	4.48E-06
503	6.50E-06	4.57E-06	553	6.37E-06	4.48E-06
504	6.49E-06	4.57E-06	554	6.36E-06	4.48E-06
505	6.49E-06	4.57E-06	555	6.36E-06	4.48E-06
506	6.49E-06	4.57E-06	556	6.36E-06	4.48E-06
507	6.49E-06	4.57E-06	557	6.36E-06	4.47E-06
508	6.48E-06	4.56E-06	558	6.35E-06	4.47E-06
509	6.48E-06	4.56E-06	559	6.35E-06	4.47E-06
510	6.48E-06	4.56E-06	560	6.35E-06	4.47E-06
511	6.47E-06	4.56E-06	561	6.35E-06	4.47E-06
512	6.47E-06	4.56E-06	562	6.35E-06	4.47E-06
513	6.47E-06	4.55E-06	563	6.34E-06	4.46E-06
514	6.47E-06	4.55E-06	564	6.34E-06	4.46E-06
515	6.46E-06	4.55E-06	565	6.34E-06	4.46E-06
516	6.46E-06	4.55E-06	566	6.34E-06	4.46E-06
517	6.46E-06	4.55E-06	567	6.33E-06	4.46E-06
518	6.46E-06	4.54E-06	568	6.33E-06	4.46E-06
519	6.45E-06	4.54E-06	569	6.33E-06	4.46E-06
520	6.45E-06	4.54E-06	570	6.33E-06	4.45E-06
521	6.45E-06	4.54E-06			
522	6.44E-06	4.54E-06			
523	6.44E-06	4.53E-06			
524	6.44E-06	4.53E-06			
525	6.44E-06	4.53E-06			
526	6.43E-06	4.53E-06			
527	6.43E-06	4.53E-06			
528	6.43E-06	4.53E-06			
529	6.43E-06	4.52E-06			
530	6.42E-06	4.52E-06			
531	6.42E-06	4.52E-06			
532	6.42E-06	4.52E-06			
533	6.42E-06	4.52E-06			
534	6.41E-06	4.51E-06			
535	6.41E-06	4.51E-06			
536	6.41E-06	4.51E-06			
537	6.41E-06	4.51E-06			
538	6.40E-06	4.51E-06			
539	6.40E-06	4.51E-06			
540	6.40E-06	4.50E-06			
541	6.40E-06	4.50E-06			
542	6.39E-06	4.50E-06			
543	6.39E-06	4.50E-06			
544	6.39E-06	4.50E-06			
545	6.39E-06	4.49E-06			
546	6.38E-06	4.49E-06			
547	6.38E-06	4.49E-06			
548	6.38E-06	4.49E-06			
549	6.38E-06	4.49E-06			
550	6.37E-06	4.49E-06			

Table 4.2.4: Standard Deviations for the Chemplex Cell

Table 4.2.4 presents the concentrations estimated by the numerical solution along with their respective standard deviations.

Time (day)	Mean (µg/l)	Standard Deviation (µg/l)	Time (day)	Mean (µg/l)	Standard Deviation (µg/l)
1	2.86E+04	3.77E+04	51	2.68E+03	1.13E+03
2	2.41E+04	3.47E+04	52	2.76E+03	1.18E+03
3	2.03E+04	3.17E+04	53	2.83E+03	1.22E+03
4	1.76E+04	3.12E+04	54	2.91E+03	1.27E+03
5	1.44E+04	2.96E+04	55	2.99E+03	1.32E+03
6	1.14E+04	2.73E+04	56	3.07E+03	1.37E+03
7	8.01E+03	2.42E+04	57	3.16E+03	1.42E+03
8	3.49E+03	1.34E+04	58	3.24E+03	1.47E+03
9	7.55E+02	2.58E+02	59	3.33E+03	1.52E+03
10	8.46E+02	6.88E+01	60	3.41E+03	1.57E+03
11	8.58E+02	7.47E+01	61	3.50E+03	1.62E+03
12	8.72E+02	8.16E+01	62	3.59E+03	1.68E+03
13	8.87E+02	8.95E+01	63	3.68E+03	1.73E+03
14	9.05E+02	9.84E+01	64	3.77E+03	1.79E+03
15	9.24E+02	1.08E+02	65	3.87E+03	1.84E+03
16	9.44E+02	1.19E+02	66	3.96E+03	1.90E+03
17	9.66E+02	1.31E+02	67	4.05E+03	1.96E+03
18	9.90E+02	1.45E+02	68	4.15E+03	2.01E+03
19	1.02E+03	1.59E+02	69	4.25E+03	2.07E+03
20	1.04E+03	1.74E+02	70	4.34E+03	2.13E+03
21	1.07E+03	1.90E+02	71	4.44E+03	2.19E+03
22	1.10E+03	2.07E+02	72	4.54E+03	2.26E+03
23	1.14E+03	2.26E+02	73	4.64E+03	2.32E+03
24	1.17E+03	2.45E+02	74	4.75E+03	2.38E+03
25	1.20E+03	2.65E+02	75	4.85E+03	2.44E+03
26	1.24E+03	2.87E+02	76	4.95E+03	2.51E+03
27	1.28E+03	3.09E+02	77	5.06E+03	2.57E+03
28	1.32E+03	3.32E+02	78	5.16E+03	2.64E+03
29	1.36E+03	3.56E+02	79	5.27E+03	2.70E+03
30	1.41E+03	3.82E+02	80	5.38E+03	2.77E+03
31	1.45E+03	4.08E+02	81	5.49E+03	2.84E+03
32	1.50E+03	4.35E+02	82	5.60E+03	2.90E+03
33	1.55E+03	4.64E+02	83	5.71E+03	2.97E+03
34	1.60E+03	4.93E+02	84	5.82E+03	3.04E+03
35	1.65E+03	5.23E+02	85	5.93E+03	3.11E+03
36	1.70E+03	5.54E+02	86	6.04E+03	3.18E+03
37	1.76E+03	5.86E+02	87	6.15E+03	3.25E+03
38	1.81E+03	6.19E+02	88	6.27E+03	3.33E+03
39	1.87E+03	6.53E+02	89	6.38E+03	3.40E+03
40	1.93E+03	6.88E+02	90	6.50E+03	3.47E+03
41	1.99E+03	7.24E+02	91	6.61E+03	3.55E+03
42	2.05E+03	7.60E+02	92	6.73E+03	3.62E+03
43	2.12E+03	7.98E+02	93	6.85E+03	3.69E+03
44	2.18E+03	8.36E+02	94	6.96E+03	3.77E+03
45	2.25E+03	8.76E+02	95	7.08E+03	3.85E+03
46	2.32E+03	9.16E+02	96	7.20E+03	3.92E+03
47	2.39E+03	9.57E+02	97	7.32E+03	4.00E+03
48	2.46E+03	9.99E+02	98	7.44E+03	4.08E+03
49	2.53E+03	1.04E+03	99	7.56E+03	4.16E+03
50	2.60E+03	1.09E+03	100	7.68E+03	4.24E+03

Table 4.2.4: Standard Deviations for the Chemplex Cell Continued

Time (day)	Mean (µg/l)	Standard Deviation (µg/l)	Time (day)	Mean (µg/l)	Standard Deviation (µg/l)
101	7.80E+03	4.32E+03	151	1.42E+04	8.95E+03
102	7.93E+03	4.40E+03	152	1.43E+04	9.06E+03
103	8.05E+03	4.48E+03	153	1.44E+04	9.16E+03
104	8.17E+03	4.56E+03	154	1.46E+04	9.27E+03
105	8.30E+03	4.64E+03	155	1.47E+04	9.37E+03
106	8.42E+03	4.72E+03	156	1.48E+04	9.48E+03
107	8.54E+03	4.80E+03	157	1.49E+04	9.59E+03
108	8.65E+03	4.89E+03	158	1.51E+04	9.69E+03
109	8.78E+03	4.98E+03	159	1.52E+04	9.80E+03
110	8.90E+03	5.06E+03	160	1.53E+04	9.91E+03
111	9.03E+03	5.15E+03	161	1.54E+04	1.00E+04
112	9.16E+03	5.23E+03	162	1.56E+04	1.01E+04
113	9.28E+03	5.32E+03	163	1.57E+04	1.02E+04
114	9.41E+03	5.40E+03	164	1.58E+04	1.03E+04
115	9.53E+03	5.49E+03	165	1.60E+04	1.04E+04
116	9.66E+03	5.58E+03	166	1.61E+04	1.06E+04
117	9.79E+03	5.67E+03	167	1.62E+04	1.07E+04
118	9.92E+03	5.76E+03	168	1.63E+04	1.08E+04
119	1.00E+04	5.85E+03	169	1.65E+04	1.09E+04
120	1.02E+04	5.94E+03	170	1.66E+04	1.10E+04
121	1.03E+04	6.03E+03	171	1.67E+04	1.11E+04
122	1.04E+04	6.12E+03	172	1.68E+04	1.12E+04
123	1.06E+04	6.21E+03	173	1.69E+04	1.13E+04
124	1.07E+04	6.30E+03	174	1.71E+04	1.14E+04
125	1.08E+04	6.39E+03	175	1.72E+04	1.16E+04
126	1.09E+04	6.49E+03	176	1.73E+04	1.17E+04
127	1.11E+04	6.58E+03	177	1.74E+04	1.18E+04
128	1.12E+04	6.67E+03	178	1.76E+04	1.19E+04
129	1.13E+04	6.77E+03	179	1.77E+04	1.20E+04
130	1.15E+04	6.86E+03	180	1.78E+04	1.21E+04
131	1.16E+04	6.96E+03	181	1.79E+04	1.22E+04
132	1.17E+04	7.05E+03	182	1.80E+04	1.24E+04
133	1.18E+04	7.15E+03	183	1.82E+04	1.25E+04
134	1.20E+04	7.24E+03	184	1.83E+04	1.26E+04
135	1.21E+04	7.34E+03	185	1.84E+04	1.27E+04
136	1.22E+04	7.44E+03	186	1.85E+04	1.28E+04
137	1.24E+04	7.54E+03	187	1.86E+04	1.29E+04
138	1.25E+04	7.64E+03	188	1.88E+04	1.31E+04
139	1.26E+04	7.73E+03	189	1.89E+04	1.32E+04
140	1.28E+04	7.83E+03	190	1.90E+04	1.33E+04
141	1.29E+04	7.93E+03	191	1.91E+04	1.34E+04
142	1.30E+04	8.03E+03	192	1.92E+04	1.35E+04
143	1.31E+04	8.13E+03	193	1.94E+04	1.36E+04
144	1.33E+04	8.23E+03	194	1.95E+04	1.38E+04
145	1.34E+04	8.34E+03	195	1.96E+04	1.39E+04
146	1.35E+04	8.44E+03	196	1.97E+04	1.40E+04
147	1.37E+04	8.54E+03	197	1.98E+04	1.41E+04
148	1.38E+04	8.64E+03	198	1.99E+04	1.42E+04
149	1.39E+04	8.75E+03	199	2.01E+04	1.43E+04
150	1.40E+04	8.85E+03	200	2.02E+04	1.45E+04

Table 4.2.4: Standard Deviations for the Chemplex Cell Continued

Time (day)	Mean (µg/l)	Standard Deviation (µg/l)	Time (day)	Mean (µg/l)	Standard Deviation (µg/l)
201	2.03E+04	1.46E+04	251	2.54E+04	2.07E+04
202	2.04E+04	1.47E+04	252	2.55E+04	2.08E+04
203	2.05E+04	1.48E+04	253	2.56E+04	2.09E+04
204	2.06E+04	1.49E+04	254	2.57E+04	2.11E+04
205	2.07E+04	1.51E+04	255	2.58E+04	2.12E+04
206	2.09E+04	1.52E+04	256	2.59E+04	2.13E+04
207	2.10E+04	1.53E+04	257	2.60E+04	2.14E+04
208	2.11E+04	1.54E+04	258	2.61E+04	2.16E+04
209	2.12E+04	1.55E+04	259	2.62E+04	2.17E+04
210	2.13E+04	1.57E+04	260	2.63E+04	2.18E+04
211	2.14E+04	1.58E+04	261	2.64E+04	2.19E+04
212	2.15E+04	1.59E+04	262	2.64E+04	2.20E+04
213	2.16E+04	1.60E+04	263	2.65E+04	2.22E+04
214	2.17E+04	1.62E+04	264	2.66E+04	2.23E+04
215	2.18E+04	1.63E+04	265	2.67E+04	2.24E+04
216	2.20E+04	1.64E+04	266	2.68E+04	2.25E+04
217	2.21E+04	1.65E+04	267	2.69E+04	2.27E+04
218	2.22E+04	1.66E+04	268	2.70E+04	2.28E+04
219	2.23E+04	1.68E+04	269	2.71E+04	2.29E+04
220	2.24E+04	1.69E+04	270	2.72E+04	2.30E+04
221	2.25E+04	1.70E+04	271	2.72E+04	2.32E+04
222	2.26E+04	1.71E+04	272	2.73E+04	2.33E+04
223	2.27E+04	1.73E+04	273	2.74E+04	2.34E+04
224	2.28E+04	1.74E+04	274	2.75E+04	2.35E+04
225	2.29E+04	1.75E+04	275	2.76E+04	2.37E+04
226	2.30E+04	1.76E+04	276	2.77E+04	2.38E+04
227	2.31E+04	1.78E+04	277	2.77E+04	2.39E+04
228	2.32E+04	1.79E+04	278	2.78E+04	2.40E+04
229	2.33E+04	1.80E+04	279	2.79E+04	2.41E+04
230	2.34E+04	1.81E+04	280	2.80E+04	2.43E+04
231	2.35E+04	1.82E+04	281	2.81E+04	2.44E+04
232	2.36E+04	1.84E+04	282	2.82E+04	2.45E+04
233	2.37E+04	1.85E+04	283	2.82E+04	2.46E+04
234	2.38E+04	1.86E+04	284	2.83E+04	2.48E+04
235	2.39E+04	1.87E+04	285	2.84E+04	2.49E+04
236	2.40E+04	1.89E+04	286	2.85E+04	2.50E+04
237	2.41E+04	1.90E+04	287	2.86E+04	2.51E+04
238	2.42E+04	1.91E+04	288	2.87E+04	2.52E+04
239	2.43E+04	1.92E+04	289	2.87E+04	2.54E+04
240	2.44E+04	1.94E+04	290	2.88E+04	2.55E+04
241	2.45E+04	1.95E+04	291	2.89E+04	2.56E+04
242	2.46E+04	1.96E+04	292	2.90E+04	2.57E+04
243	2.47E+04	1.97E+04	293	2.90E+04	2.59E+04
244	2.48E+04	1.99E+04	294	2.91E+04	2.60E+04
245	2.49E+04	1.99E+04	295	2.92E+04	2.61E+04
246	2.50E+04	2.01E+04	296	2.93E+04	2.62E+04
247	2.51E+04	2.02E+04	297	2.94E+04	2.63E+04
248	2.51E+04	2.03E+04	298	2.94E+04	2.65E+04
249	2.52E+04	2.04E+04	299	2.95E+04	2.66E+04
250	2.53E+04	2.06E+04	300	2.96E+04	2.67E+04

Table 4.2.4: Standard Deviations for the Chemplex Cell Continued

Time (day)	Mean (µg/l)	Standard Deviation (µg/l)	Time (day)	Mean (µg/l)	Standard Deviation (µg/l)
301	2.97E+04	2.68E+04	351	3.30E+04	3.26E+04
302	2.97E+04	2.69E+04	352	3.31E+04	3.27E+04
303	2.98E+04	2.71E+04	353	3.31E+04	3.28E+04
304	2.99E+04	2.72E+04	354	3.32E+04	3.29E+04
305	3.00E+04	2.73E+04	355	3.32E+04	3.30E+04
306	3.00E+04	2.74E+04	356	3.33E+04	3.31E+04
307	3.01E+04	2.75E+04	357	3.34E+04	3.32E+04
308	3.02E+04	2.77E+04	358	3.34E+04	3.33E+04
309	3.03E+04	2.78E+04	359	3.35E+04	3.35E+04
310	3.03E+04	2.79E+04	360	3.35E+04	3.36E+04
311	3.04E+04	2.80E+04	361	3.36E+04	3.37E+04
312	3.05E+04	2.81E+04	362	3.36E+04	3.38E+04
313	3.05E+04	2.82E+04	363	3.37E+04	3.39E+04
314	3.06E+04	2.84E+04	364	3.38E+04	3.40E+04
315	3.07E+04	2.85E+04	365	3.38E+04	3.41E+04
316	3.08E+04	2.86E+04	366	3.39E+04	3.42E+04
317	3.08E+04	2.87E+04	367	3.39E+04	3.43E+04
318	3.09E+04	2.88E+04	368	3.40E+04	3.44E+04
319	3.10E+04	2.89E+04	369	3.40E+04	3.45E+04
320	3.10E+04	2.91E+04	370	3.41E+04	3.46E+04
321	3.11E+04	2.92E+04	371	3.41E+04	3.47E+04
322	3.12E+04	2.93E+04	372	3.42E+04	3.48E+04
323	3.12E+04	2.94E+04	373	3.42E+04	3.49E+04
324	3.13E+04	2.95E+04	374	3.43E+04	3.50E+04
325	3.14E+04	2.96E+04	375	3.43E+04	3.51E+04
326	3.14E+04	2.98E+04	376	3.44E+04	3.52E+04
327	3.15E+04	2.99E+04	377	3.44E+04	3.54E+04
328	3.16E+04	3.00E+04	378	3.45E+04	3.55E+04
329	3.16E+04	3.01E+04	379	3.45E+04	3.56E+04
330	3.17E+04	3.02E+04	380	3.46E+04	3.57E+04
331	3.18E+04	3.03E+04	381	3.46E+04	3.58E+04
332	3.18E+04	3.05E+04	382	3.47E+04	3.59E+04
333	3.19E+04	3.06E+04	383	3.48E+04	3.60E+04
334	3.20E+04	3.07E+04	384	3.48E+04	3.61E+04
335	3.20E+04	3.08E+04	385	3.48E+04	3.62E+04
336	3.21E+04	3.09E+04	386	3.49E+04	3.63E+04
337	3.22E+04	3.10E+04	387	3.49E+04	3.64E+04
338	3.22E+04	3.11E+04	388	3.50E+04	3.65E+04
339	3.23E+04	3.12E+04	389	3.50E+04	3.66E+04
340	3.23E+04	3.14E+04	390	3.51E+04	3.67E+04
341	3.24E+04	3.15E+04	391	3.51E+04	3.68E+04
342	3.25E+04	3.16E+04	392	3.52E+04	3.69E+04
343	3.25E+04	3.17E+04	393	3.52E+04	3.70E+04
344	3.26E+04	3.18E+04	394	3.53E+04	3.71E+04
345	3.27E+04	3.19E+04	395	3.53E+04	3.72E+04
346	3.27E+04	3.20E+04	396	3.54E+04	3.73E+04
347	3.28E+04	3.21E+04	397	3.54E+04	3.74E+04
348	3.28E+04	3.23E+04	398	3.55E+04	3.75E+04
349	3.29E+04	3.24E+04	399	3.55E+04	3.76E+04
350	3.30E+04	3.25E+04	400	3.56E+04	3.77E+04

Table 4.2.4: Standard Deviations for the Chemplex Cell Continued

Time (day)	Mean (µg/l)	Standard Deviation (µg/l)
401	3.56E+04	3.77E+04
402	3.57E+04	3.78E+04
403	3.57E+04	3.79E+04
404	3.57E+04	3.80E+04
405	3.58E+04	3.81E+04
406	3.58E+04	3.82E+04
407	3.59E+04	3.83E+04
408	3.59E+04	3.84E+04
409	3.60E+04	3.85E+04
410	3.60E+04	3.86E+04

Table 4.2.5: Standard Deviations for the PGDP Cell

Table 4.2.5 presents the concentrations estimated by the numerical solution along with their respective standard deviations.

Time (day)	Mean (µg/l)	Standard Deviation (µg/l)	Time (day)	Mean (µg/l)	Standard Deviation (µg/l)
1	231.26	91.23	51	1.80	0.59
2	9.47	3.12	52	1.84	0.61
3	3.86	1.27	53	1.87	0.62
4	2.49	0.82	54	1.90	0.63
5	1.93	0.64	55	1.94	0.64
6	1.64	0.54	56	1.98	0.65
7	1.46	0.48	57	2.01	0.66
8	1.35	0.45	58	2.05	0.68
9	1.28	0.42	59	2.09	0.69
10	1.23	0.40	60	2.13	0.70
11	1.19	0.39	61	2.17	0.71
12	1.17	0.38	62	2.21	0.73
13	1.15	0.38	63	2.25	0.74
14	1.14	0.38	64	2.29	0.76
15	1.13	0.37	65	2.34	0.77
16	1.13	0.37	66	2.38	0.78
17	1.13	0.37	67	2.43	0.80
18	1.13	0.37	68	2.47	0.81
19	1.14	0.37	69	2.52	0.83
20	1.14	0.38	70	2.57	0.85
21	1.15	0.38	71	2.62	0.86
22	1.16	0.38	72	2.67	0.88
23	1.17	0.39	73	2.72	0.90
24	1.18	0.39	74	2.77	0.91
25	1.20	0.39	75	2.83	0.93
26	1.21	0.40	76	2.88	0.95
27	1.22	0.40	77	2.94	0.97
28	1.24	0.41	78	2.99	0.99
29	1.26	0.41	79	3.05	1.01
30	1.27	0.42	80	3.11	1.03
31	1.29	0.43	81	3.17	1.05
32	1.31	0.43	82	3.23	1.07
33	1.33	0.44	83	3.30	1.09
34	1.35	0.45	84	3.36	1.11
35	1.37	0.45	85	3.43	1.13
36	1.39	0.46	86	3.49	1.15
37	1.42	0.47	87	3.56	1.17
38	1.44	0.47	88	3.63	1.20
39	1.46	0.48	89	3.70	1.22
40	1.49	0.49	90	3.78	1.24
41	1.51	0.50	91	3.85	1.27
42	1.54	0.51	92	3.93	1.29
43	1.57	0.52	93	4.00	1.32
44	1.59	0.52	94	4.08	1.35
45	1.62	0.53	95	4.16	1.37
46	1.65	0.54	96	4.25	1.40
47	1.68	0.55	97	4.33	1.43
48	1.71	0.56	98	4.42	1.45
49	1.74	0.57	99	4.50	1.48
50	1.77	0.58	100	4.59	1.51

Table 4.2.6: Standard Deviations for the Valmont EW-1 Cell

Table 4.2.6 presents the concentrations estimated by the numerical solution along with their respective standard deviations.

Time (day)	Mean (µg/l)	Standard Deviation (µg/l)	Time (day)	Mean (µg/l)	Standard Deviation (µg/l)
1	2.02E+03	4.37E+02	51	5.94E+00	2.17E+00
2	1.97E+03	5.48E+02	52	5.94E+00	2.17E+00
3	3.43E+02	1.22E+02	53	5.94E+00	2.17E+00
4	1.13E+02	4.09E+01	54	5.94E+00	2.17E+00
5	5.72E+01	2.08E+01	55	5.94E+00	2.17E+00
6	3.63E+01	1.33E+01	56	5.95E+00	2.17E+00
7	2.63E+01	9.60E+00	57	5.95E+00	2.17E+00
8	2.06E+01	7.54E+00	58	5.95E+00	2.17E+00
9	1.71E+01	6.26E+00	59	5.96E+00	2.18E+00
10	1.48E+01	5.39E+00	60	5.96E+00	2.18E+00
11	1.31E+01	4.78E+00	61	5.97E+00	2.18E+00
12	1.18E+01	4.33E+00	62	5.98E+00	2.18E+00
13	1.09E+01	3.98E+00	63	5.99E+00	2.19E+00
14	1.01E+01	3.71E+00	64	5.99E+00	2.19E+00
15	9.55E+00	3.49E+00	65	6.00E+00	2.19E+00
16	9.06E+00	3.31E+00	66	6.01E+00	2.20E+00
17	8.65E+00	3.16E+00	67	6.02E+00	2.20E+00
18	8.31E+00	3.04E+00	68	6.04E+00	2.20E+00
19	8.02E+00	2.93E+00	69	6.05E+00	2.21E+00
20	7.77E+00	2.84E+00	70	6.06E+00	2.21E+00
21	7.56E+00	2.76E+00	71	6.07E+00	2.22E+00
22	7.37E+00	2.69E+00	72	6.09E+00	2.22E+00
23	7.21E+00	2.63E+00	73	6.10E+00	2.23E+00
24	7.06E+00	2.58E+00	74	6.11E+00	2.23E+00
25	6.94E+00	2.53E+00	75	6.13E+00	2.24E+00
26	6.82E+00	2.49E+00	76	6.14E+00	2.24E+00
27	6.72E+00	2.46E+00	77	6.16E+00	2.25E+00
28	6.63E+00	2.42E+00	78	6.18E+00	2.26E+00
29	6.55E+00	2.39E+00	79	6.19E+00	2.26E+00
30	6.48E+00	2.37E+00	80	6.21E+00	2.27E+00
31	6.42E+00	2.34E+00	81	6.23E+00	2.27E+00
32	6.36E+00	2.32E+00	82	6.24E+00	2.28E+00
33	6.31E+00	2.30E+00	83	6.26E+00	2.29E+00
34	6.26E+00	2.29E+00	84	6.28E+00	2.29E+00
35	6.22E+00	2.27E+00	85	6.30E+00	2.30E+00
36	6.18E+00	2.26E+00	86	6.32E+00	2.31E+00
37	6.15E+00	2.25E+00	87	6.34E+00	2.31E+00
38	6.12E+00	2.23E+00	88	6.36E+00	2.32E+00
39	6.09E+00	2.23E+00	89	6.38E+00	2.33E+00
40	6.07E+00	2.22E+00	90	6.40E+00	2.34E+00
41	6.05E+00	2.21E+00	91	6.42E+00	2.34E+00
42	6.03E+00	2.20E+00	92	6.44E+00	2.35E+00
43	6.01E+00	2.20E+00	93	6.46E+00	2.36E+00
44	6.00E+00	2.19E+00	94	6.48E+00	2.37E+00
45	5.98E+00	2.19E+00	95	6.50E+00	2.38E+00
46	5.97E+00	2.18E+00	96	6.52E+00	2.38E+00
47	5.96E+00	2.18E+00	97	6.55E+00	2.39E+00
48	5.96E+00	2.18E+00	98	6.57E+00	2.40E+00
49	5.95E+00	2.17E+00	99	6.59E+00	2.41E+00
50	5.95E+00	2.17E+00	100	6.62E+00	2.42E+00

Table 4.2.6: Standard Deviations for the Valmont EW-1 Cell Continued

Time (day)	Mean (µg/l)	Standard Deviation (µg/l)	Time (day)	Mean (µg/l)	Standard Deviation (µg/l)
101	6.64E+00	2.42E+00	151	8.10E+00	2.96E+00
102	6.66E+00	2.43E+00	152	8.14E+00	2.97E+00
103	6.69E+00	2.44E+00	153	8.17E+00	2.99E+00
104	6.71E+00	2.45E+00	154	8.21E+00	3.00E+00
105	6.73E+00	2.46E+00	155	8.25E+00	3.01E+00
106	6.76E+00	2.47E+00	156	8.28E+00	3.02E+00
107	6.78E+00	2.48E+00	157	8.32E+00	3.04E+00
108	6.81E+00	2.49E+00	158	8.35E+00	3.05E+00
109	6.84E+00	2.50E+00	159	8.39E+00	3.06E+00
110	6.86E+00	2.51E+00	160	8.43E+00	3.08E+00
111	6.89E+00	2.52E+00	161	8.46E+00	3.09E+00
112	6.91E+00	2.52E+00	162	8.50E+00	3.10E+00
113	6.94E+00	2.53E+00	163	8.54E+00	3.12E+00
114	6.97E+00	2.54E+00	164	8.57E+00	3.13E+00
115	6.99E+00	2.55E+00	165	8.61E+00	3.15E+00
116	7.02E+00	2.56E+00	166	8.65E+00	3.16E+00
117	7.05E+00	2.57E+00	167	8.69E+00	3.17E+00
118	7.07E+00	2.58E+00	168	8.73E+00	3.19E+00
119	7.10E+00	2.59E+00	169	8.77E+00	3.20E+00
120	7.13E+00	2.60E+00	170	8.80E+00	3.22E+00
121	7.16E+00	2.61E+00	171	8.84E+00	3.23E+00
122	7.19E+00	2.62E+00	172	8.88E+00	3.24E+00
123	7.22E+00	2.64E+00	173	8.92E+00	3.26E+00
124	7.24E+00	2.65E+00	174	8.96E+00	3.27E+00
125	7.27E+00	2.66E+00	175	9.00E+00	3.29E+00
126	7.30E+00	2.67E+00	176	9.04E+00	3.30E+00
127	7.33E+00	2.68E+00	177	9.08E+00	3.32E+00
128	7.36E+00	2.69E+00	178	9.12E+00	3.33E+00
129	7.39E+00	2.70E+00	179	9.16E+00	3.35E+00
130	7.42E+00	2.71E+00	180	9.20E+00	3.36E+00
131	7.45E+00	2.72E+00	181	9.25E+00	3.38E+00
132	7.48E+00	2.73E+00	182	9.29E+00	3.39E+00
133	7.51E+00	2.74E+00	183	9.33E+00	3.41E+00
134	7.54E+00	2.76E+00	184	9.37E+00	3.42E+00
135	7.58E+00	2.77E+00	185	9.41E+00	3.44E+00
136	7.61E+00	2.78E+00	186	9.45E+00	3.45E+00
137	7.64E+00	2.79E+00	187	9.50E+00	3.47E+00
138	7.67E+00	2.80E+00	188	9.54E+00	3.48E+00
139	7.70E+00	2.81E+00	189	9.58E+00	3.50E+00
140	7.73E+00	2.83E+00	190	9.63E+00	3.52E+00
141	7.77E+00	2.84E+00	191	9.67E+00	3.53E+00
142	7.80E+00	2.85E+00	192	9.71E+00	3.55E+00
143	7.83E+00	2.86E+00	193	9.76E+00	3.56E+00
144	7.87E+00	2.87E+00	194	9.80E+00	3.58E+00
145	7.90E+00	2.89E+00	195	9.85E+00	3.60E+00
146	7.93E+00	2.90E+00	196	9.89E+00	3.61E+00
147	7.97E+00	2.91E+00	197	9.94E+00	3.63E+00
148	8.00E+00	2.92E+00	198	9.98E+00	3.65E+00
149	8.04E+00	2.94E+00	199	1.00E+01	3.66E+00
150	8.07E+00	2.95E+00	200	1.01E+01	3.68E+00

Table 4.2.6: Standard Deviations for the Valmont EW-1 Cell Continued

Time (day)	Mean (µg/l)	Standard Deviation (µg/l)
201	1.01E+01	3.70E+00
202	1.02E+01	3.71E+00
203	1.02E+01	3.73E+00
204	1.03E+01	3.75E+00
205	1.03E+01	3.76E+00
206	1.04E+01	3.78E+00
207	1.04E+01	3.80E+00
208	1.04E+01	3.82E+00
209	1.05E+01	3.83E+00
210	1.05E+01	3.85E+00
211	1.06E+01	3.87E+00
212	1.06E+01	3.89E+00
213	1.07E+01	3.90E+00
214	1.07E+01	3.92E+00
215	1.08E+01	3.94E+00
216	1.08E+01	3.96E+00
217	1.09E+01	3.98E+00
218	1.09E+01	4.00E+00
219	1.10E+01	4.01E+00
220	1.10E+01	4.03E+00
221	1.11E+01	4.05E+00
222	1.11E+01	4.07E+00
223	1.12E+01	4.09E+00
224	1.12E+01	4.11E+00
225	1.13E+01	4.13E+00
226	1.13E+01	4.15E+00
227	1.14E+01	4.17E+00
228	1.15E+01	4.18E+00
229	1.15E+01	4.20E+00
230	1.16E+01	4.22E+00
231	1.16E+01	4.24E+00
232	1.17E+01	4.26E+00
233	1.17E+01	4.28E+00
234	1.18E+01	4.30E+00
235	1.18E+01	4.32E+00
236	1.19E+01	4.34E+00
237	1.19E+01	4.36E+00
238	1.20E+01	4.38E+00
239	1.21E+01	4.40E+00
240	1.21E+01	4.42E+00

Table 4.2.7: Standard Deviations for the Valmont EW-5 Cell

Table 4.2.7 presents the concentrations estimated by the numerical solution along with their respective standard deviations.

Time (day)	Mean (µg/l)	Standard Deviation (µg/l)	Time (day)	Mean (µg/l)	Standard Deviation (µg/l)
1	7.72E+02	6.41E+02	51	2.35E+01	8.74E+00
2	2.32E+02	2.79E+02	52	2.35E+01	8.75E+00
3	1.51E+02	2.64E+02	53	2.35E+01	8.76E+00
4	1.33E+02	2.77E+02	54	2.36E+01	8.76E+00
5	1.24E+02	2.71E+02	55	2.36E+01	8.77E+00
6	1.21E+02	2.84E+02	56	2.36E+01	8.78E+00
7	1.17E+02	2.74E+02	57	2.36E+01	8.79E+00
8	1.16E+02	2.83E+02	58	2.37E+01	8.80E+00
9	1.11E+02	2.61E+02	59	2.37E+01	8.81E+00
10	5.12E+01	5.30E+01	60	2.37E+01	8.82E+00
11	3.96E+01	2.39E+01	61	2.37E+01	8.83E+00
12	3.50E+01	1.67E+01	62	2.38E+01	8.84E+00
13	3.25E+01	1.39E+01	63	2.38E+01	8.86E+00
14	3.07E+01	1.24E+01	64	2.38E+01	8.87E+00
15	2.95E+01	1.16E+01	65	2.39E+01	8.88E+00
16	2.85E+01	1.10E+01	66	2.39E+01	8.90E+00
17	2.77E+01	1.06E+01	67	2.40E+01	8.91E+00
18	2.71E+01	1.03E+01	68	2.40E+01	8.93E+00
19	2.66E+01	1.00E+01	69	2.40E+01	8.94E+00
20	2.62E+01	9.82E+00	70	2.41E+01	8.96E+00
21	2.58E+01	9.66E+00	71	2.41E+01	8.97E+00
22	2.55E+01	9.52E+00	72	2.42E+01	8.99E+00
23	2.52E+01	9.41E+00	73	2.42E+01	9.00E+00
24	2.50E+01	9.31E+00	74	2.42E+01	9.02E+00
25	2.48E+01	9.23E+00	75	2.43E+01	9.04E+00
26	2.46E+01	9.16E+00	76	2.43E+01	9.05E+00
27	2.44E+01	9.10E+00	77	2.44E+01	9.07E+00
28	2.43E+01	9.04E+00	78	2.44E+01	9.09E+00
29	2.42E+01	9.00E+00	79	2.45E+01	9.11E+00
30	2.41E+01	8.95E+00	80	2.45E+01	9.13E+00
31	2.40E+01	8.92E+00	81	2.46E+01	9.14E+00
32	2.39E+01	8.89E+00	82	2.46E+01	9.16E+00
33	2.38E+01	8.86E+00	83	2.47E+01	9.18E+00
34	2.37E+01	8.83E+00	84	2.47E+01	9.20E+00
35	2.37E+01	8.81E+00	85	2.48E+01	9.22E+00
36	2.36E+01	8.80E+00	86	2.48E+01	9.24E+00
37	2.36E+01	8.78E+00	87	2.49E+01	9.26E+00
38	2.36E+01	8.77E+00	88	2.49E+01	9.28E+00
39	2.35E+01	8.76E+00	89	2.50E+01	9.30E+00
40	2.35E+01	8.75E+00	90	2.51E+01	9.32E+00
41	2.35E+01	8.74E+00	91	2.51E+01	9.34E+00
42	2.35E+01	8.73E+00	92	2.52E+01	9.36E+00
43	2.35E+01	8.73E+00	93	2.52E+01	9.38E+00
44	2.35E+01	8.73E+00	94	2.53E+01	9.40E+00
45	2.35E+01	8.73E+00	95	2.53E+01	9.42E+00
46	2.35E+01	8.73E+00	96	2.54E+01	9.45E+00
47	2.35E+01	8.73E+00	97	2.55E+01	9.47E+00
48	2.35E+01	8.73E+00	98	2.55E+01	9.49E+00
49	2.35E+01	8.73E+00	99	2.56E+01	9.51E+00
50	2.35E+01	8.74E+00	100	2.56E+01	9.53E+00

Table 4.2.7: Standard Deviations for the Valmont EW-5 Continued

Time (day)	Mean (µg/l)	Standard Deviation (µg/l)	Time (day)	Mean (µg/l)	Standard Deviation (µg/l)
101	2.57E+01	9.56E+00	151	2.91E+01	1.08E+01
102	2.57E+01	9.58E+00	152	2.92E+01	1.09E+01
103	2.58E+01	9.60E+00	153	2.93E+01	1.09E+01
104	2.59E+01	9.62E+00	154	2.94E+01	1.09E+01
105	2.59E+01	9.65E+00	155	2.95E+01	1.10E+01
106	2.60E+01	9.67E+00	156	2.95E+01	1.10E+01
107	2.61E+01	9.69E+00	157	2.96E+01	1.10E+01
108	2.61E+01	9.72E+00	158	2.97E+01	1.10E+01
109	2.62E+01	9.74E+00	159	2.98E+01	1.11E+01
110	2.62E+01	9.76E+00	160	2.99E+01	1.11E+01
111	2.63E+01	9.79E+00	161	2.99E+01	1.11E+01
112	2.64E+01	9.81E+00	162	3.00E+01	1.12E+01
113	2.64E+01	9.84E+00	163	3.01E+01	1.12E+01
114	2.65E+01	9.86E+00	164	3.02E+01	1.12E+01
115	2.66E+01	9.88E+00	165	3.02E+01	1.13E+01
116	2.66E+01	9.91E+00	166	3.03E+01	1.13E+01
117	2.67E+01	9.93E+00	167	3.04E+01	1.14E+01
118	2.68E+01	9.96E+00	168	3.05E+01	1.14E+01
119	2.68E+01	9.98E+00	169	3.05E+01	1.14E+01
120	2.69E+01	1.00E+01	170	3.06E+01	1.14E+01
121	2.70E+01	1.00E+01	171	3.07E+01	1.15E+01
122	2.70E+01	1.01E+01	172	3.08E+01	1.15E+01
123	2.71E+01	1.01E+01	173	3.09E+01	1.15E+01
124	2.72E+01	1.01E+01	174	3.10E+01	1.16E+01
125	2.72E+01	1.01E+01	175	3.10E+01	1.16E+01
126	2.73E+01	1.02E+01	176	3.11E+01	1.16E+01
127	2.74E+01	1.02E+01	177	3.12E+01	1.17E+01
128	2.75E+01	1.02E+01	178	3.13E+01	1.17E+01
129	2.75E+01	1.02E+01	179	3.14E+01	1.17E+01
130	2.76E+01	1.03E+01	180	3.15E+01	1.18E+01
131	2.77E+01	1.03E+01	181	3.16E+01	1.18E+01
132	2.77E+01	1.03E+01	182	3.16E+01	1.18E+01
133	2.78E+01	1.03E+01	183	3.17E+01	1.19E+01
134	2.79E+01	1.04E+01	184	3.18E+01	1.19E+01
135	2.79E+01	1.04E+01	185	3.19E+01	1.19E+01
136	2.80E+01	1.04E+01	186	3.20E+01	1.20E+01
137	2.81E+01	1.05E+01	187	3.21E+01	1.20E+01
138	2.82E+01	1.05E+01	188	3.22E+01	1.20E+01
139	2.82E+01	1.05E+01	189	3.23E+01	1.21E+01
140	2.83E+01	1.05E+01	190	3.23E+01	1.21E+01
141	2.84E+01	1.06E+01	191	3.24E+01	1.21E+01
142	2.85E+01	1.06E+01	192	3.25E+01	1.22E+01
143	2.85E+01	1.06E+01	193	3.26E+01	1.22E+01
144	2.86E+01	1.06E+01	194	3.27E+01	1.22E+01
145	2.87E+01	1.07E+01	195	3.28E+01	1.23E+01
146	2.88E+01	1.07E+01	196	3.29E+01	1.23E+01
147	2.88E+01	1.07E+01	197	3.30E+01	1.23E+01
148	2.89E+01	1.08E+01	198	3.31E+01	1.24E+01
149	2.90E+01	1.08E+01	199	3.32E+01	1.24E+01
150	2.91E+01	1.08E+01	200	3.32E+01	1.24E+01

Table 4.2.7: Standard Deviations for the Valmont EW-5 Continued

Time (day)	Mean (µg/l)	Standard Deviation (µg/l)
201	3.33E+01	1.25E+01
202	3.34E+01	1.25E+01
203	3.35E+01	1.25E+01
204	3.36E+01	1.26E+01
205	3.37E+01	1.26E+01
206	3.38E+01	1.26E+01
207	3.39E+01	1.27E+01
208	3.40E+01	1.27E+01
209	3.41E+01	1.27E+01
210	3.42E+01	1.28E+01
211	3.43E+01	1.28E+01
212	3.44E+01	1.28E+01
213	3.45E+01	1.29E+01
214	3.46E+01	1.29E+01
215	3.47E+01	1.30E+01
216	3.48E+01	1.30E+01
217	3.48E+01	1.30E+01
218	3.49E+01	1.31E+01
219	3.50E+01	1.31E+01
220	3.51E+01	1.31E+01
221	3.52E+01	1.32E+01
222	3.53E+01	1.32E+01
223	3.54E+01	1.32E+01
224	3.55E+01	1.33E+01
225	3.56E+01	1.33E+01

Table 4.2.8: Standard Deviations for the Watervliet IW-1 Cell

Table 4.2.8 presents the concentrations estimated by the numerical solution along with their respective standard deviations.

Time (day)	Mean (μg/l)	Standard Deviation (μg/l)	Time (day)	Mean (μg/l)	Standard Deviation (μg/l)
1	1.90E+03	1.72E+02	51	1.01E+00	7.74E-01
2	1.61E+03	1.85E+02	52	1.00E+00	7.68E-01
3	1.28E+03	1.83E+02	53	1.00E+00	7.62E-01
4	9.74E+02	1.67E+02	54	1.00E+00	7.57E-01
5	7.17E+02	1.43E+02	55	1.00E+00	7.53E-01
6	5.16E+02	1.19E+02	56	1.00E+00	7.49E-01
7	3.67E+02	9.55E+01	57	1.01E+00	7.46E-01
8	2.60E+02	7.56E+01	58	1.01E+00	7.43E-01
9	1.84E+02	5.93E+01	59	1.02E+00	7.41E-01
10	1.31E+02	4.63E+01	60	1.02E+00	7.39E-01
11	9.35E+01	3.61E+01	61	1.03E+00	7.38E-01
12	6.76E+01	2.82E+01	62	1.03E+00	7.37E-01
13	4.95E+01	2.21E+01	63	1.04E+00	7.36E-01
14	3.67E+01	1.75E+01	64	1.05E+00	7.36E-01
15	2.77E+01	1.40E+01	65	1.06E+00	7.36E-01
16	2.11E+01	1.12E+01	66	1.06E+00	7.36E-01
17	1.64E+01	9.15E+00	67	1.07E+00	7.36E-01
18	1.29E+01	7.52E+00	68	1.08E+00	7.36E-01
19	1.03E+01	6.25E+00	69	1.09E+00	7.37E-01
20	8.39E+00	5.25E+00	70	1.10E+00	7.38E-01
21	6.90E+00	4.46E+00	71	1.11E+00	7.39E-01
22	5.76E+00	3.82E+00	72	1.12E+00	7.40E-01
23	4.87E+00	3.32E+00	73	1.14E+00	7.41E-01
24	4.17E+00	2.90E+00	74	1.15E+00	7.43E-01
25	3.62E+00	2.57E+00	75	1.16E+00	7.44E-01
26	3.17E+00	2.29E+00	76	1.17E+00	7.46E-01
27	2.81E+00	2.06E+00	77	1.18E+00	7.48E-01
28	2.51E+00	1.87E+00	78	1.20E+00	7.50E-01
29	2.27E+00	1.71E+00	79	1.21E+00	7.52E-01
30	2.07E+00	1.58E+00	80	1.22E+00	7.54E-01
31	1.90E+00	1.46E+00	81	1.23E+00	7.57E-01
32	1.76E+00	1.37E+00	82	1.25E+00	7.59E-01
33	1.64E+00	1.28E+00	83	1.26E+00	7.62E-01
34	1.54E+00	1.21E+00	84	1.28E+00	7.65E-01
35	1.46E+00	1.15E+00	85	1.29E+00	7.67E-01
36	1.38E+00	1.10E+00	86	1.30E+00	7.70E-01
37	1.32E+00	1.05E+00	87	1.32E+00	7.73E-01
38	1.27E+00	1.01E+00	88	1.33E+00	7.77E-01
39	1.22E+00	9.75E-01	89	1.35E+00	7.80E-01
40	1.18E+00	9.45E-01	90	1.36E+00	7.83E-01
41	1.15E+00	9.17E-01	91	1.38E+00	7.87E-01
42	1.12E+00	8.94E-01	92	1.40E+00	7.90E-01
43	1.10E+00	8.73E-01	93	1.41E+00	7.94E-01
44	1.08E+00	8.54E-01	94	1.43E+00	7.98E-01
45	1.06E+00	8.38E-01	95	1.44E+00	8.02E-01
46	1.05E+00	8.24E-01	96	1.46E+00	8.06E-01
47	1.03E+00	8.11E-01	97	1.48E+00	8.10E-01
48	1.02E+00	8.00E-01	98	1.49E+00	8.14E-01
49	1.02E+00	7.90E-01	99	1.51E+00	8.19E-01
50	1.01E+00	7.82E-01	100	1.53E+00	8.23E-01

Table 4.2.8: Standard Deviations for the Watervliet IW-1 Cell Continued

Time (day)	Mean (µg/l)	Standard Deviation (µg/l)	Time (day)	Mean (µg/l)	Standard Deviation (µg/l)
101	1.55E+00	8.28E-01	151	2.65E+00	1.23E+00
102	1.56E+00	8.33E-01	152	2.68E+00	1.24E+00
103	1.58E+00	8.38E-01	153	2.71E+00	1.25E+00
104	1.60E+00	8.43E-01	154	2.73E+00	1.27E+00
105	1.62E+00	8.48E-01	155	2.76E+00	1.28E+00
106	1.64E+00	8.53E-01	156	2.79E+00	1.29E+00
107	1.65E+00	8.58E-01	157	2.82E+00	1.30E+00
108	1.67E+00	8.64E-01	158	2.85E+00	1.31E+00
109	1.69E+00	8.70E-01	159	2.87E+00	1.33E+00
110	1.71E+00	8.75E-01	160	2.90E+00	1.34E+00
111	1.73E+00	8.81E-01	161	2.93E+00	1.35E+00
112	1.75E+00	8.87E-01	162	2.96E+00	1.37E+00
113	1.77E+00	8.93E-01	163	2.99E+00	1.38E+00
114	1.79E+00	9.00E-01	164	3.02E+00	1.39E+00
115	1.81E+00	9.06E-01	165	3.05E+00	1.41E+00
116	1.83E+00	9.13E-01	166	3.08E+00	1.42E+00
117	1.85E+00	9.19E-01	167	3.11E+00	1.43E+00
118	1.87E+00	9.26E-01	168	3.14E+00	1.45E+00
119	1.89E+00	9.33E-01	169	3.17E+00	1.46E+00
120	1.91E+00	9.40E-01	170	3.20E+00	1.48E+00
121	1.93E+00	9.48E-01	171	3.23E+00	1.49E+00
122	1.95E+00	9.55E-01	172	3.26E+00	1.50E+00
123	1.98E+00	9.62E-01	173	3.29E+00	1.52E+00
124	2.00E+00	9.70E-01	174	3.32E+00	1.53E+00
125	2.02E+00	9.78E-01	175	3.35E+00	1.55E+00
126	2.04E+00	9.86E-01	176	3.39E+00	1.56E+00
127	2.06E+00	9.94E-01	177	3.42E+00	1.58E+00
128	2.09E+00	1.00E+00	178	3.45E+00	1.59E+00
129	2.11E+00	1.01E+00	179	3.48E+00	1.61E+00
130	2.13E+00	1.02E+00	180	3.52E+00	1.63E+00
131	2.15E+00	1.03E+00	181	3.55E+00	1.64E+00
132	2.18E+00	1.04E+00	182	3.58E+00	1.66E+00
133	2.20E+00	1.05E+00	183	3.61E+00	1.67E+00
134	2.22E+00	1.05E+00	184	3.65E+00	1.69E+00
135	2.25E+00	1.06E+00	185	3.68E+00	1.71E+00
136	2.27E+00	1.07E+00	186	3.71E+00	1.72E+00
137	2.30E+00	1.08E+00	187	3.75E+00	1.74E+00
138	2.32E+00	1.09E+00	188	3.78E+00	1.76E+00
139	2.34E+00	1.10E+00	189	3.82E+00	1.77E+00
140	2.37E+00	1.11E+00	190	3.85E+00	1.79E+00
141	2.39E+00	1.12E+00	191	3.89E+00	1.81E+00
142	2.42E+00	1.13E+00	192	3.92E+00	1.82E+00
143	2.44E+00	1.14E+00	193	3.96E+00	1.84E+00
144	2.47E+00	1.15E+00	194	3.99E+00	1.86E+00
145	2.50E+00	1.16E+00	195	4.03E+00	1.88E+00
146	2.52E+00	1.17E+00	196	4.06E+00	1.89E+00
147	2.55E+00	1.18E+00	197	4.10E+00	1.91E+00
148	2.57E+00	1.20E+00	198	4.14E+00	1.93E+00
149	2.60E+00	1.21E+00	199	4.17E+00	1.95E+00
150	2.63E+00	1.22E+00	200	4.21E+00	1.97E+00

Table 4.2.8: Standard Deviations for the Watervliet IW-1 Cell Continued

Time (day)	Mean (µg/l)	Standard Deviation (µg/l)	Time (day)	Mean (µg/l)	Standard Deviation (µg/l)
201	4.25E+00	1.99E+00	251	6.37E+00	3.10E+00
202	4.28E+00	2.01E+00	252	6.42E+00	3.12E+00
203	4.32E+00	2.02E+00	253	6.47E+00	3.15E+00
204	4.36E+00	2.04E+00	254	6.52E+00	3.17E+00
205	4.40E+00	2.06E+00	255	6.56E+00	3.20E+00
206	4.43E+00	2.08E+00	256	6.61E+00	3.23E+00
207	4.47E+00	2.10E+00	257	6.66E+00	3.25E+00
208	4.51E+00	2.12E+00	258	6.71E+00	3.28E+00
209	4.55E+00	2.14E+00	259	6.76E+00	3.31E+00
210	4.59E+00	2.16E+00	260	6.81E+00	3.33E+00
211	4.63E+00	2.18E+00	261	6.86E+00	3.36E+00
212	4.67E+00	2.20E+00	262	6.91E+00	3.39E+00
213	4.71E+00	2.22E+00	263	6.96E+00	3.41E+00
214	4.75E+00	2.24E+00	264	7.02E+00	3.44E+00
215	4.79E+00	2.26E+00	265	7.07E+00	3.47E+00
216	4.83E+00	2.28E+00	266	7.12E+00	3.50E+00
217	4.87E+00	2.30E+00	267	7.17E+00	3.52E+00
218	4.91E+00	2.33E+00	268	7.22E+00	3.55E+00
219	4.95E+00	2.35E+00	269	7.27E+00	3.58E+00
220	4.99E+00	2.37E+00	270	7.33E+00	3.61E+00
221	5.03E+00	2.39E+00	271	7.38E+00	3.64E+00
222	5.07E+00	2.41E+00	272	7.43E+00	3.67E+00
223	5.11E+00	2.43E+00	273	7.49E+00	3.70E+00
224	5.15E+00	2.45E+00	274	7.54E+00	3.72E+00
225	5.20E+00	2.48E+00	275	7.59E+00	3.75E+00
226	5.24E+00	2.50E+00	276	7.65E+00	3.78E+00
227	5.28E+00	2.52E+00	277	7.70E+00	3.81E+00
228	5.32E+00	2.54E+00	278	7.76E+00	3.84E+00
229	5.37E+00	2.56E+00	279	7.81E+00	3.87E+00
230	5.41E+00	2.59E+00	280	7.87E+00	3.90E+00
231	5.45E+00	2.61E+00	281	7.92E+00	3.93E+00
232	5.50E+00	2.63E+00	282	7.98E+00	3.96E+00
233	5.54E+00	2.66E+00	283	8.03E+00	3.99E+00
234	5.59E+00	2.68E+00	284	8.09E+00	4.02E+00
235	5.63E+00	2.70E+00	285	8.14E+00	4.05E+00
236	5.67E+00	2.73E+00	286	8.20E+00	4.08E+00
237	5.72E+00	2.75E+00	287	8.26E+00	4.11E+00
238	5.76E+00	2.77E+00	288	8.31E+00	4.14E+00
239	5.81E+00	2.80E+00	289	8.37E+00	4.18E+00
240	5.85E+00	2.82E+00	290	8.43E+00	4.21E+00
241	5.90E+00	2.85E+00	291	8.49E+00	4.24E+00
242	5.95E+00	2.87E+00	292	8.54E+00	4.27E+00
243	5.99E+00	2.89E+00	293	8.60E+00	4.30E+00
244	6.04E+00	2.92E+00	294	8.66E+00	4.33E+00
245	6.09E+00	2.94E+00	295	8.72E+00	4.36E+00
246	6.13E+00	2.97E+00	296	8.78E+00	4.40E+00
247	6.18E+00	2.99E+00	297	8.84E+00	4.43E+00
248	6.23E+00	3.02E+00	298	8.90E+00	4.46E+00
249	6.27E+00	3.04E+00	299	8.96E+00	4.49E+00
250	6.32E+00	3.07E+00	300	9.02E+00	4.53E+00

Table 4.2.8: Standard Deviations for the Watervliet IW-1 Cell Continued

Time (day)	Mean (µg/l)	Standard Deviation (µg/l)	Time (day)	Mean (µg/l)	Standard Deviation (µg/l)
301	9.08E+00	4.56E+00	351	1.24E+01	6.41E+00
302	9.14E+00	4.59E+00	352	1.25E+01	6.45E+00
303	9.20E+00	4.63E+00	353	1.26E+01	6.49E+00
304	9.26E+00	4.66E+00	354	1.26E+01	6.53E+00
305	9.32E+00	4.69E+00	355	1.27E+01	6.57E+00
306	9.38E+00	4.73E+00	356	1.28E+01	6.62E+00
307	9.44E+00	4.76E+00	357	1.29E+01	6.66E+00
308	9.50E+00	4.79E+00	358	1.29E+01	6.70E+00
309	9.57E+00	4.83E+00	359	1.30E+01	6.74E+00
310	9.63E+00	4.86E+00	360	1.31E+01	6.78E+00
311	9.69E+00	4.90E+00	361	1.32E+01	6.83E+00
312	9.76E+00	4.93E+00	362	1.32E+01	6.87E+00
313	9.82E+00	4.97E+00	363	1.33E+01	6.91E+00
314	9.88E+00	5.00E+00	364	1.34E+01	6.95E+00
315	9.95E+00	5.04E+00	365	1.35E+01	7.00E+00
316	1.00E+01	5.07E+00	366	1.36E+01	7.04E+00
317	1.01E+01	5.11E+00	367	1.36E+01	7.08E+00
318	1.01E+01	5.14E+00	368	1.37E+01	7.13E+00
319	1.02E+01	5.18E+00	369	1.38E+01	7.17E+00
320	1.03E+01	5.21E+00	370	1.39E+01	7.22E+00
321	1.03E+01	5.25E+00	371	1.39E+01	7.26E+00
322	1.04E+01	5.29E+00	372	1.40E+01	7.30E+00
323	1.05E+01	5.32E+00	373	1.41E+01	7.35E+00
324	1.05E+01	5.36E+00	374	1.42E+01	7.39E+00
325	1.06E+01	5.39E+00	375	1.43E+01	7.44E+00
326	1.07E+01	5.43E+00	376	1.43E+01	7.48E+00
327	1.07E+01	5.47E+00	377	1.44E+01	7.53E+00
328	1.08E+01	5.51E+00	378	1.45E+01	7.57E+00
329	1.09E+01	5.54E+00	379	1.46E+01	7.62E+00
330	1.09E+01	5.58E+00	380	1.47E+01	7.66E+00
331	1.10E+01	5.62E+00	381	1.48E+01	7.71E+00
332	1.11E+01	5.66E+00	382	1.48E+01	7.76E+00
333	1.11E+01	5.70E+00	383	1.49E+01	7.80E+00
334	1.12E+01	5.74E+00	384	1.50E+01	7.85E+00
335	1.13E+01	5.78E+00	385	1.51E+01	7.89E+00
336	1.13E+01	5.82E+00	386	1.52E+01	7.94E+00
337	1.14E+01	5.85E+00	387	1.53E+01	7.99E+00
338	1.15E+01	5.89E+00	388	1.53E+01	8.03E+00
339	1.16E+01	5.93E+00	389	1.54E+01	8.08E+00
340	1.16E+01	5.97E+00	390	1.55E+01	8.13E+00
341	1.17E+01	6.01E+00	391	1.56E+01	8.18E+00
342	1.18E+01	6.05E+00	392	1.57E+01	8.22E+00
343	1.18E+01	6.09E+00	393	1.58E+01	8.27E+00
344	1.19E+01	6.13E+00	394	1.58E+01	8.32E+00
345	1.20E+01	6.17E+00	395	1.59E+01	8.37E+00
346	1.20E+01	6.21E+00	396	1.60E+01	8.42E+00
347	1.21E+01	6.25E+00	397	1.61E+01	8.46E+00
348	1.22E+01	6.29E+00	398	1.62E+01	8.51E+00
349	1.23E+01	6.33E+00	399	1.63E+01	8.56E+00
350	1.23E+01	6.37E+00	400	1.64E+01	8.61E+00

Table 4.2.8: Standard Deviations for the Watervliet IW-1 Cell Continued

Time (day)	Mean (µg/l)	Standard Deviation (µg/l)	Time (day)	Mean (µg/l)	Standard Deviation (µg/l)
401	1.65E+01	8.66E+00	451	2.95E+01	1.30E+02
402	1.65E+01	8.71E+00	452	2.87E+01	1.16E+02
403	1.66E+01	8.76E+00	453	2.74E+01	9.48E+01
404	1.67E+01	8.81E+00	454	2.61E+01	7.28E+01
405	1.68E+01	8.86E+00	455	2.50E+01	5.36E+01
406	1.69E+01	8.91E+00	456	2.41E+01	3.86E+01
407	1.70E+01	8.96E+00	457	2.35E+01	2.77E+01
408	1.71E+01	9.01E+00	458	2.31E+01	2.06E+01
409	1.72E+01	9.06E+00	459	2.28E+01	1.62E+01
410	1.73E+01	9.11E+00	460	2.27E+01	1.39E+01
411	1.74E+01	9.16E+00	461	2.26E+01	1.28E+01
412	1.74E+01	9.21E+00	462	2.26E+01	1.23E+01
413	1.75E+01	9.26E+00	463	2.26E+01	1.22E+01
414	1.76E+01	9.32E+00	464	2.28E+01	1.22E+01
415	1.77E+01	9.37E+00	465	2.28E+01	1.22E+01
416	1.78E+01	9.42E+00	466	2.28E+01	1.22E+01
417	2.21E+01	9.25E+01	467	2.29E+01	1.23E+01
418	2.17E+01	8.18E+01	468	2.30E+01	1.24E+01
419	2.11E+01	6.65E+01	469	2.31E+01	1.25E+01
420	2.04E+01	5.07E+01	470	2.32E+01	1.25E+01
421	1.99E+01	3.71E+01	471	2.33E+01	1.26E+01
422	1.95E+01	2.66E+01	472	2.35E+01	1.27E+01
423	1.92E+01	1.93E+01	473	2.36E+01	1.27E+01
424	1.91E+01	1.47E+01	474	2.37E+01	1.28E+01
425	1.90E+01	1.21E+01	475	2.38E+01	1.29E+01
426	1.90E+01	1.09E+01	476	2.39E+01	1.29E+01
427	1.90E+01	1.04E+01	477	2.40E+01	1.30E+01
428	1.91E+01	1.02E+01	478	2.41E+01	1.31E+01
429	1.91E+01	1.01E+01	479	2.42E+01	1.31E+01
430	1.92E+01	1.02E+01	480	2.43E+01	1.32E+01
431	1.93E+01	1.02E+01	481	2.45E+01	1.33E+01
432	1.94E+01	1.03E+01	482	2.46E+01	1.33E+01
433	1.94E+01	1.03E+01	483	2.47E+01	1.34E+01
434	1.95E+01	1.04E+01	484	2.48E+01	1.35E+01
435	1.96E+01	1.04E+01	485	2.49E+01	1.35E+01
436	1.97E+01	1.05E+01	486	2.50E+01	1.36E+01
437	1.98E+01	1.06E+01	487	2.52E+01	1.37E+01
438	1.99E+01	1.06E+01	488	2.53E+01	1.37E+01
439	2.00E+01	1.07E+01	489	2.54E+01	1.38E+01
440	2.01E+01	1.07E+01	490	2.55E+01	1.39E+01
441	2.02E+01	1.08E+01	491	2.56E+01	1.39E+01
442	2.03E+01	1.08E+01	492	2.57E+01	1.40E+01
443	2.04E+01	1.09E+01	493	2.59E+01	1.41E+01
444	2.05E+01	1.10E+01	494	2.60E+01	1.41E+01
445	2.06E+01	1.10E+01	495	2.61E+01	1.42E+01
446	2.07E+01	1.11E+01	496	2.62E+01	1.43E+01
447	2.08E+01	1.11E+01	497	2.63E+01	1.43E+01
448	2.09E+01	1.12E+01	498	2.65E+01	1.44E+01
449	2.10E+01	1.13E+01	499	2.66E+01	1.45E+01
450	2.11E+01	1.13E+01	500	2.67E+01	1.45E+01

Table 4.2.8: Standard Deviations for the Watervliet IW-1 Cell Continued

Time (day)	Mean (µg/l)	Standard Deviation (µg/l)	Time (day)	Mean (µg/l)	Standard Deviation (µg/l)
501	2.68E+01	1.46E+01	551	3.34E+01	1.83E+01
502	2.69E+01	1.47E+01	552	3.35E+01	1.84E+01
503	2.71E+01	1.47E+01	553	3.37E+01	1.85E+01
504	2.72E+01	1.48E+01	554	3.38E+01	1.86E+01
505	2.73E+01	1.49E+01	555	3.39E+01	1.86E+01
506	2.74E+01	1.50E+01	556	3.41E+01	1.87E+01
507	2.76E+01	1.50E+01	557	3.42E+01	1.88E+01
508	2.77E+01	1.51E+01	558	3.44E+01	1.89E+01
509	2.78E+01	1.52E+01	559	3.45E+01	1.90E+01
510	2.79E+01	1.52E+01	560	3.47E+01	1.91E+01
511	2.81E+01	1.53E+01	561	3.48E+01	1.91E+01
512	2.82E+01	1.54E+01	562	3.49E+01	1.92E+01
513	2.83E+01	1.54E+01	563	3.51E+01	1.93E+01
514	2.84E+01	1.55E+01	564	3.52E+01	1.94E+01
515	2.86E+01	1.56E+01	565	3.54E+01	1.95E+01
516	2.87E+01	1.57E+01	566	3.55E+01	1.96E+01
517	2.88E+01	1.57E+01	567	3.57E+01	1.96E+01
518	2.89E+01	1.58E+01	568	3.58E+01	1.97E+01
519	2.91E+01	1.59E+01	569	3.60E+01	1.98E+01
520	2.92E+01	1.60E+01	570	3.60E+01	1.98E+01
521	2.93E+01	1.60E+01			
522	2.95E+01	1.61E+01			
523	2.96E+01	1.62E+01			
524	2.97E+01	1.62E+01			
525	2.98E+01	1.63E+01			
526	3.00E+01	1.64E+01			
527	3.01E+01	1.65E+01			
528	3.02E+01	1.65E+01			
529	3.04E+01	1.66E+01			
530	3.05E+01	1.67E+01			
531	3.06E+01	1.68E+01			
532	3.08E+01	1.68E+01			
533	3.09E+01	1.69E+01			
534	3.10E+01	1.70E+01			
535	3.12E+01	1.71E+01			
536	3.13E+01	1.72E+01			
537	3.14E+01	1.72E+01			
538	3.16E+01	1.73E+01			
539	3.17E+01	1.74E+01			
540	3.18E+01	1.75E+01			
541	3.20E+01	1.75E+01			
542	3.21E+01	1.76E+01			
543	3.23E+01	1.77E+01			
544	3.24E+01	1.78E+01			
545	3.25E+01	1.78E+01			
546	3.27E+01	1.79E+01			
547	3.28E+01	1.80E+01			
548	3.29E+01	1.81E+01			
549	3.31E+01	1.82E+01			
550	3.32E+01	1.82E+01			

Table 4.2.9: Standard Deviations for the Watervliet IW4 Cell

Table 4.2.9 presents the concentrations estimated by the numerical solution along with their respective standard deviations.

Time (day)	Mean (µg/l)	Standard Deviation (µg/l)	Time (day)	Mean (µg/l)	Standard Deviation (µg/l)
1	7.25E+00	1.45E+01	51	1.46E-02	3.34E-02
2	2.15E+00	4.34E+00	52	1.62E-02	3.70E-02
3	2.81E-01	5.89E-01	53	1.79E-02	4.09E-02
4	2.22E-02	4.97E-02	54	1.98E-02	4.52E-02
5	1.37E-03	3.28E-03	55	2.18E-02	4.99E-02
6	1.68E-04	3.72E-04	56	2.40E-02	5.50E-02
7	1.18E-04	2.67E-04	57	2.64E-02	6.05E-02
8	1.25E-04	2.86E-04	58	2.90E-02	6.64E-02
9	1.37E-04	3.12E-04	59	3.18E-02	7.29E-02
10	1.52E-04	3.47E-04	60	3.49E-02	7.98E-02
11	1.68E-04	3.84E-04	61	3.81E-02	8.73E-02
12	1.87E-04	4.27E-04	62	4.17E-02	9.53E-02
13	2.09E-04	4.78E-04	63	4.54E-02	1.04E-01
14	2.31E-04	5.26E-04	64	4.94E-02	1.13E-01
15	2.57E-04	5.87E-04	65	5.37E-02	1.23E-01
16	2.89E-04	6.59E-04	66	5.82E-02	1.33E-01
17	3.22E-04	7.37E-04	67	6.31E-02	1.45E-01
18	3.62E-04	8.27E-04	68	6.82E-02	1.56E-01
19	4.03E-04	9.21E-04	69	7.36E-02	1.69E-01
20	4.53E-04	1.04E-03	70	7.94E-02	1.82E-01
21	5.09E-04	1.16E-03	71	8.54E-02	1.96E-01
22	5.71E-04	1.30E-03	72	9.17E-02	2.10E-01
23	6.39E-04	1.46E-03	73	9.84E-02	2.26E-01
24	7.18E-04	1.64E-03	74	1.05E-01	2.42E-01
25	8.07E-04	1.84E-03	75	1.13E-01	2.58E-01
26	9.02E-04	2.06E-03	76	1.20E-01	2.76E-01
27	1.01E-03	2.32E-03	77	1.28E-01	2.94E-01
28	1.14E-03	2.60E-03	78	1.36E-01	3.13E-01
29	1.28E-03	2.92E-03	79	1.45E-01	3.33E-01
30	1.43E-03	3.28E-03	80	1.54E-01	3.53E-01
31	1.61E-03	3.68E-03	81	1.63E-01	3.74E-01
32	1.80E-03	4.12E-03	82	1.73E-01	3.96E-01
33	2.02E-03	4.62E-03	83	1.83E-01	4.19E-01
34	2.27E-03	5.19E-03	84	1.93E-01	4.42E-01
35	2.54E-03	5.81E-03	85	2.03E-01	4.66E-01
36	2.85E-03	6.51E-03	86	2.14E-01	4.91E-01
37	3.19E-03	7.29E-03	87	2.25E-01	5.17E-01
38	3.57E-03	8.17E-03	88	2.36E-01	5.43E-01
39	4.00E-03	9.14E-03	89	2.48E-01	5.70E-01
40	4.47E-03	1.02E-02	90	2.60E-01	5.97E-01
41	5.00E-03	1.14E-02	91	2.72E-01	6.25E-01
42	5.59E-03	1.28E-02	92	2.85E-01	6.54E-01
43	6.24E-03	1.43E-02	93	2.97E-01	6.83E-01
44	6.96E-03	1.59E-02	94	3.10E-01	7.13E-01
45	7.76E-03	1.77E-02	95	3.24E-01	7.44E-01
46	8.64E-03	1.98E-02	96	3.37E-01	7.75E-01
47	9.62E-03	2.20E-02	97	3.51E-01	8.07E-01
48	1.07E-02	2.45E-02	98	3.65E-01	8.40E-01
49	1.19E-02	2.72E-02	99	3.79E-01	8.73E-01
50	1.32E-02	3.02E-02	100	3.94E-01	9.06E-01

Table 4.2.9: Standard Deviations for the Watervliet IW4 Cell Continued

Time (day)	Mean (µg/l)	Standard Deviation (µg/l)	Time (day)	Mean (µg/l)	Standard Deviation (µg/l)
101	4.09E-01	9.40E-01	151	1.42E+00	3.27E+00
102	4.24E-01	9.75E-01	152	1.44E+00	3.33E+00
103	4.39E-01	1.01E+00	153	1.47E+00	3.39E+00
104	4.55E-01	1.05E+00	154	1.50E+00	3.45E+00
105	4.70E-01	1.08E+00	155	1.52E+00	3.51E+00
106	4.86E-01	1.12E+00	156	1.55E+00	3.57E+00
107	5.03E-01	1.16E+00	157	1.57E+00	3.63E+00
108	5.19E-01	1.19E+00	158	1.60E+00	3.69E+00
109	5.36E-01	1.23E+00	159	1.63E+00	3.75E+00
110	5.53E-01	1.27E+00	160	1.65E+00	3.82E+00
111	5.70E-01	1.31E+00	161	1.68E+00	3.88E+00
112	5.87E-01	1.35E+00	162	1.71E+00	3.94E+00
113	6.04E-01	1.39E+00	163	1.74E+00	4.01E+00
114	6.22E-01	1.43E+00	164	1.76E+00	4.07E+00
115	6.40E-01	1.47E+00	165	1.79E+00	4.13E+00
116	6.58E-01	1.52E+00	166	1.82E+00	4.20E+00
117	6.77E-01	1.56E+00	167	1.85E+00	4.26E+00
118	6.95E-01	1.60E+00	168	1.88E+00	4.33E+00
119	7.14E-01	1.64E+00	169	1.91E+00	4.40E+00
120	7.33E-01	1.69E+00	170	1.94E+00	4.46E+00
121	7.52E-01	1.73E+00	171	1.97E+00	4.53E+00
122	7.71E-01	1.78E+00	172	1.99E+00	4.60E+00
123	7.91E-01	1.82E+00	173	2.02E+00	4.67E+00
124	8.11E-01	1.87E+00	174	2.05E+00	4.74E+00
125	8.31E-01	1.91E+00	175	2.08E+00	4.81E+00
126	8.51E-01	1.96E+00	176	2.11E+00	4.88E+00
127	8.71E-01	2.01E+00	177	2.15E+00	4.95E+00
128	8.92E-01	2.05E+00	178	2.18E+00	5.02E+00
129	9.13E-01	2.10E+00	179	2.21E+00	5.09E+00
130	9.34E-01	2.15E+00	180	2.24E+00	5.16E+00
131	9.55E-01	2.20E+00	181	2.27E+00	5.23E+00
132	9.76E-01	2.25E+00	182	2.30E+00	5.31E+00
133	9.98E-01	2.30E+00	183	2.33E+00	5.38E+00
134	1.02E+00	2.35E+00	184	2.36E+00	5.45E+00
135	1.04E+00	2.40E+00	185	2.40E+00	5.53E+00
136	1.06E+00	2.45E+00	186	2.43E+00	5.60E+00
137	1.09E+00	2.50E+00	187	2.46E+00	5.68E+00
138	1.11E+00	2.55E+00	188	2.49E+00	5.75E+00
139	1.13E+00	2.61E+00	189	2.53E+00	5.83E+00
140	1.15E+00	2.66E+00	190	2.56E+00	5.91E+00
141	1.18E+00	2.71E+00	191	2.59E+00	5.98E+00
142	1.20E+00	2.77E+00	192	2.63E+00	6.06E+00
143	1.22E+00	2.82E+00	193	2.66E+00	6.14E+00
144	1.25E+00	2.88E+00	194	2.70E+00	6.22E+00
145	1.27E+00	2.93E+00	195	2.73E+00	6.30E+00
146	1.30E+00	2.99E+00	196	2.77E+00	6.38E+00
147	1.32E+00	3.04E+00	197	2.80E+00	6.46E+00
148	1.34E+00	3.10E+00	198	2.84E+00	6.54E+00
149	1.37E+00	3.16E+00	199	2.87E+00	6.62E+00
150	1.39E+00	3.21E+00	200	2.91E+00	6.70E+00

Table 4.2.9: Standard Deviations for the Watervliet IW4 Cell Continued

Time (day)	Mean (µg/l)	Standard Deviation (µg/l)	Time (day)	Mean (µg/l)	Standard Deviation (µg/l)
201	2.94E+00	6.79E+00	251	5.02E+00	1.16E+01
202	2.98E+00	6.87E+00	252	5.07E+00	1.17E+01
203	3.01E+00	6.95E+00	253	5.12E+00	1.18E+01
204	3.05E+00	7.04E+00	254	5.17E+00	1.19E+01
205	3.09E+00	7.12E+00	255	5.21E+00	1.20E+01
206	3.12E+00	7.21E+00	256	5.26E+00	1.21E+01
207	3.16E+00	7.29E+00	257	5.31E+00	1.23E+01
208	3.20E+00	7.38E+00	258	5.36E+00	1.24E+01
209	3.24E+00	7.46E+00	259	5.41E+00	1.25E+01
210	3.27E+00	7.55E+00	260	5.46E+00	1.26E+01
211	3.31E+00	7.64E+00	261	5.51E+00	1.27E+01
212	3.35E+00	7.73E+00	262	5.56E+00	1.28E+01
213	3.39E+00	7.82E+00	263	5.61E+00	1.29E+01
214	3.43E+00	7.90E+00	264	5.66E+00	1.31E+01
215	3.47E+00	7.99E+00	265	5.71E+00	1.32E+01
216	3.50E+00	8.08E+00	266	5.76E+00	1.33E+01
217	3.54E+00	8.18E+00	267	5.82E+00	1.34E+01
218	3.58E+00	8.27E+00	268	5.87E+00	1.35E+01
219	3.62E+00	8.36E+00	269	5.92E+00	1.37E+01
220	3.66E+00	8.45E+00	270	5.97E+00	1.38E+01
221	3.70E+00	8.54E+00	271	6.02E+00	1.39E+01
222	3.74E+00	8.64E+00	272	6.08E+00	1.40E+01
223	3.79E+00	8.73E+00	273	6.13E+00	1.41E+01
224	3.83E+00	8.83E+00	274	6.18E+00	1.43E+01
225	3.87E+00	8.92E+00	275	6.24E+00	1.44E+01
226	3.91E+00	9.02E+00	276	6.29E+00	1.45E+01
227	3.95E+00	9.11E+00	277	6.35E+00	1.46E+01
228	3.99E+00	9.21E+00	278	6.40E+00	1.48E+01
229	4.03E+00	9.31E+00	279	6.45E+00	1.49E+01
230	4.08E+00	9.41E+00	280	6.51E+00	1.50E+01
231	4.12E+00	9.50E+00	281	6.56E+00	1.51E+01
232	4.16E+00	9.60E+00	282	6.62E+00	1.53E+01
233	4.21E+00	9.70E+00	283	6.68E+00	1.54E+01
234	4.25E+00	9.80E+00	284	6.73E+00	1.55E+01
235	4.29E+00	9.90E+00	285	6.79E+00	1.57E+01
236	4.34E+00	1.00E+01	286	6.84E+00	1.58E+01
237	4.38E+00	1.01E+01	287	6.90E+00	1.59E+01
238	4.42E+00	1.02E+01	288	6.96E+00	1.61E+01
239	4.47E+00	1.03E+01	289	7.02E+00	1.62E+01
240	4.51E+00	1.04E+01	290	7.07E+00	1.63E+01
241	4.56E+00	1.05E+01	291	7.13E+00	1.65E+01
242	4.60E+00	1.06E+01	292	7.19E+00	1.66E+01
243	4.65E+00	1.07E+01	293	7.25E+00	1.67E+01
244	4.70E+00	1.08E+01	294	7.31E+00	1.69E+01
245	4.74E+00	1.09E+01	295	7.36E+00	1.70E+01
246	4.79E+00	1.10E+01	296	7.42E+00	1.71E+01
247	4.83E+00	1.12E+01	297	7.48E+00	1.73E+01
248	4.88E+00	1.13E+01	298	7.54E+00	1.74E+01
249	4.93E+00	1.14E+01	299	7.60E+00	1.75E+01
250	4.98E+00	1.15E+01	300	7.66E+00	1.77E+01

Table 4.2.9: Standard Deviations for the Watervliet IW4 Cell Continued

Time (day)	Mean (µg/l)	Standard Deviation (µg/l)	Time (day)	Mean (µg/l)	Standard Deviation (µg/l)
301	7.72E+00	1.78E+01	351	1.11E+01	2.56E+01
302	7.78E+00	1.80E+01	352	1.12E+01	2.58E+01
303	7.85E+00	1.81E+01	353	1.13E+01	2.60E+01
304	7.91E+00	1.82E+01	354	1.13E+01	2.62E+01
305	7.97E+00	1.84E+01	355	1.14E+01	2.63E+01
306	8.03E+00	1.85E+01	356	1.15E+01	2.65E+01
307	8.09E+00	1.87E+01	357	1.16E+01	2.67E+01
308	8.15E+00	1.88E+01	358	1.16E+01	2.69E+01
309	8.22E+00	1.90E+01	359	1.17E+01	2.71E+01
310	8.28E+00	1.91E+01	360	1.18E+01	2.72E+01
311	8.34E+00	1.93E+01	361	1.19E+01	2.74E+01
312	8.41E+00	1.94E+01	362	1.20E+01	2.76E+01
313	8.47E+00	1.95E+01	363	1.20E+01	2.78E+01
314	8.54E+00	1.97E+01	364	1.21E+01	2.80E+01
315	8.60E+00	1.98E+01	365	1.22E+01	2.81E+01
316	8.66E+00	2.00E+01	366	1.23E+01	2.83E+01
317	8.73E+00	2.01E+01	367	1.24E+01	2.85E+01
318	8.80E+00	2.03E+01	368	1.24E+01	2.87E+01
319	8.86E+00	2.04E+01	369	1.25E+01	2.89E+01
320	8.93E+00	2.06E+01	370	1.26E+01	2.91E+01
321	8.99E+00	2.08E+01	371	1.27E+01	2.93E+01
322	9.06E+00	2.09E+01	372	1.28E+01	2.95E+01
323	9.13E+00	2.11E+01	373	1.28E+01	2.96E+01
324	9.19E+00	2.12E+01	374	1.29E+01	2.98E+01
325	9.26E+00	2.14E+01	375	1.30E+01	3.00E+01
326	9.33E+00	2.15E+01	376	1.31E+01	3.02E+01
327	9.40E+00	2.17E+01	377	1.32E+01	3.04E+01
328	9.46E+00	2.18E+01	378	1.33E+01	3.06E+01
329	9.53E+00	2.20E+01	379	1.33E+01	3.08E+01
330	9.60E+00	2.22E+01	380	1.34E+01	3.10E+01
331	9.67E+00	2.23E+01	381	1.35E+01	3.12E+01
332	9.74E+00	2.25E+01	382	1.36E+01	3.14E+01
333	9.81E+00	2.26E+01	383	1.37E+01	3.16E+01
334	9.88E+00	2.28E+01	384	1.38E+01	3.18E+01
335	9.95E+00	2.30E+01	385	1.39E+01	3.20E+01
336	1.00E+01	2.31E+01	386	1.39E+01	3.22E+01
337	1.01E+01	2.33E+01	387	1.40E+01	3.24E+01
338	1.02E+01	2.34E+01	388	1.41E+01	3.26E+01
339	1.02E+01	2.36E+01	389	1.42E+01	3.28E+01
340	1.03E+01	2.38E+01	390	1.43E+01	3.30E+01
341	1.04E+01	2.39E+01	391	1.44E+01	3.32E+01
342	1.04E+01	2.41E+01	392	1.45E+01	3.34E+01
343	1.05E+01	2.43E+01	393	1.46E+01	3.36E+01
344	1.06E+01	2.44E+01	394	1.46E+01	3.38E+01
345	1.07E+01	2.46E+01	395	1.47E+01	3.40E+01
346	1.07E+01	2.48E+01	396	1.48E+01	3.42E+01
347	1.08E+01	2.50E+01	397	1.49E+01	3.44E+01
348	1.09E+01	2.51E+01	398	1.50E+01	3.46E+01
349	1.10E+01	2.53E+01	399	1.51E+01	3.48E+01
350	1.10E+01	2.55E+01	400	1.52E+01	3.50E+01

Table 4.2.9: Standard Deviations for the Watervliet IW4 Cell Continued

Time (day)	Mean (µg/l)	Standard Deviation (µg/l)	Time (day)	Mean (µg/l)	Standard Deviation (µg/l)
401	1.53E+01	3.52E+01	451	2.03E+01	4.68E+01
402	1.54E+01	3.55E+01	452	2.04E+01	4.71E+01
403	1.55E+01	3.57E+01	453	2.05E+01	4.73E+01
404	1.55E+01	3.59E+01	454	2.06E+01	4.76E+01
405	1.56E+01	3.61E+01	455	2.07E+01	4.78E+01
406	1.57E+01	3.63E+01	456	2.08E+01	4.81E+01
407	1.58E+01	3.65E+01	457	2.09E+01	4.83E+01
408	1.59E+01	3.67E+01	458	2.11E+01	4.86E+01
409	1.60E+01	3.70E+01	459	2.12E+01	4.89E+01
410	1.61E+01	3.72E+01	460	2.13E+01	4.91E+01
411	1.62E+01	3.74E+01	461	2.14E+01	4.94E+01
412	1.63E+01	3.76E+01	462	2.15E+01	4.96E+01
413	1.64E+01	3.78E+01	463	2.16E+01	4.99E+01
414	1.65E+01	3.81E+01	464	2.19E+01	5.04E+01
415	1.66E+01	3.83E+01	465	2.19E+01	5.04E+01
416	1.67E+01	3.85E+01	466	2.20E+01	5.07E+01
417	1.68E+01	3.87E+01	467	2.21E+01	5.10E+01
418	1.69E+01	3.89E+01	468	2.22E+01	5.12E+01
419	1.70E+01	3.92E+01	469	2.23E+01	5.15E+01
420	1.71E+01	3.94E+01	470	2.24E+01	5.18E+01
421	1.72E+01	3.96E+01	471	2.25E+01	5.20E+01
422	1.73E+01	3.98E+01	472	2.27E+01	5.23E+01
423	1.74E+01	4.01E+01	473	2.28E+01	5.26E+01
424	1.75E+01	4.03E+01	474	2.29E+01	5.28E+01
425	1.76E+01	4.05E+01	475	2.30E+01	5.31E+01
426	1.77E+01	4.08E+01	476	2.31E+01	5.34E+01
427	1.78E+01	4.10E+01	477	2.33E+01	5.37E+01
428	1.79E+01	4.12E+01	478	2.34E+01	5.39E+01
429	1.80E+01	4.15E+01	479	2.35E+01	5.42E+01
430	1.81E+01	4.17E+01	480	2.36E+01	5.45E+01
431	1.82E+01	4.19E+01	481	2.37E+01	5.48E+01
432	1.83E+01	4.22E+01	482	2.39E+01	5.51E+01
433	1.84E+01	4.24E+01	483	2.40E+01	5.53E+01
434	1.85E+01	4.26E+01	484	2.41E+01	5.56E+01
435	1.86E+01	4.29E+01	485	2.42E+01	5.59E+01
436	1.87E+01	4.31E+01	486	2.43E+01	5.62E+01
437	1.88E+01	4.34E+01	487	2.45E+01	5.65E+01
438	1.89E+01	4.36E+01	488	2.46E+01	5.68E+01
439	1.90E+01	4.38E+01	489	2.47E+01	5.70E+01
440	1.91E+01	4.41E+01	490	2.48E+01	5.73E+01
441	1.92E+01	4.43E+01	491	2.50E+01	5.76E+01
442	1.93E+01	4.46E+01	492	2.51E+01	5.79E+01
443	1.94E+01	4.48E+01	493	2.52E+01	5.82E+01
444	1.95E+01	4.51E+01	494	2.53E+01	5.85E+01
445	1.96E+01	4.53E+01	495	2.55E+01	5.88E+01
446	1.97E+01	4.56E+01	496	2.56E+01	5.91E+01
447	1.98E+01	4.58E+01	497	2.57E+01	5.94E+01
448	2.00E+01	4.61E+01	498	2.59E+01	5.97E+01
449	2.01E+01	4.63E+01	499	2.60E+01	6.00E+01
450	2.02E+01	4.66E+01	500	2.61E+01	6.03E+01

Table 4.2.9: Standard Deviations for the Watervliet IW4 Cell Continued

Time (day)	Mean (µg/l)	Standard Deviation (µg/l)	Time (day)	Mean (µg/l)	Standard Deviation (µg/l)
501	2.62E+01	6.06E+01	551	3.33E+01	7.67E+01
502	2.64E+01	6.09E+01	552	3.34E+01	7.71E+01
503	2.65E+01	6.12E+01	553	3.36E+01	7.74E+01
504	2.66E+01	6.15E+01	554	3.37E+01	7.78E+01
505	2.68E+01	6.18E+01	555	3.39E+01	7.81E+01
506	2.69E+01	6.21E+01	556	3.40E+01	7.85E+01
507	2.70E+01	6.24E+01	557	3.42E+01	7.89E+01
508	2.72E+01	6.27E+01	558	3.43E+01	7.92E+01
509	2.73E+01	6.30E+01	559	3.45E+01	7.96E+01
510	2.74E+01	6.33E+01	560	3.46E+01	7.99E+01
511	2.76E+01	6.36E+01	561	3.48E+01	8.03E+01
512	2.77E+01	6.39E+01	562	3.49E+01	8.07E+01
513	2.78E+01	6.42E+01	563	3.51E+01	8.10E+01
514	2.80E+01	6.45E+01	564	3.53E+01	8.14E+01
515	2.81E+01	6.48E+01	565	3.54E+01	8.17E+01
516	2.82E+01	6.51E+01	566	3.56E+01	8.21E+01
517	2.84E+01	6.55E+01	567	3.57E+01	8.25E+01
518	2.85E+01	6.58E+01	568	3.59E+01	8.28E+01
519	2.86E+01	6.61E+01	569	3.61E+01	8.32E+01
520	2.88E+01	6.64E+01	570	3.62E+01	8.36E+01
521	2.89E+01	6.67E+01	571	3.64E+01	8.40E+01
522	2.91E+01	6.70E+01	572	3.65E+01	8.43E+01
523	2.92E+01	6.74E+01	573	3.67E+01	8.47E+01
524	2.93E+01	6.77E+01	574	3.69E+01	8.51E+01
525	2.95E+01	6.80E+01	575	3.70E+01	8.55E+01
526	2.96E+01	6.83E+01	576	3.72E+01	8.58E+01
527	2.97E+01	6.87E+01	577	3.74E+01	8.62E+01
528	2.99E+01	6.90E+01	578	3.75E+01	8.66E+01
529	3.00E+01	6.93E+01	579	3.77E+01	8.70E+01
530	3.02E+01	6.96E+01	580	3.78E+01	8.73E+01
531	3.03E+01	7.00E+01	581	3.80E+01	8.77E+01
532	3.05E+01	7.03E+01	582	3.82E+01	8.81E+01
533	3.06E+01	7.06E+01	583	3.83E+01	8.85E+01
534	3.07E+01	7.09E+01	584	3.85E+01	8.89E+01
535	3.09E+01	7.13E+01	585	3.87E+01	8.93E+01
536	3.10E+01	7.16E+01	586	3.89E+01	8.97E+01
537	3.12E+01	7.19E+01	587	3.90E+01	9.00E+01
538	3.13E+01	7.23E+01	588	3.92E+01	9.04E+01
539	3.15E+01	7.26E+01	589	3.94E+01	9.08E+01
540	3.16E+01	7.30E+01	590	3.95E+01	9.12E+01
541	3.18E+01	7.33E+01	591	3.97E+01	9.16E+01
542	3.19E+01	7.36E+01	592	3.99E+01	9.20E+01
543	3.21E+01	7.40E+01	593	4.00E+01	9.24E+01
544	3.22E+01	7.43E+01	594	4.02E+01	9.28E+01
545	3.24E+01	7.47E+01	595	4.04E+01	9.32E+01
546	3.25E+01	7.50E+01	596	4.06E+01	9.36E+01
547	3.26E+01	7.53E+01	597	4.07E+01	9.40E+01
548	3.28E+01	7.57E+01	598	4.09E+01	9.44E+01
549	3.30E+01	7.60E+01	599	4.11E+01	9.48E+01
550	3.31E+01	7.64E+01	600	4.13E+01	9.52E+01

Table 4.2.9: Standard Deviations for the Watervliet IW4 Cell Continued

Time (day)	Mean (µg/l)	Standard Deviation (µg/l)	Time (day)	Mean (µg/l)	Standard Deviation (µg/l)
601	4.14E+01	9.56E+01	651	5.09E+01	1.18E+02
602	4.16E+01	9.60E+01	652	5.11E+01	1.18E+02
603	4.18E+01	9.64E+01	653	5.13E+01	1.18E+02
604	4.20E+01	9.69E+01	654	5.15E+01	1.19E+02
605	4.21E+01	9.73E+01	655	5.17E+01	1.19E+02
606	4.23E+01	9.77E+01	656	5.19E+01	1.20E+02
607	4.25E+01	9.81E+01	657	5.22E+01	1.20E+02
608	4.27E+01	9.85E+01	658	5.24E+01	1.21E+02
609	4.29E+01	9.89E+01	659	5.26E+01	1.21E+02
610	4.30E+01	9.93E+01	660	5.28E+01	1.22E+02
611	4.32E+01	9.98E+01	661	4.38E+02	0.00E+00
612	4.34E+01	1.00E+02	662	5.32E+01	1.23E+02
613	4.38E+01	1.01E+02	663	5.34E+01	1.23E+02
614	4.40E+01	1.01E+02	664	5.36E+01	1.24E+02
615	4.40E+01	1.01E+02	665	5.38E+01	1.24E+02
616	4.41E+01	1.02E+02	666	5.40E+01	1.25E+02
617	4.43E+01	1.02E+02	667	5.43E+01	1.25E+02
618	4.45E+01	1.03E+02	668	5.45E+01	1.26E+02
619	4.47E+01	1.03E+02	669	5.47E+01	1.26E+02
620	4.49E+01	1.04E+02	670	5.49E+01	1.27E+02
621	4.51E+01	1.04E+02	671	5.51E+01	1.27E+02
622	4.53E+01	1.04E+02	672	5.53E+01	1.28E+02
623	4.54E+01	1.05E+02	673	5.55E+01	1.28E+02
624	4.56E+01	1.05E+02	674	5.58E+01	1.29E+02
625	4.58E+01	1.06E+02	675	5.60E+01	1.29E+02
626	4.60E+01	1.06E+02	676	5.62E+01	1.30E+02
627	4.62E+01	1.07E+02	677	5.64E+01	1.30E+02
628	4.64E+01	1.07E+02	678	5.66E+01	1.31E+02
629	4.66E+01	1.07E+02	679	5.69E+01	1.31E+02
630	4.68E+01	1.08E+02	680	5.71E+01	1.32E+02
631	4.70E+01	1.08E+02	681	5.73E+01	1.32E+02
632	4.72E+01	1.09E+02	682	5.75E+01	1.33E+02
633	4.73E+01	1.09E+02	683	5.77E+01	1.33E+02
634	4.75E+01	1.10E+02	684	5.80E+01	1.34E+02
635	4.77E+01	1.10E+02	685	5.82E+01	1.34E+02
636	4.79E+01	1.11E+02	686	5.84E+01	1.35E+02
637	4.81E+01	1.11E+02	687	5.86E+01	1.35E+02
638	4.83E+01	1.12E+02	688	5.89E+01	1.36E+02
639	4.85E+01	1.12E+02	689	5.91E+01	1.36E+02
640	4.87E+01	1.12E+02	690	5.93E+01	1.37E+02
641	4.89E+01	1.13E+02	691	5.95E+01	1.37E+02
642	4.91E+01	1.13E+02	692	5.98E+01	1.38E+02
643	4.93E+01	1.14E+02	693	6.00E+01	1.38E+02
644	4.95E+01	1.14E+02	694	6.02E+01	1.39E+02
645	4.97E+01	1.15E+02	695	6.05E+01	1.40E+02
646	4.99E+01	1.15E+02	696	6.07E+01	1.40E+02
647	5.01E+01	1.16E+02	697	6.09E+01	1.41E+02
648	5.03E+01	1.16E+02	698	6.12E+01	1.41E+02
649	5.05E+01	1.17E+02	699	6.14E+01	1.42E+02
650	5.07E+01	1.17E+02	700	6.16E+01	1.42E+02

Table 4.2.9: Standard Deviations for the Watervliet IW4 Cell Continued

Time (day)	Mean (µg/l)	Standard Deviation (µg/l)	Time (day)	Mean (µg/l)	Standard Deviation (µg/l)
701	6.19E+01	1.43E+02	751	7.44E+01	1.72E+02
702	6.21E+01	1.43E+02	752	7.47E+01	1.72E+02
703	6.23E+01	1.44E+02	753	7.49E+01	1.73E+02
704	6.26E+01	1.44E+02	754	7.52E+01	1.74E+02
705	6.28E+01	1.45E+02	755	7.55E+01	1.74E+02
706	6.30E+01	1.45E+02	756	7.58E+01	1.75E+02
707	6.33E+01	1.46E+02	757	7.60E+01	1.75E+02
708	6.35E+01	1.47E+02	758	7.63E+01	1.76E+02
709	6.38E+01	1.47E+02	759	7.66E+01	1.77E+02
710	6.40E+01	1.48E+02	760	7.68E+01	1.77E+02
711	6.42E+01	1.48E+02	761	7.71E+01	1.78E+02
712	6.45E+01	1.49E+02	762	7.74E+01	1.79E+02
713	6.47E+01	1.49E+02	763	7.77E+01	1.79E+02
714	6.50E+01	1.50E+02	764	7.80E+01	1.80E+02
715	6.52E+01	1.50E+02	765	7.82E+01	1.81E+02
716	6.54E+01	1.51E+02	766	7.85E+01	1.81E+02
717	6.57E+01	1.52E+02	767	7.88E+01	1.82E+02
718	6.59E+01	1.52E+02	768	7.91E+01	1.82E+02
719	6.62E+01	1.53E+02	769	7.94E+01	1.83E+02
720	6.64E+01	1.53E+02	770	7.96E+01	1.84E+02
721	6.67E+01	1.54E+02	771	7.99E+01	1.84E+02
722	6.69E+01	1.54E+02	772	8.02E+01	1.85E+02
723	6.72E+01	1.55E+02	773	8.05E+01	1.86E+02
724	6.74E+01	1.56E+02	774	8.08E+01	1.86E+02
725	6.77E+01	1.56E+02	775	8.11E+01	1.87E+02
726	6.79E+01	1.57E+02	776	8.13E+01	1.88E+02
727	6.82E+01	1.57E+02	777	8.16E+01	1.88E+02
728	6.84E+01	1.58E+02	778	8.19E+01	1.89E+02
729	6.87E+01	1.58E+02	779	8.22E+01	1.90E+02
730	6.89E+01	1.59E+02	780	8.25E+01	1.90E+02
731	6.92E+01	1.60E+02	781	8.28E+01	1.91E+02
732	6.94E+01	1.60E+02	782	8.31E+01	1.92E+02
733	6.97E+01	1.61E+02	783	8.34E+01	1.92E+02
734	6.99E+01	1.61E+02	784	8.37E+01	1.93E+02
735	7.02E+01	1.62E+02	785	8.39E+01	1.94E+02
736	7.05E+01	1.63E+02	786	8.42E+01	1.94E+02
737	7.07E+01	1.63E+02	787	8.45E+01	1.95E+02
738	7.10E+01	1.64E+02	788	8.48E+01	1.96E+02
739	7.12E+01	1.64E+02	789	8.51E+01	1.96E+02
740	7.15E+01	1.65E+02	790	8.54E+01	1.97E+02
741	7.18E+01	1.66E+02	791	8.57E+01	1.98E+02
742	7.20E+01	1.66E+02	792	8.60E+01	1.99E+02
743	7.23E+01	1.67E+02	793	8.63E+01	1.99E+02
744	7.25E+01	1.67E+02	794	8.66E+01	2.00E+02
745	7.28E+01	1.68E+02	795	8.69E+01	2.01E+02
746	7.31E+01	1.69E+02	796	8.72E+01	2.01E+02
747	7.33E+01	1.69E+02	797	8.75E+01	2.02E+02
748	7.36E+01	1.70E+02	798	8.78E+01	2.03E+02
749	7.39E+01	1.70E+02	799	8.81E+01	2.03E+02
750	7.41E+01	1.71E+02	800	8.84E+01	2.04E+02

Table 4.2.9: Standard Deviations for the Watervliet IW4 Cell Continued

Time (day)	Mean (µg/l)	Standard Deviation (µg/l)	Time (day)	Mean (µg/l)	Standard Deviation (µg/l)
801	8.87E+01	2.05E+02	851	1.04E+02	2.41E+02
802	8.90E+01	2.06E+02	852	1.04E+02	2.42E+02
803	8.94E+01	2.06E+02	853	1.05E+02	2.43E+02
804	8.97E+01	2.07E+02	854	1.05E+02	2.43E+02
805	9.00E+01	2.08E+02	855	1.05E+02	2.44E+02
806	9.03E+01	2.08E+02	856	1.06E+02	2.45E+02
807	9.06E+01	2.09E+02	857	1.06E+02	2.46E+02
808	9.09E+01	2.10E+02	858	1.07E+02	2.47E+02
809	9.12E+01	2.11E+02	859	1.07E+02	2.47E+02
810	9.15E+01	2.11E+02	860	1.07E+02	2.48E+02
811	9.18E+01	2.12E+02	861	1.08E+02	2.49E+02
812	9.22E+01	2.13E+02	862	1.08E+02	2.50E+02
813	9.25E+01	2.13E+02	863	1.08E+02	2.51E+02
814	9.28E+01	2.14E+02	864	1.09E+02	2.52E+02
815	9.31E+01	2.15E+02	865	1.09E+02	2.52E+02
816	9.34E+01	2.16E+02	866	1.09E+02	2.53E+02
817	9.37E+01	2.16E+02	867	1.10E+02	2.54E+02
818	9.41E+01	2.17E+02	868	1.10E+02	2.55E+02
819	9.44E+01	2.18E+02	869	1.10E+02	2.56E+02
820	9.47E+01	2.19E+02	870	1.11E+02	2.56E+02
821	9.50E+01	2.19E+02	871	1.11E+02	2.57E+02
822	9.53E+01	2.20E+02	872	1.12E+02	2.58E+02
823	9.57E+01	2.21E+02	873	1.12E+02	2.59E+02
824	9.60E+01	2.22E+02	874	1.12E+02	2.60E+02
825	9.50E+01	2.19E+02	875	1.13E+02	2.61E+02
826	9.66E+01	2.23E+02	876	1.13E+02	2.62E+02
827	9.70E+01	2.24E+02	877	1.13E+02	2.62E+02
828	9.73E+01	2.25E+02	878	1.14E+02	2.63E+02
829	9.76E+01	2.25E+02	879	1.14E+02	2.64E+02
830	9.71E+01	2.25E+02	880	1.14E+02	2.65E+02
831	9.74E+01	2.25E+02	881	1.15E+02	2.66E+02
832	9.77E+01	2.26E+02	882	1.15E+02	2.67E+02
833	9.80E+01	2.27E+02	883	1.16E+02	2.68E+02
834	9.84E+01	2.28E+02	884	1.16E+02	2.68E+02
835	9.87E+01	2.28E+02	885	1.16E+02	2.69E+02
836	9.90E+01	2.29E+02	886	1.17E+02	2.70E+02
837	9.94E+01	2.30E+02	887	1.17E+02	2.71E+02
838	9.97E+01	2.31E+02	888	1.17E+02	2.72E+02
839	1.00E+02	2.32E+02	889	1.18E+02	2.73E+02
840	1.00E+02	2.32E+02	890	1.18E+02	2.74E+02
841	1.01E+02	2.33E+02	891	1.19E+02	2.75E+02
842	1.01E+02	2.34E+02	892	1.19E+02	2.75E+02
843	1.01E+02	2.35E+02	893	1.19E+02	2.76E+02
844	1.02E+02	2.35E+02	894	1.20E+02	2.77E+02
845	1.02E+02	2.36E+02	895	1.20E+02	2.78E+02
846	1.02E+02	2.37E+02	896	1.21E+02	2.79E+02
847	1.03E+02	2.38E+02	897	1.21E+02	2.80E+02
848	1.03E+02	2.39E+02	898	1.21E+02	2.81E+02
849	1.03E+02	2.39E+02	899	1.22E+02	2.82E+02
850	1.04E+02	2.40E+02	900	1.22E+02	2.83E+02

Table 4.2.9: Standard Deviations for the Watervliet IW4 Cell Continued

Time (day)	Mean (µg/l)	Standard Deviation (µg/l)	Time (day)	Mean (µg/l)	Standard Deviation (µg/l)
901	1.22E+02	2.83E+02	951	1.43E+02	3.32E+02
902	1.23E+02	2.84E+02	952	1.44E+02	3.33E+02
903	1.23E+02	2.85E+02	953	1.44E+02	3.34E+02
904	1.24E+02	2.86E+02	954	1.45E+02	3.35E+02
905	1.24E+02	2.87E+02	955	1.45E+02	3.36E+02
906	1.24E+02	2.88E+02	956	1.45E+02	3.37E+02
907	1.25E+02	2.89E+02	957	1.46E+02	3.38E+02
908	1.25E+02	2.90E+02	958	1.46E+02	3.39E+02
909	1.26E+02	2.91E+02	959	1.47E+02	3.40E+02
910	1.26E+02	2.92E+02	960	1.47E+02	3.41E+02
911	1.26E+02	2.93E+02	961	1.48E+02	3.42E+02
912	1.27E+02	2.94E+02	962	1.48E+02	3.43E+02
913	1.27E+02	2.95E+02	963	1.49E+02	3.44E+02
914	1.28E+02	2.95E+02	964	1.49E+02	3.45E+02
915	1.28E+02	2.96E+02	965	1.50E+02	3.46E+02
916	1.28E+02	2.97E+02	966	1.50E+02	3.47E+02
917	1.29E+02	2.98E+02	967	1.50E+02	3.48E+02
918	1.29E+02	2.99E+02	968	1.51E+02	3.49E+02
919	1.30E+02	3.00E+02	969	1.51E+02	3.51E+02
920	1.30E+02	3.01E+02	970	1.52E+02	3.52E+02
921	1.30E+02	3.02E+02	971	1.52E+02	3.52E+02
922	1.31E+02	3.03E+02	972	1.53E+02	3.54E+02
923	1.31E+02	3.04E+02	973	1.53E+02	3.55E+02
924	1.32E+02	3.05E+02	974	1.54E+02	3.56E+02
925	1.32E+02	3.06E+02	975	1.54E+02	3.57E+02
926	1.33E+02	3.07E+02			
927	1.33E+02	3.08E+02			
928	1.33E+02	3.09E+02			
929	1.34E+02	3.10E+02			
930	1.34E+02	3.11E+02			
931	1.35E+02	3.12E+02			
932	1.35E+02	3.13E+02			
933	1.35E+02	3.14E+02			
934	1.36E+02	3.15E+02			
935	1.36E+02	3.16E+02			
936	1.37E+02	3.17E+02			
937	1.37E+02	3.18E+02			
938	1.38E+02	3.19E+02			
939	1.38E+02	3.20E+02			
940	1.38E+02	3.21E+02			
941	1.39E+02	3.22E+02			
942	1.39E+02	3.23E+02			
943	1.40E+02	3.24E+02			
944	1.40E+02	3.25E+02			
945	1.41E+02	3.26E+02			
946	1.41E+02	3.27E+02			
947	1.41E+02	3.28E+02			
948	1.42E+02	3.29E+02			
949	1.42E+02	3.30E+02			
950	1.43E+02	3.31E+02			

Figure 4.3.1: Sensitivity Analysis for Advection

Figure 4.3.1 shows the change in concentration over 180 days as all variable are fixed and only the average linear velocity is varied from 9.98 x 10^{-8} m/s to 9.98 x 10^{-12} m/s.

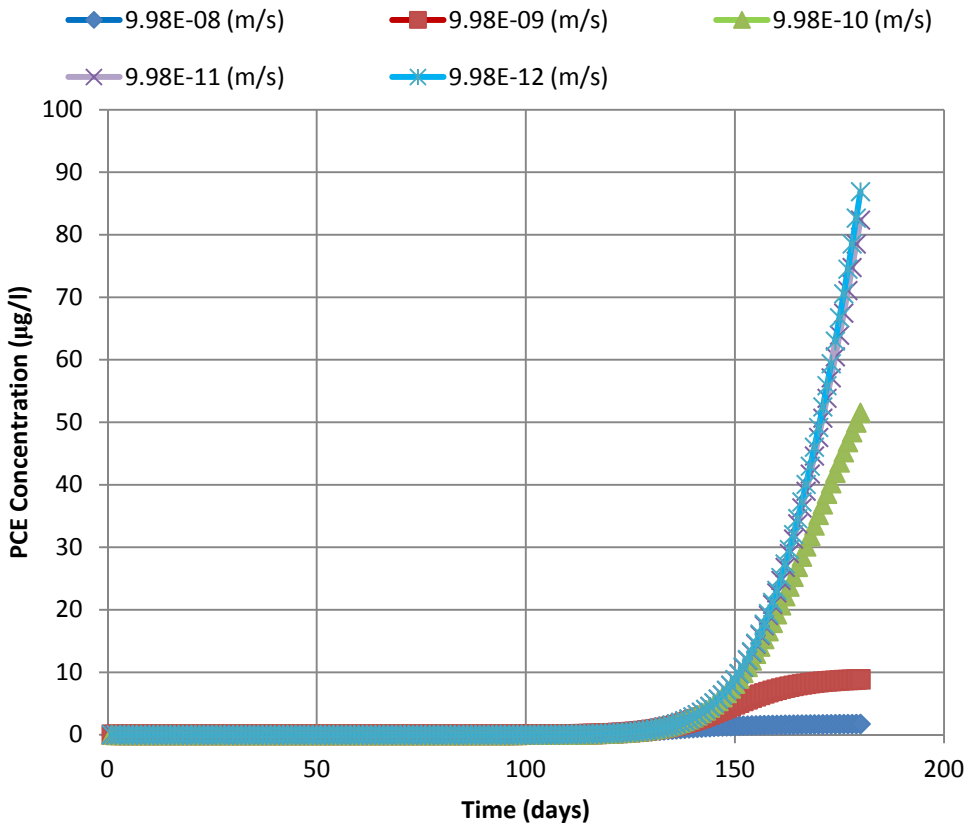

Figure 4.3.2: Sensitivity Analysis for Dispersivity

Figure 4.3.2 shows the change in concentration over 180 days as all variable are fixed and only the longitudinal dispersivity and transverse dispersivity are varied from 1 m to 100 m.

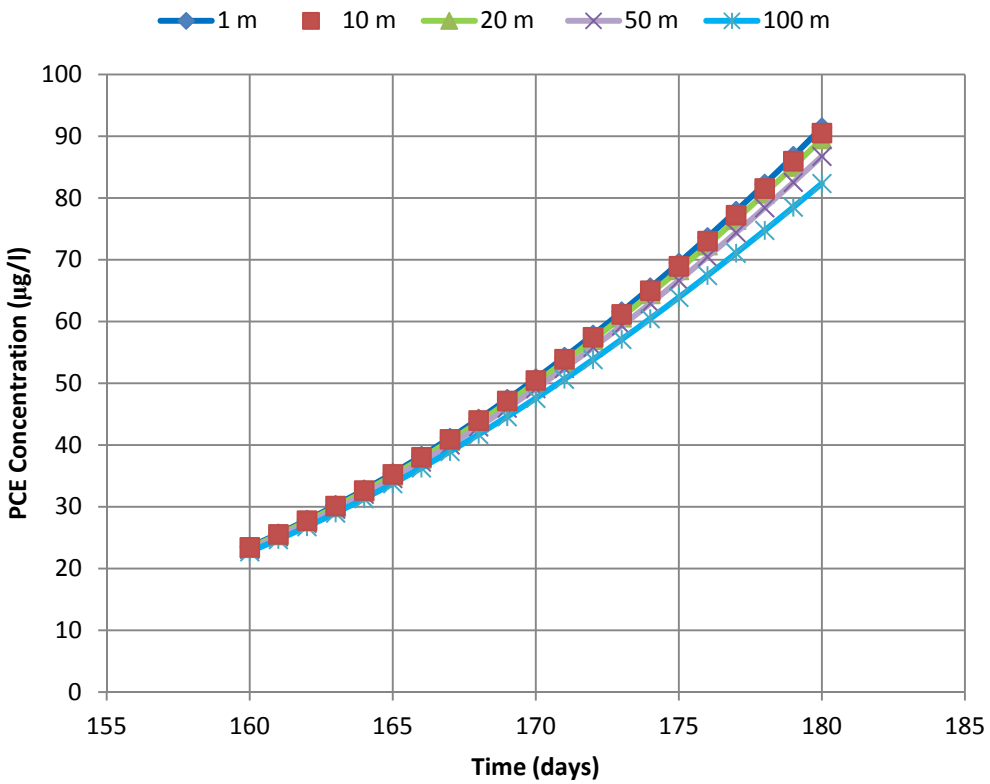

Figure 4.3.3: Sensitivity Analysis for α_L/α_T

Figure 4.3.3 shows the change in concentration over 180 days as all variable are fixed and only the ratio between longitudinal dispersivity and transverse dispersivity is varied from 1 to 20.

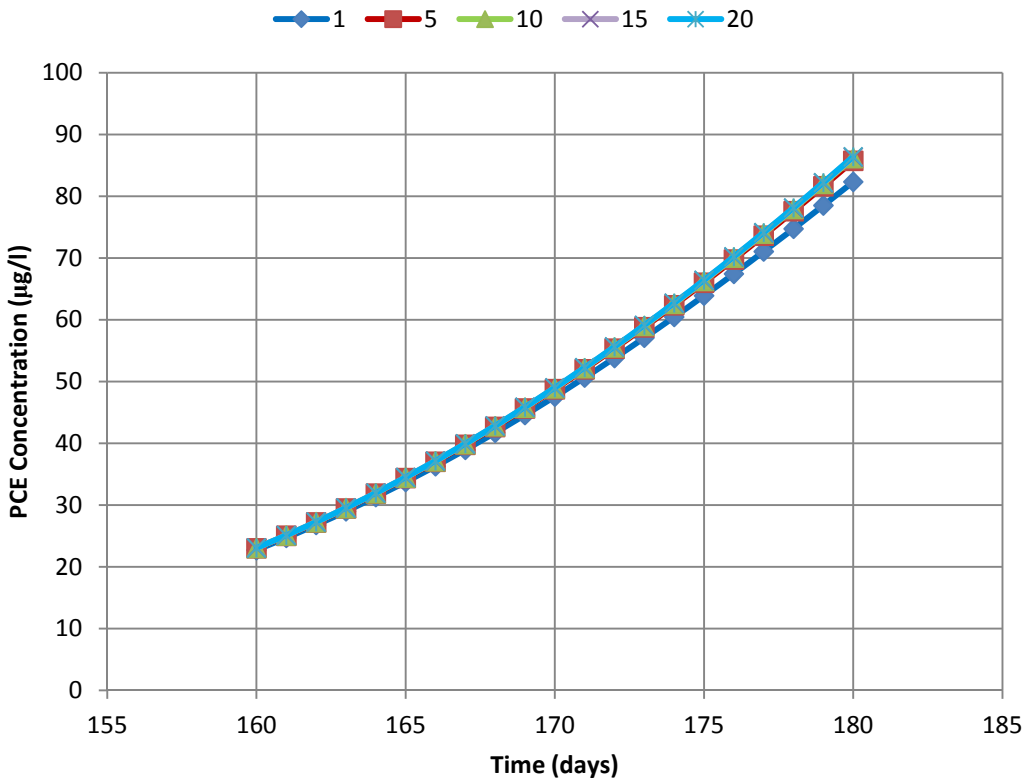

Figure 4.3.4: Sensitivity Analysis for Retardation Factor

Figure 4.3.4 shows the change in concentration over 180 days as all variable are fixed and only the retardation factor is varied from 1 to 200.

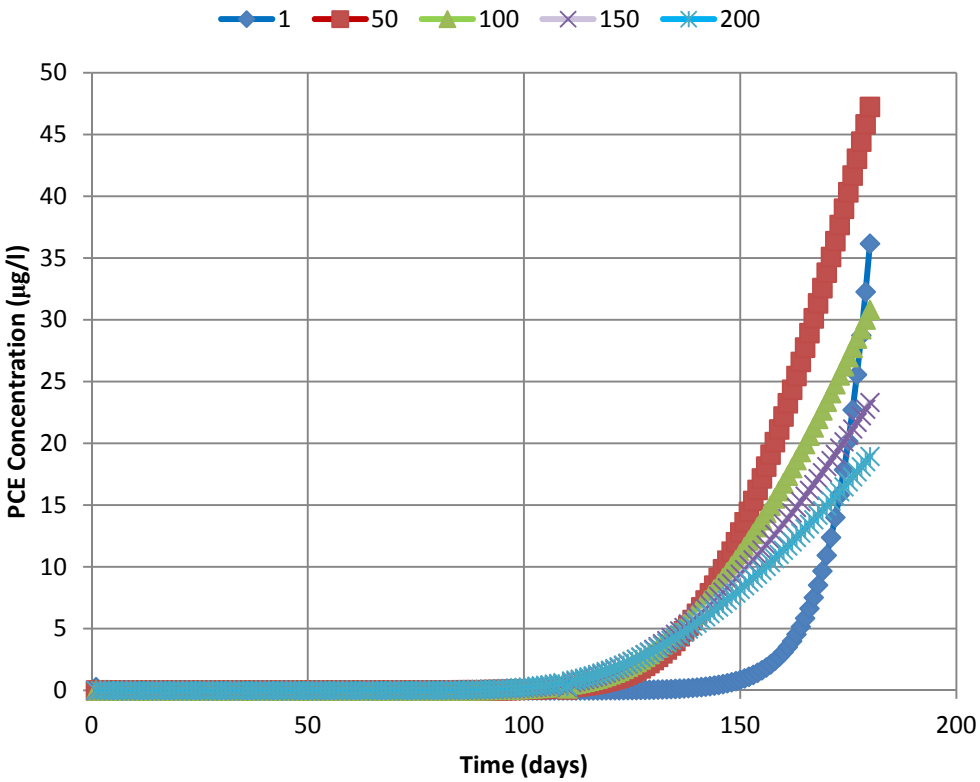

Figure 4.3.5: Sensitivity Analysis for Solubility

Figure 4.3.5 shows the change in concentration over 180 days as all variable are fixed and only the solubility is varied from 100 mg/l to 1500 mg/l.

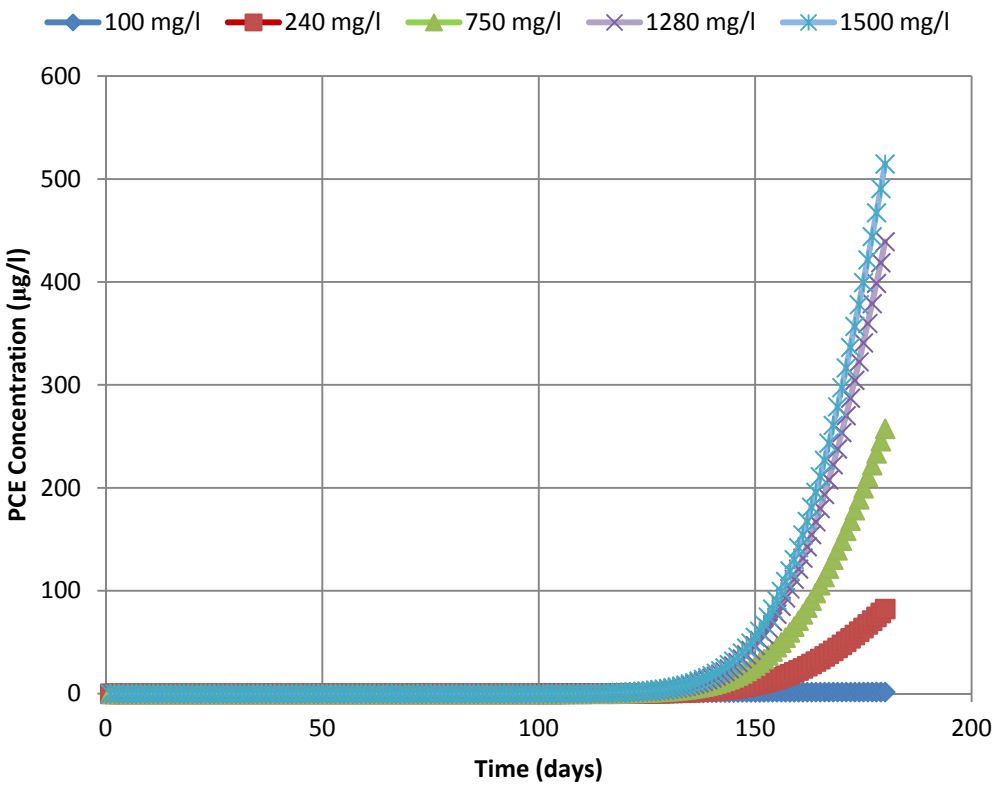

Figure 4.3.6: Sensitivity Analysis for Rate of Natural Oxidant Demand

Figure 4.3.6 shows the change in concentration over 180 days as all variable are fixed and only the natural oxidant demand rate is varied from 2.31 x 10^{-10} 1/s to 2.32 x 10^{-7} 1/s.

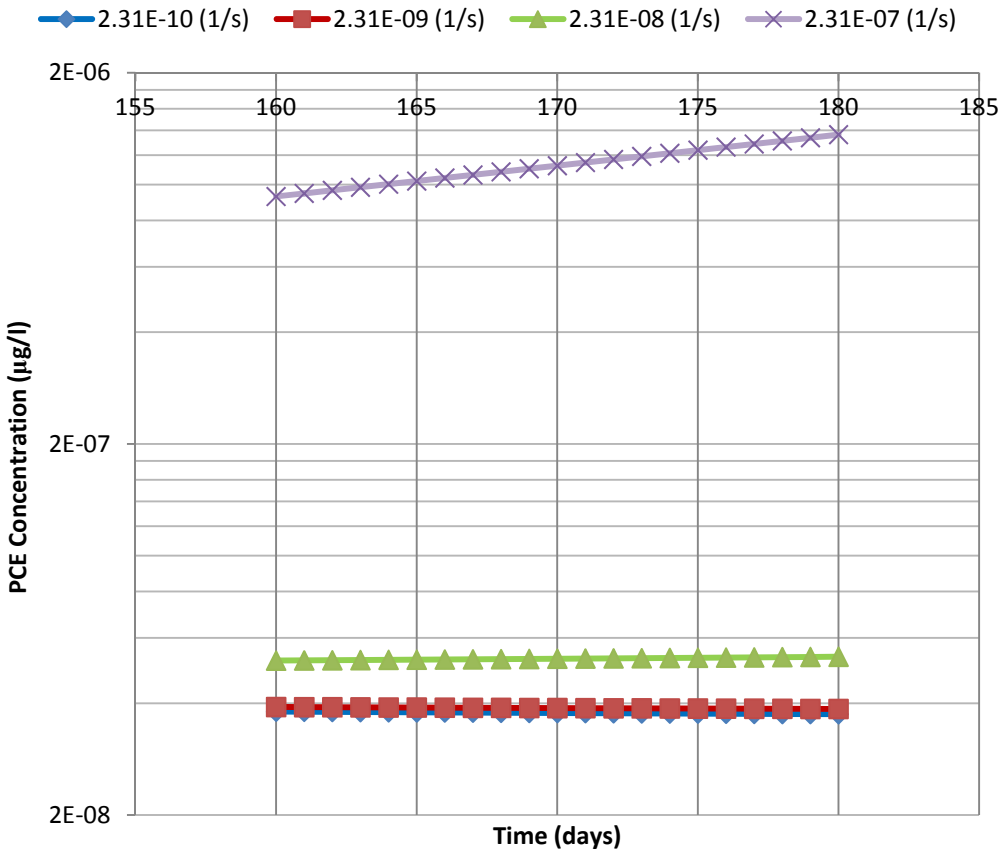

Figure 4.3.7: Sensitivity Analysis for Rate of Oxidation

Figure 4.3.7 shows the change in concentration over 180 days as all variable are fixed and only the rate of oxidation is varied from 0.00435 1/(M s) to 43.5 1/(M s).

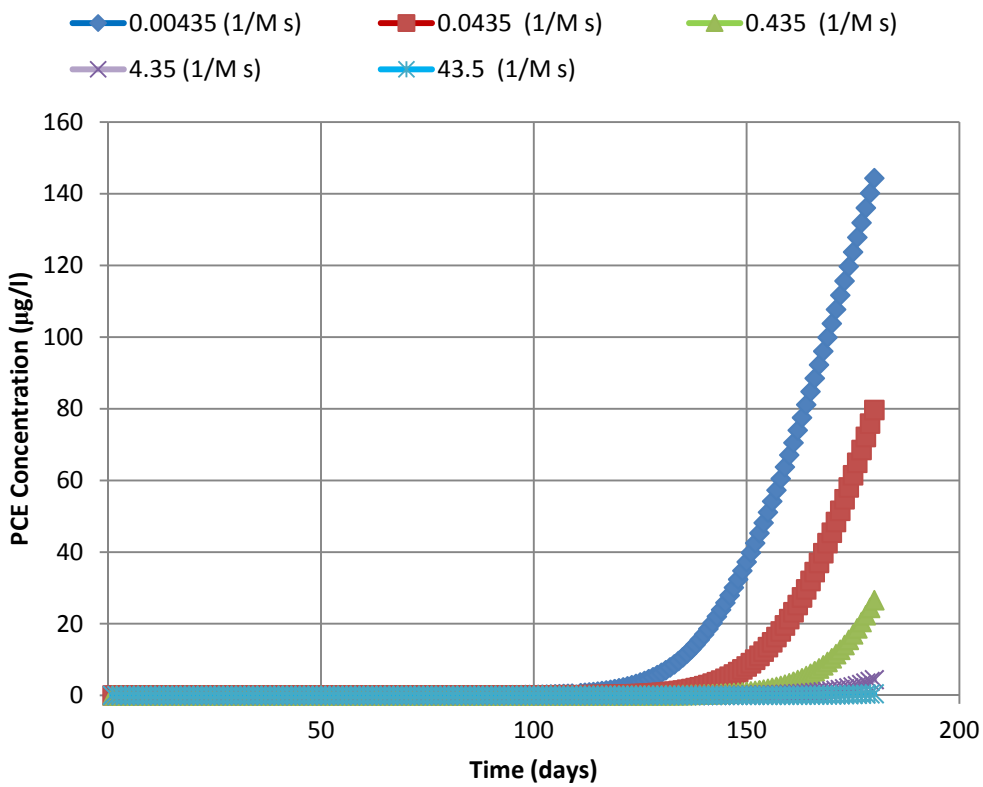

Figure 4.3.8: Sensitivity Analysis for Rate of Concentration Rebound

Figure 4.3.8 shows the change in concentration over 180 days as all variable are fixed and only the rate of concentration rebound is varied from 1.16 x 10^{-11} 1/s to 1.16 x 10^{-7} 1/s.

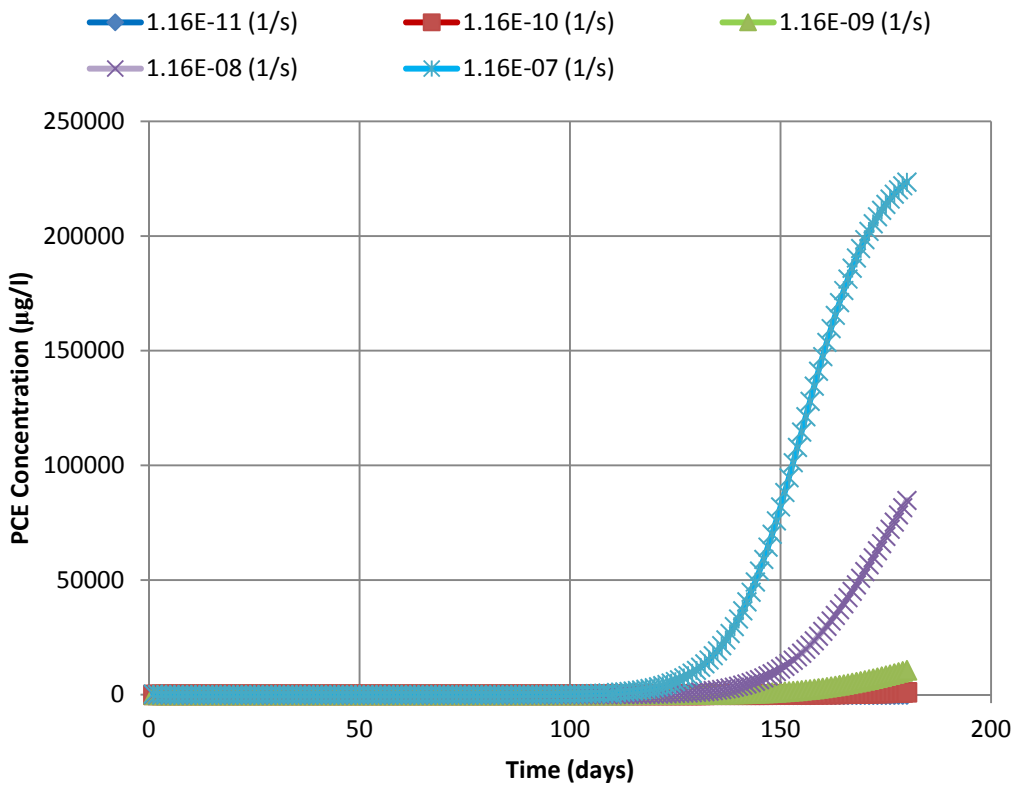

Figure 4.3.9: Hydraulic Conductivity Reduced at 250 days

Figure 4.3.9 shows how concentration rebound will increase as the hydraulic conductivity is reduced from 8.97 $x10^{-8}$ m/s to $3.63x10^{-8}$m/s at 250 days. As pore velocity is decreased with a reduced hydraulic conductivity, less mass is transported and the concentration rebound increases.

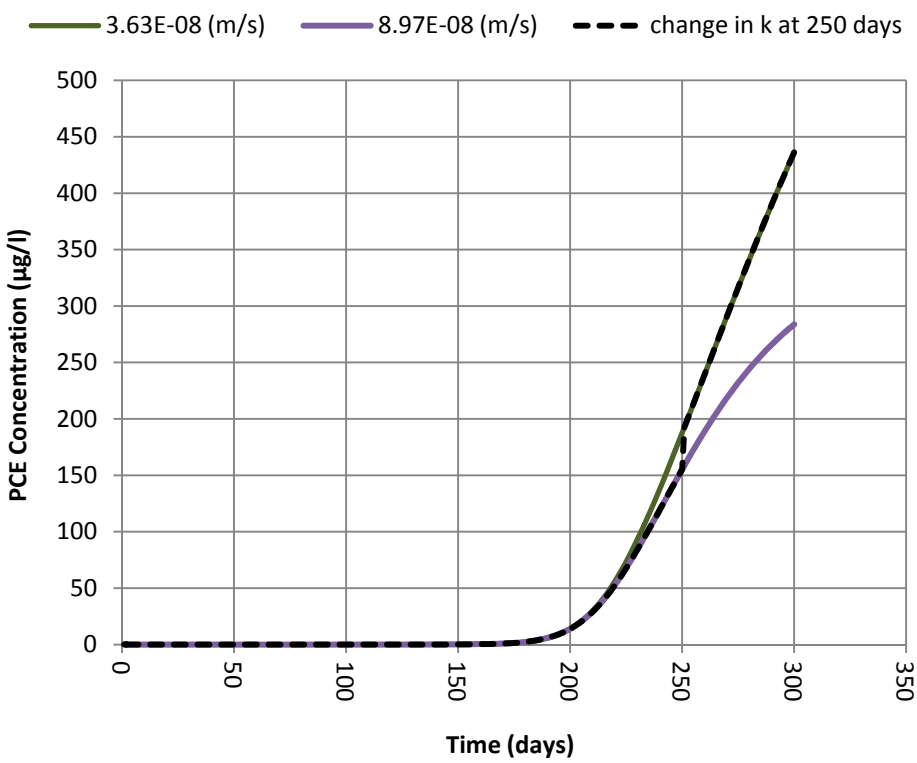

Table 4.4.1: Mass Reduction Summary

Table 4.4.1 presents the estimations of the mass in the aqueous phase and the sorbed phase both before and 100 days after the permanganate injections. It also presents the amount of mass reduced at 100 days as a percentage.

Site		Aqueous Phase (kg)	Solid Phase(kg)
Busch	Pre ISCO	6.78E-02	2.07E-01
	Post ISCO	1.35E-04	4.12E-04
	% Reduction	99.80%	99.80%
Cape Canaveral (2S)	Pre ISCO	9.57E+01	3.18E+01
	Post ISCO	7.80E-04	2.59E-04
	% Reduction	100.00%	100.00%
Cape Canaveral (5S)	Pre ISCO	9.76E+01	3.24E+01
	Post ISCO	5.77E-01	1.92E-01
	% Reduction	99.41%	99.41%
Chemplex	Pre ISCO	0.006	0.0163
	Post ISCO	0.0057	0.0153
	% Reduction	5.00%	6.13%
PGDP	Pre ISCO	3.89E+01	1.55E+01
	Post ISCO	1.40E-03	5.41E-03
	% Reduction	100.00%	99.97%
Valmont (EW-1)	Pre ISCO	3.95E-01	2.54E-01
	Post ISCO	6.21E-02	3.98E-02
	% Reduction	84.28%	84.33%
Valmont (EW-5)	Pre ISCO	0.1116	0.0716
	Post ISCO	0.1055	0.0677
	% Reduction	5.47%	5.45%
Watervliet (IW-1)	Pre ISCO	1.55	4.74E+02
	Post ISCO	5.62E-01	1.27E+02
	% Reduction	63.74%	73.21%
Watervliet (IW-4)	Pre ISCO	3.41E-02	1.04E+01
	Post ISCO	3.01E-04	9.21E-04
	% Reduction	99.12%	99.99%

Table 4.5.1: Precipitate Accumulation in Pore Volumes

Table 4.5.1 summarizes the results of the precipitate accumulation analysis. The percentage of pore space remaining demonstrates that the change in pore space is negligible.

Site	Porosity (n)	Mass Injected (mol)	Volume Injected (l)	Total Volume of Cell (l)	Total Volume of Pores (l)	Volume Injected/Pore Volume	% of Initial Volume
Busch	0.20	13474	233	707921	141584	1.65E-03	99.84%
Cape Canaveral 2S	0.26	3227	56	707921	184060	3.03E-04	99.97%
Cape Canaveral 5S	0.26	3227	56	707921	184060	3.03E-04	99.97%
Chemplex	0.36	1790	31	25485162	9174658	3.37E-06	100.00%
PGDP	0.30	12402	215	707921	212376	1.01E-03	99.90%
Valmont EW-1	0.12	13421	232	70792116	8495054	2.73E-05	100.00%
Valmont EW-5	0.12	6263	108	11326739	1359209	7.97E-05	99.99%
Watervliet IW-1	0.02	4553	79	707921	16282	4.84E-03	99.52%
Watervliet IW-4	0.02	2553	44	707921	16282	2.71E-03	99.73%

Table 4.6.1: Rejection of Outliers

Table 4.6.1 shows that the concentration rebound rate from the PGDP cell (0.10 1/s) can be rejected as an outlier since the Q is greater than the Q_{crit}. (Rorabacher, 1991)

k_{cr} (1/s)	Q_{crit} (99% Confidence Level)	Q
1.00E-07	5.98E-01	0.00E+00
2.50E-07	5.98E-01	1.50E-06
7.50E-07	5.98E-01	6.50E-06
3.50E-05	5.98E-01	3.49E-04
1.20E-03	5.98E-01	1.20E-02
1.35E-03	5.98E-01	1.35E-02
1.50E-03	5.98E-01	1.50E-02
2.00E-03	5.98E-01	2.00E-02
1.00E-01	5.98E-01	1.00E+00

Figure 4.6.1: Regression Analysis for Concentration Rebound Rate and Diffusion Coefficient in Water

Figure 4.6.1 presents the correlation between concentration rate rebound and the diffusion coefficient in pure water (R^2=0.9257).

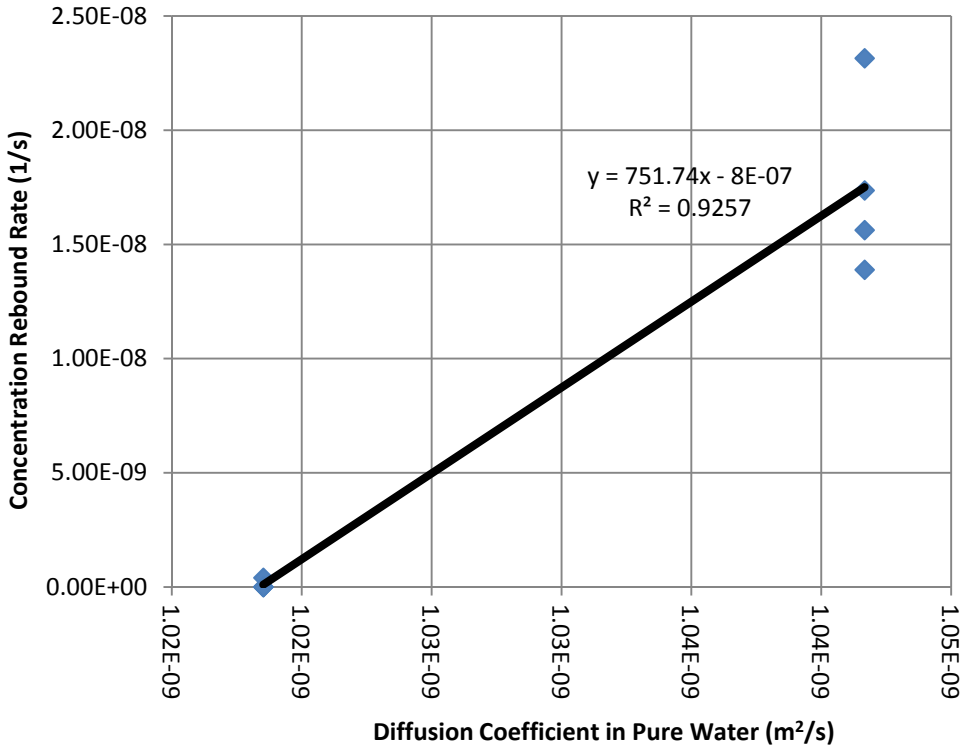

Figure 4.6.2: Regression Analysis for Concentration Rebound Rate and Mass Reduction

Figure 4.6.2 presents the correlation between the rate of concentration rebound and the percentage of mass reduced (R^2=0.0151).

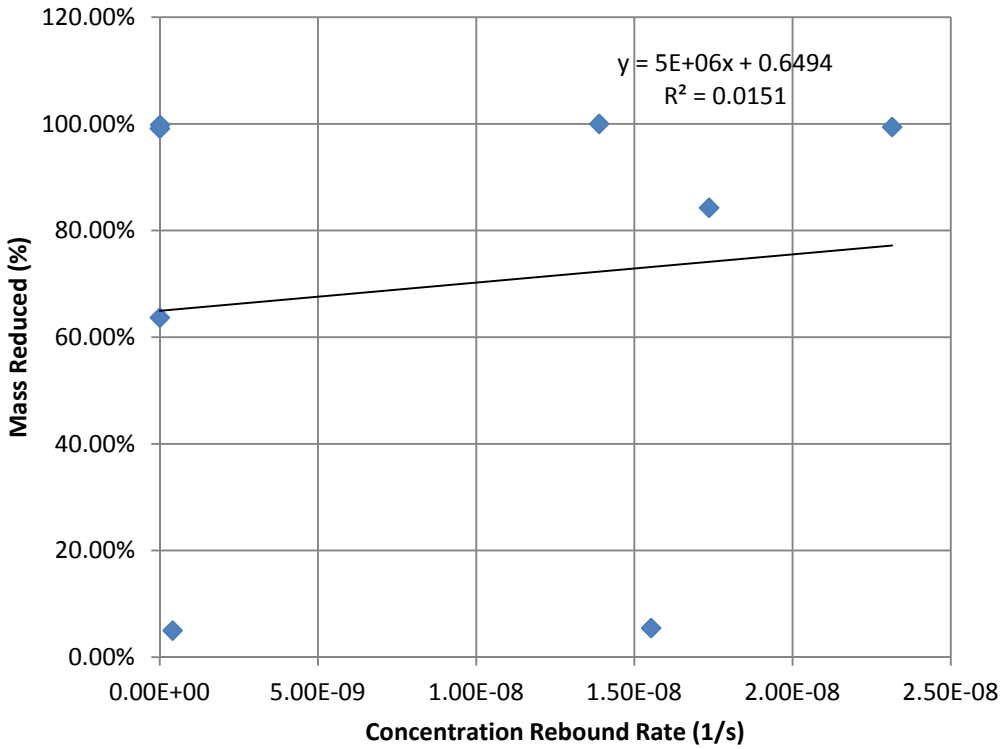

Chapter 5: Discussion

This investigation simulated a total of 9 cells simulated from 6 sites where an ISCO was used to remediate PCE or TCE. The simulations were completed in order to estimate each cell's rate of concentration rebound. Afterwards, this study correlated those concentration rebound rates to the diffusion coefficients in pure water for both PCE and TCE and found a correlation (R^2 =0.9527) via a regression analysis. The following section presents the conclusions of this project and recommendations for further research.

5.1 Uncertainty Analysis Conclusions

When the outputs of the Monte Carlo analyses are compared to the outputs of their respective simulated cell (e.g., when the Monte Carlos analysis for the Busch Campus is compared to the field calibrated concentration rebound for the Busch Campus) there are three groups to be discussed. First, there are three cells (PGDP and both Valmont cells) that have expected values of means and standard deviations. The simulations all entailed a large number of variables that can vary widely in the field, so the large standard deviations were expected. There are two cells that have much lower than expected values for means and standard deviations. Both Cape Canaveral cells have much lower than expected standard deviations. Cape Canaveral cells are comprised of sand and sand has a much higher hydraulic conductivity than the rest of the cells. With a coefficient of variation of 200% a large range of randomized average linear velocities were generated and many of the randomized average linear velocities were probably higher than the average linear velocity used for the calibration. The sensitivity analysis revealed that concentration rebound decreases as average linear velocity increased. The

higher average linear velocities resulted in much lower means and standard deviations values than was expected. The third group of cells includes all of the PCE cells. The coefficient of variation for the rate of concentration rebound used for all PCE sites was 167%. The high coefficient of variation results from a small sample and is probably much higher than the actual coefficient of variation. The high coefficient of variation resulted in much higher than expected values for means and standard deviations.

The coefficient of variation for the rate of concentration rebound rates was based upon two small samples. Further research will probably identify better coefficients of variation, but it can be assumed that the coefficient of variation used for the TCE rates is probably more accurate than the large coefficient of variation used for the PCE cells.

5.2 Sensitivity Analysis Conclusions

The following subsection discusses the results for each of the parameters examined in the sensitivity analysis. All of the parameters can be categorized into two groups. The first has concentration rebound that increases as a parameter increases and the second has concentration rebound that increases when a parameter decreases.

There are four parameters that cause an increase in concentration rebound when they increase. When the ratio between longitudinal dispersivity and transverse dispersivity increases[6], the transport becomes less influential and concentration rebound increases. As solubility increases, the concentration rebound increases because more DNAPL will transfer to the aqueous phase. The rate of NOD increasing will also increase the concentration rebound at a site. As more permanganate mass is consumed by natural

[6] If the ratio is 1, than $\alpha_x=\alpha_y$. If the ratio is 20, than $\alpha_y=\alpha_x/20$. So as the ratio increases, less mass is transported via dispersion.

organic matter, less DNAPL is oxidized. The last parameter that increases concentration rebound as it increases is the rate of concentration rebound. As the rate of concentration increases, the untreated and entrapped DNAPLs enter the aqueous phase faster.

The second group includes the five parameters that will increase the concentration rebound as they decrease. As advection decreases, mass transport allows the rate on concentration rebound to be more influential. This is also why a decreased hydraulic conductivity causes the concentration to increase. Decreasing hydraulic conductivity will also decrease advection. Reduced mass transport is the explanation for another set of parameters (i.e., dispersivities) that increase concentration rebound as they decrease. A parameter that does not alter transport, but increases concentration rebound when it decreases is the rate of oxidation. As the rate of oxidation decreases, less DNAPL mass in oxidized resulting in more concentration rebound. The last parameter that increases concentration rebound as it decreases is the retardation factor.

5.3 Mass Reduction Analysis Conclusions

The mass reduction analysis confirmed two previously established points. First, it confirms previous research by Schnarr et al. (1998) and West et al. (1997) that established that permanganate injections can reduce the DNAPL mass in a subsurface system. Second, it confirms the research completed by Goldstein et al. (2004) that stated concentration rebound and mass reduction are not correlated.

5.4 Precipitate Accumulation Analysis Results

In the literature review, it was established that precipitates have an impact where advection and dispersion do not occur. The alteration of pore volume by the volume of precipitates was negligible in the nine cells simulated in this study. It is doubtful that the average linear velocity was altered by the accumulation of manganese oxides. However, this analysis ignores how the fate and transport of manganese dioxides may influence outcomes. By assuming an equal distribution of manganese oxides throughout the entire volume of the cell simulation, the heterogeneities of the site are ignored as well as temporary effects during transport.

5.5 Molecular Diffusion/ Rate of Concentration Rebound Correlation Conclusions

The important role that molecular diffusion plays for dissolution is clear from Equation 3.1.5. The terms used in Equation 3.1.5 show that the rate that mass transfer will occur is a function of the molecular diffusion coefficient, film thickness, and specific surface area. In addition, Johnson and Pankow (1992) offer evidence of molecular diffusion's important role for the fate and transport of contaminants at DNAPL contaminated sites. Since concentration rebound is caused by dissolution (Brusseau et al., 2007), it can be deduced that molecular diffusion will be influential in concentration rebound. The second process that causes is concentration rebound is back diffusion, which is also driven by molecular diffusion. This study offers support of the casual relationship (R^2=0.9527) between the diffusion coefficient in pure water and the rate of concentration rebound.

5.5 Recommendations

There are four topics that have not been addressed by this study and are important topics to progress this research. Most ISCO project uses iterative injections. The affect that multiple injections have on the rate of concentration rebound is unclear. Further research into this topic may make it possible to estimate the frequency of injections that would be necessary to manage concentration rebound. This study has also ignored how competing reactions will impact concentration rebound. For example, a site with several DNAPLs will have several contaminants competing to react with permanganate. Since these competing reactions influence that amount of DNAPL mass oxidized, it will affect the amount of liquid mass that will drive the rate of concentration rebound. It is unclear how this impacts the rate of concentration rebound and most contaminated sites have much more than one contaminant. Thirdly, this project did not investigate how biodegradation impacts the rate of concentration rebound. An investigation that couples the rate of concentration rebound with the population rebound of microorganisms that metabolize DNAPLS could confirm or refute the assumption made in the literature review. Lastly, source architecture is not accounted for in this study. The literature review establishes that source architecture is important. Unfortunately, source architecture is difficult to estimate and there is much more research to be completed before the effects of source architecture on concentration rebound can be examined.

References

1. Andersen, M.R.; Johnson, R.L.; Pankow, J.F. Dissolution of Dense Chlorinated Solvents into Ground Water: 1. Dissolution from a Well-Defined Residual Source. *Ground Water*. **1992a**, 30, 250-256.

2. Andersen, M.R.; Johnson, R.L.; Pankow, J.F. Dissolution of Dense Chlorinated Solvents into Ground Water: 3. Modeling Contaminant Plumes from Fingers and Pools of Solvent. *Environmental Science & Technology*. **1992b**, 26, 901-908.

3. Ataie-Ashtiani, B.; Hosseini, S.A. Error Analysis if Finite Difference Methods for Two-Dimensional Advection-Dispersion-Reaction Equation. *Advances in Water Resources*. **2005**, 28,793-806.

4. Ball, W.P.; Liu, C.; Xia, G.; Young, D.F. A Diffusion Based Interpretation of Tetrachloroethene and Trichloroethene Concentration Profiles in a Groundwater Aquitard. *Water Resources Research*. **1997**, 33, 2741-2758.

5. Barker, J.F.; Sudicky, E.A.; Mayfield, C.I.; Gillham, R.W. *The Fate and Persistence of Aromatic Hydrocarbons Dissolved in Groundwater: Results from Controlled Field Experiments* 1989, American Association of Petroleum Geologists Symposium Volume-Environmental Concerns in the Petroleum Industry. 1989

6. Battelle. Demonstration of ISCO Treatment of a DNAPL Source at Launch Complex 34 in Cape Canaveral Air Station.: Final Innovative Technology Evaluation Report. 2002.

7. Bird, R.; Stewart, E.; Lightfoot, E. *Transport Phenomena*. John Wiley, New York, NY, 1960.

8. Bradford, S.A.; Phelan, T.J; Abriola, L.M. Dissolution of Residual Tetrachloroethylene in Fractional Wettability Porous Media: Correlation Development and Application. *Journal of Contaminant Hydrology*. **2000**, 45, 35-61.

9. Bradford, S.A.; Rathfelder, K.M.; Lang, J.; Abriola, L.M. Entrapment and Dissolution of DNAPLs in Heterogeneous Porous Media. *Journal of Contaminant Hydrology*. **2003**, 67, 133– 157.

10. Brusseau, M.L.; Nelson, N.T.; Zhang, Z.; Blue, J.E.; Roher, J.; Allen, T. Source-Zone Characterization of a Chlorinated-Solvent Contaminated Superfund Site in Tucson, AZ. *Journal of Contaminant Hydrology*. **2007**. 90, 21-40.

11. Chapman, S. W.; Parker, B. L. Plume Persistence Due to Aquitard Back Diffusion Following DNAPL Source Removal or Isolation. *Water Resources Research*. **2005**. 41: W12411.

12. Christ, J.A.; Ramsburg, C.A.; Pennell, K.D.; Abriola, L.M. Estimating Mass Discharge from Dense Nonaqueous Phase Liquid Source Zones Using Upscaled Mass Transfer Coefficients: An Evaluation Using Multiphase Numerical Simulations. *Water Resources Research*. **2006**, 42, 1-13.

13. Crimi, M.L.; Siegrist, R.L. Impact of Reaction Conditions on MnO_2 Genesis during Permanganate Oxidation. *Journal of Environmental Engineering*. **2004**, 130, 562-572

14. Crimi, M.L.; Siegrist, R.L. Factors Affecting Effectiveness and Efficiency of DNAPL Destruction Using Potassium Permanganate and Catalyzed Hydrogen Peroxide. **2005**. *Journal of Environmental Engineering*. Dec. 1724-1732.

15. Curtis, G.P.; Roberts, P.V. Reinhard, M. A Natural Gradient Experiment of Solute Transport in a Sand Aquifer 4. Sorption of Organic Solutes and its Influence on Mobility. *Water Resources Research*. **1984**. 22, 2059-2067.

16. Dai, Q; Reitsma, S. Kinetic Study of Permanganate Oxidation of Tetrachloroethylene at a High pH Under Acidic Conditions. **2004**. *Remediation*. 67-79.

17. Delgado, J.M.P.Q. Longitudinal and Transverse Dispersion I Porous Media. *Chemical Engineering Research and Design*. **2007**. 85, 1245-1252.

18. Doherty, R. A History of the Production and Use of Carbon Tetrachloride, Tetrachloroethylene, Trichloroethylene and 1,1,1-Trichloroethane in the United States: Part 1-Historical Background; Carbon Tetrachloride and Tetrachloroethylene. *Journal of Environmental Forensics*. **2000a**. 1, 69-81.

19. Doherty, R. A History of the Production and Use of Carbon Tetrachloride, Tetrachloroethylene, Trichloroethylene and 1,1,1-Trichloroethane in the United States: Part 2-Historical Background: Trichloroethylene and 1,1,1-Trichloroethane. *Journal of Environmental Forensics*. **2000b**. 1, 83-93.

20. Domenico, P.A.; Schwartz, F.W. *Physical and Chemical Hydrogeology*, John Wiley & Sons, New York. 1990

21. EPA Guidance Document. Development of Site-Specific Impact to Ground Water Soil Remediation Standards Using the Soil-Water Partition Equation. 2008.

22. EPA, Intermedia Transfer Factors for Contaminants Found at Hazardous Waste Sites: Tetrachloroethylene. 1994a

23. EPA, Intermedia Transfer Factors for Contaminants Found at Hazardous Waste Sites: Trichloroethylene. 1994b

24. EPA, Third Five-Year Review Report for Chemplex Site Clinton, County, IO. 2009

25. Feenstra, S; Cherry, J.A. *Subsurface Contamination by Dense Non-Aqueous Phase Liquids (DNAPL) Chemicals. 1988*. The International Groundwater Symposium International, May 1-4 . Association of Hydrogeologists, 1988.

26. Feenstra, S.; Guiger, N.. Diagnosis and assessment of DNAPL sites. In *Dense Chlorinated Solvents and Other DNAPLs in Groundwater: History, Behavior, and* Remediation; Pankow, J.F., Cherry, J.A. Eds. Waterloo Press, Portland, OR. 1996. 395-473.

27. Feenstra, S.; Cherry, J.A. Dissolution of Dense Non Aqueous Phase Liquids (DNAPLS) in the Subsurface. In *Dense Chlorinated Solvents and Other DNAPLs in Groundwater: History, Behavior, and* Remediation; Pankow, J.F., Cherry, J.A. Eds. Waterloo Press, Portland, OR. 1996. 395-473.

28. Fetter, C.W. *Contaminant Hydrogeology.*2nd Ed.; Prentice Hall: Upper Saddle River, NJ. 1993.

29. Freyberg, D.L. A Natural Gradient Experiment on Solute Transport in a Sand Aquifer 2. Spatial Moments and the Advection and Dispersion of Nonreactive Tracers. *Water Resources Research*, **1984**. 22, 2031-2046

30. Frind, E. O.; Molson, J. W.; Schirmer, M.; Guiger, N. Dissolution and Mass Transfer of Multiple Organics under Field Conditions: The Borden Emplaced Source. *Water Resources Research*. **1999**. 35, 683–694.

31. Fure, A.D.; Jawitz, J.W.; Annable, M.D. DNAPL Source Depletion: Linking Architecture and Flux Response. **2006**. *Journal of Contaminant Hydrology*. 85, 118-140.

32. Geller, J.T.; Hunt, J.R. Mass Transfer from Nonaqueous Phase Organic Liquids in Water-Saturated Porous Media. *Water Resources Research*. **1993**. 29, 833-845.

33. Goldstein, K.J.; Vitolins, A.R.; Navon, D.; Parker, B.L.; Chapman, S.; Anderson, G. A. Characterization and Pilot-Scale Studies for Chemical Oxidation Remediation of Fractured Shale. *Remediation*. **2004**. Autumn: 19-37

34. Gonullu, M.T. Modeling Dissolution of an Organic Mixture in the Subsurface. *Water Resources Research*. **1996**. 30, 649-653.

35. Grant, G.P.; Gerhard, J.I. *The Sensitivity of Predicted DNAPL Source Zone Longevity to Mass Transfer Correlation Model*, in Geoenvironmental Engineering: Integrated Management of Groundwater and Contaminated Land. Ed.; Young, R.N.; Thomas, H.R. Thomas Telford, Stratford-upon-Avon, U. K. 2004. pp. 59-66.

36. Grant, G.P.; Gerhard, J.I. Simulating the Dissolution of a Complex Dense Nonaqueous Phase Liquid Source Zone: 2. Experimental Validation of an Interfacial Area-Based Mass Transfer Model. *Water Resources Research*. **2007**. 43, 1-18.

37. Guiguer, N. Dissolution and Mass Transfer Processes for Residual Organics in the Saturated Groundwater Zone: Numerical modeling. Ph.D. Thesis, University of Waterloo, Waterloo, ON. 1993.

38. Guilbeault, M.A.; Parker, B.L.; Cherry, J.A. Mass and Flux Distributions from DNAPL Zones in Sandy Aquifers. *Ground Water*. **2005**. 43, 70-86.

39. Hansen, S.K.; Kueper, B.H. An Analytical Solution to Multi-Component NAPL Dissolution Equations. *Advances in Water Resources*. **2007**. 30, 382-388.

40. Hatcher, W.J. Reaction and Mass Transport in Two-Phase Reactors. In: Cheremisinoff, N.P. (Ed.), Handbook of Heat and Mass Transfer. Mass Transfer and Reactor Design, **1986**. Vol. 2 Gulf Publishing, Houston.

41. Heiderscheidt, J.L.; Siegrist, R.L.; Illangasekare, T.H. Intermediate-Scale 2D Experimental Investigation using Potassium Permanganate for Remediation of Complex DNAPL Source Zones. *Journal of Contaminant Hydrology*. **2008**. 102, 3-16.

42. Holzbecher, E. *Environmental Modeling Using MATLAB*. Springer: Berlin: 2007.

43. Honning, J.; Broholm, M.M.; and Bjerg, P.L. Role of Diffusion in Chemical Oxidation of PCE in a Dual Permeability System. *Environmental Science & Technology*. **2007**. 41, 8426-8432.

44. Hood, E.D.; Thomson, N.R.; Grossi, D.; Farquahr, G.J. Experimental Determination of the Kinetic Rate Law for the Oxidation of Perchloroethylene by Potassium Permanganate. *Chemosphere*. **2000**. 40, 1383-1388 2000

45. Hrapovic, L: Sleep, B.E.; Major, D.J.; Hood, E.D. Laboratory Study of Treatment of Trichloroethene by Chemical Oxidation Followed by Bioremediation. *Environmental Science & Technology*. **2005**. 39, 2888-2897.

46. Huang, K.C; Hoag, G.E.; Chheda, P.; Woody, B.A.; Dobbs, G.M. Kinetic Study of Oxidation of Trichloroethylene by Potassium Permanganate. *Environmental Engineering Science*. **1999**. 16. 265-274.

47. Huang, K.C.; Hoag, G.; Chheda, P.; Woody, B.A.; Dobbs, G.M. Oxidation of Chlorinated Ethenes by Potassium Permanganate: A Kinetics Study. *Journal of Hazardous Materials*. **2001**. B87, 155-169.

48. Huang, K.C.; Hoag, G.; Chheda, P.; Woody, B.A.; Dobbs, G.M. Kinetics and Mechanism of Oxidation of Tetrachloroethylene with Permanganate. *Chemosphere*. **2002a**. 46, 815-825.

49. Huang, K.C.; Hoag, G.E.; Chheda, P.; Woody, W.A.; Dobbs, G.M. Chemical Oxidation of Trichloroethylene with Potassium Permanganate in a Porous Medium. *Advances in Environmental Research*. **2002b**. 7, 217-229.

50. Illangasekare, T.H.; Armbruster III, E.J.; Yates, D.N. Non-Aqueous-Phase Fluids in Heterogeneous Aquifer—Experimental Study. *Journal of Environmental Engineering*. **1995a.** 12, 571-579.

51. Illangasekare, T.H.; Ramsey, J.L.; Jensen, K.H.; Butts, M. Experimental Study of Movement and Distribution of Dense Organic Contaminants in Heterogeneous Aquifers: an Experimental Study. *Journal of Contaminant Hydrology*. **1995b**. 20, 1-25.

52. Illangasekare, T.H.; Munakata Marr, J.; Siegrist, R.L.; Soga, K.; Glover, K.C.; Moreno-Barbero, E.; Heiderscheidt, J.L.; Saenton, S.; Matthew, M.; Kaplan, A.R.; Kim, Y.; Dai, D.; Page, J.W.E. Mass Transfer from Entrapped DNAPL Sources Undergoing Remediation: Characterization Methods and Prediction Tools. **2006**. SERDP Project No. CU-1294 Colorado School of Mines.

53. Imhoff, P.T.; Jaffe, P.R.; Pinder, G.F. An Experimental Study of Complete Dissolution of a Non Aqueous Phase Liquid in Saturated Porous Media, *Water Resources Research*. **1993**. 30. 307-320

54. Imhoff, P.T.; Arthur, M.H.; Miller, C.T. Complete Dissolution of Trichloroethylene in Saturated Porous Media. *Environmental Science & Technology*. **1998**. 32, 2417-2424.

55. Johnson, R.L.; Pankow, J.F. Dissolution of Dense Chlorinated Solvents into Groundwater. 2. Source Functions for Pools of Solvent. *Environmental Science & Technology*. **1992**. 26, 896-901.

56. Kao, C.M.; Huang, K.D.; Wang, J.Y.; Chen, T.Y.; Chien, H.Y. Application of Potassium Permanganate as an Oxidant for *In Situ* Oxidation of Trichloroethylene-Contaminated Groundwater: A Laboratory and Kinetics Study. *Journal of Hazardous Materials*. **2008**. 153, 919-927.

57. Knauss, K.G.; Dibley, M.J.; Leif, R.N.; Mew, D.A.; Aines, R.D. The Aqueous Solubility of Trichloroethene (TCE) and Tetrachloroethene (PCE) as a Function of Temperature. *Applied Geochemistry*. **2000**. 15, 501-512.

58. Kueper, B.; Abbot, W.; Farquhar, G. Experimental observations of multiphase flow in heterogeneous porous media. *Journal of Contaminant. Hydrology*. **1989**. 5, 83-95.

59. Kueper, B.H.; Redman, D.; Starr, R.C.; Reitsma, S.; Mah, M. A field experiment to study the behavior of tetracholoroethylene below the water table; spatial distribution of residual and pooled DNAPL. *Ground Water*. **1993**. 31. 756-766.

60. Kueper, B.H.; Frind, E.O. Two-Phase Flow in Heterogeneous Porous Media, 1. Model Development. *Water Resources Research*. **1991a**. 27, 1049-1057.

61. Kueper, B.H.; Frind, E.O. Two-Phase Flow in Heterogeneous Porous Media, 1. Model Application. *Water Resources Research*. **1991b**. 27, 1059-1070.

62. Kueper, B.H., and McWhorter, D.B., Physics Governing the Migration of Dense Non-Aqueous Phase (DNAPLS) in Fractured Media. In: Pankow, J.F., and Cherry, J.A., Dense Chlorinated Solvents and Other DNAPLS in Groundwater: History, Behavior, and Remediation. 1996 Waterloo Press, Portland, 337-353.

63. Langan Engineering and Environmental Services Inc.. Groundwater Remedial Investigation Report. Busch Maintenance Garage. 2011. NJDEP Case Number: 94-04-19-1002-49.

64. Lee, K.Y.; Chrysikopoulos, C.V. Numerical modeling of three-dimensional contaminant migration from dissolution of multicomponent NAPL pools in saturated porous media. *Environmental Geology*. **1995**. 26, 157-165.

65. Lee, E.S.; Seol, Y.; Fang, Y.C.; Schwartz, F.W. Destruction Efficiencies and Dynamics of Reaction Fronts Associated with the Permanganate Oxidation of Trichloroethylene. *Environmental Science & Technology*. **2003**. 37, 2540-2546.

66. Lee, K.Y. Transport of Dissolved Contaminants Originating From a Rectangular Prism-Shaped, Multicomponent nonaqueous-Phase Liquid Source in Saturated Porous Media. *Environmental Geology*. **2002**. 43, 132–137.

67. Li, X.D.; Schwartz, F.W. Efficiency Problems Related to Permanganate Oxidation Schemes. In: Wickramanayake, G.B., Gavaskar, G.B., Chen A.R., (Eds.) Chemical Oxidation and Reactive Barriers: The Second International Conference on Remediation of Chlorinated and Recalcitrant Compounds. Batelle Press, Columbus, OH, 2000. 41-48.

68. Liu, C.; Ball, W.P. Back Diffusion of Chlorinated Solvent Contaminants from a Natural Aquitard to a Remediated Aquifer under Well-Controlled Field Conditions: Predictions and Measurements. *Ground Water*. **2002**. 40, 175-184.

69. Macdonald, J.A.; Kavanaugh, M.C. Restoring Contaminated Groundwater: An Achievable Goal?. *Environmental Science & Technology*. **1994**. 28, 362-368.

70. Mackay, D.M.; Cherry, J.A. Groundwater Contamination: Pump-and-Treat Remediation. *Environmental Science & Technology*. **1989**. 23, 630-636.

71. Mackay. D. M.; Freyburg, D.L.; Roberts, P.V. A Natural Gradient Experiment on Solute Transport in a Sand Aquifer 1. Approach and Overview of Plume Movement. *Water Resources Research*. **1986**. 22, 2017-2029.

72. MacKinnon, L.K.; Thomson, N.R. Laboratory-Scale *In Situ* Chemical Oxidation of a Perchloroethylene Pool Using Permanganate. *Journal of Contaminant Hydrology*. **2002**. 49-74.

73. Marble, J.C.; Carroll, K.C.; Janousek, H.; Brusseau, M.L. In Situ Oxidation and Associated Mass-Flux-Reduction/Mass-Removal Behavior for Systems with Organic Liquid Located in Lower Permeability Sediments. *Journal of Contaminant Hydrology*. **2010**. 117, 82-93.

74. Marvin, B.K.; and Chambers, J.; Leavitt, A.; Scheier, C.G. Chemical and Engineering Challenges to In Situ Permanganate Remediation. In: Gavaskar, A.R., and Chen, A.S.C., Remediation of Chlorinated and Recalcitrant Compounds: 3rd International Conference of Chlorinated and Recalcitrant Compounds-Monterey, CA . 2002. Batelle Press, Columbus,OH.

75. Mayer, A. S.; Miller, C.T. The influence of mass transfer characteristics and porous media heterogeneity on nonaqueous phase dissolution, *Water Resources Research*. **1996**. 32, 1551–1568.

76. McKay, L.D.; Stafford, P.L.; Toran, L.E. EPM Modeling of a Field-Scale Tritium Tracer Experiment in Fractured, Weathered Shale. *Ground Water*. **1997**. 35, 997-1007.

77. Mercer, J.; Cohen, R. A Review of Immiscible Fluids in the Subsurface: Properties, Models, Characterization and Remediation. *Journal of Contaminant Hydrology*. **1990**. 6. 107-163.

78. Miller, C.M.; Poirier-McNeil, M.M.; Mayer, A.S. Dissolution of Trapped Non-Aqueous Phase Liquids: Mass Transfer Characteristics. *Water Resources Research*. **1990**. 23, 2783-2793.

79. Mumford, K.G.; Thomson, N.R.; Allen-King, R.M. Bench-Scale Investigation of Permanganate Natural Oxidant Demand Kinetics. *Environmental Science & Technology*. **2005**. 39, 2835-2840.

80. Mundle, K.; Reynolds, D.A.; West, M.R.; Kueper, B. H. Concentration Rebound Following In Situ Chemical Oxidation in Fractured Clay. *Ground Water*. **2007**. 45: 692-702.

81. MWH, Hot Spot Pilot Test Evaluation Report for Chemplex Site in Clinton, IO. 2010

82. Nambi, I. NAPL Dissolution in Heterogeneous Systems: an Experimental Investigation in a Simple Heterogeneous System. *Journal of Contaminant Hydrology*. **2000**. 44. 161-184.

83. Park, E; Parker, J.C. Evaluation of an Upscaled Model for DNAPL Dissolution Kinetics in Heterogenous Aquifers. *Advances in Water Resources*. **2005**. 28, 1280-1291.

84. Parker, J.C.; Katyal, A.K.; Kaluarachchi, J.J.; Lenhard, R.J.; Johnson, T.J.; Jayaraman, K.; Unlu, K.; Zhu, J.L. Modeling Multiphase Organic Chemical Transport in Soils and Ground Water. USEPA Report 600/2– 91/042. USEP, Washington, D. C. 1991.

85. Parker, B.L., Cherry, J.A., and Gillham, R.W., The Effects of Molecular Diffusion on DNAPL Behavior in Fractured Porous Media. In: Pankow, J.F., and Cherry, J.A., Dense Chlorinated Solvents and Other DNPLS in Groundwater: History, Behavior, and Remediation. 1996. Waterloo Press, Portland, 355-393.

86. Parker, B.L.; Cherry, J.A.; Chapman, S.W.; Guilbeault, M.A. Review and Analysis of Chlorinated Solvent Dense Non-Aqueous Phase Liquid Distributions in Five Sandy Aquifers. *Vadose Zone Journal*. **2003**. 2, 116-137.

87. Parker, J.C.; Park, E. Modeling Field-Scale Dense Nonaqueous Phase Liquid Dissolution Kinetics in Heterogeneous Aquifers. *Water Resources Research*. **2004**. 40, 1-12.

88. Parker, B.L.; Chapman, S. W.; Guilbeault, M. A. Plume Persistence Caused by Back Diffusion from Thin Clay Layers in a Sand Aquifer Following TCE Source-Zone Hydraulic Isolation. *Journal of Contaminant Hydrology*. **2008**. 102: 86-104.

89. Petri, B.G.; Siegrist, R.L.; Crimi, M.L. Effects of Groundwater Velocity and Permanganate Concentration on DNAPL Mass Depletion Rates During *In Situ* Oxidation. *Journal of Environmental Engineering*. **2008**. January, 1-13.

90. Pfannkuch, H. 0. Determination of the Contaminant Source Strength from Mass Exchange Processes at the Petroleum/Groundwater Interface in Shallow Aquifer Systems. In: Petroleum Hydrocarbons and Organic Chemicals in Groundwater, National Water Well Association, Worthington, Ohio, 1984, pp. 111-129.

91. Poulsen, M. M.; Kueper, B.H. A Field Experiment to Study the Behavior of Tetrachloroethylene in Unsaturated Porous Media. *Environmental Science & Technology*. **1992**. 26. 889– 895.

92. Powers, S. E.; Abriola, L.M.; Weber, W.J. An Experimental investigation of Nonaqueous Phase Liquid Dissolution in Saturated Subsurface Systems: Steady State mass Transfer Rates. *Water Resources Research*. **1992**. 28. 2691-2705.

93. Powers, S.E.; Abriola, L.M.; Weber, W.J.; An Experimental Investigation of Nonaqueous Phase Liquid Dissolution in Saturated Subsurface Systems: Transient Mass Transfer Rates. *Water Resources Research*. **1994**. 30, 321-332.

94. Remson, I; Hornberger, G.M.; Molz, F.J. Numerical Methods in Subsurface Hydrology: With an Introduction to the Finite Difference Method. Wiley-Interscience: New York 1971.

95. Reitsma, S.; and Dai, Q.L. Reaction-Enhanced Mass Transfer and Transport from Non-Aqueous Phase Liquid Source Zones. *Journal of Contaminant Hydrology*. **2001**. 49, 49-66.

96. Rivett, M.O.; Feenstra, S.; Cherry, J.A.; Field Experimental Studies of Residual Solvent Source Emplaced in the Groundwater Zone. **1991**. Proceedings of the Petroleum Hydrocarbons and Organic Chemicals in Ground Water: Prevention, Detection, and Restoration. NWWA/API Houston TX, 283-300.

97. Roberts, P V.; Goltz. M. N.; Mackay. D. M. A Natural Gradient Experiment on Solute Transport in a Sand Aquifer 3. Retardation Estimates and Mass Balances for Organic Solutes. *Water Resources Research*, **1986**. 22 2047-2058.

98. Rorabacher, D.B. Statistical Treatment for Rejection of Deviant Values: Critical Values of Dixon Q Parameter and Related Subrange Ratios at the 95 Percent Confidence Level. *Analytical Chemistry*. **1991**. 83, 139-146.

99. Roy, J.W.; Smith J.E.; Gillham, R.W. Natural Remobilization of Multicomponent DNAPL Pools Due to Dissolution. *Journal of Contaminant Hydrology*. **2002**. 59, 163–186.

100. RWMA. Groundwater Movement at PORTS. 2002

101. Saba, T.A. Upscaling of Mass Transfer from Entrapped NAPLs Under Natural and Enhanced Conditions, Ph.D. Dissertation, University of Colorado, Boulder CO, 1999.

102. Saba, T.A.; Illangasekare, T.H. Effect of Groundwater Flow Dimensionality on Mass Transfer from Entrapped Non-Aqueous Phase Liquid Contaminants, *Water Resources Research*. **2000**. 36, 971-979.

103. Saenton, S.; Illangasekare, T.H. Evaluation of Benefits of Partial Source Zone Treatment Using Intermediate-Scale Physical Model Testing and Numerical Analysis. In Groundwater Engineering—Recent Advances: Proceedings of the International Symposium, Okayama, Japan, 28– 30 May 2003.: Eds.: Kono, I; Nishigaki, M.; Komatsu, M. Taylor and Francis, Philadelphia, Pa. pp. 25-34.

104. Sale, T. C.; McWhorter, D. B. Steady State Mass Transfer from Single-Component Dense Nonaqueous phase Liquids in Uniform Flow Fields. *Water Resources Research*. **2001**. 37, 393–404.

105. Sahl, J.W.; Munakata-Marr, J.; Crimi, M.L.; Siegrist, R.L. Coupling Permanganate Oxidation with Microbial Dechlorination of Tetrachloroethane. *Water Environment Research*. **2007.** 79, 5-12.

106. Schnarr, M.; Truax, C.; Farquhar, G.; Hood, E., Gonullu, T.; Stickney, B. Laboratory and Controlled Field Experiments using Potassium Permanganate to Remediate Trichloroethylene and Perchloroethylene DNAPLs in Porous Media. *Journal of Contaminant Hydrology*. **1998**. 29, 205-224.

107. Schnoor, J.L. *Environmental Modeling: Fate and Transport of Pollutants in Water, Air, and Soil*. Wiley Interscience.: New York, NY, 1996.

108. Schwille, F. *Dense Chlorinated Solvents in Porous and Fractured Media*, Lewis Publishers, Chelsea, MI, 1988.

109. Schroth, M.H.; Oostrom, M.; Wietsma, T.W.; Istok, J.D. *In-Situ* Oxidation of Trichloroethene by Permanganate: Effects of Porous Medium Hydraulic Properties. *Journal of Contaminant Hydrology*. **2001**. 50, 79-98.

110. Seol, Y.; Zhang, H.; Schwartz, F.W. A Review of *In Situ* Chemical Oxidation and Heterogeneity. Environmental and Engineering. *Geoscience*. **2003**. 1, 37-49.

111. Soga, K.; Page, J.W.E.; Illangasekare, T.H. A Review of NAPL Source Zone Remediation Efficiency and Mass Flux Approach. *Journal of Hazardous Materials*. **2004**. 110, 13-27.

112. Stuse, A.M.; Siegrist, R.L.; Dawson, H.E.; Urynowicz, M.A. Diffusive Transport of Permanganate During *In Situ* Oxidation. *Journal of Environmental Engineering*. **2002**. April, 327-334.

113. Sudicky, E.A. An Advection-Diffusion Theory of Contaminant Transport for Stratified Porous Media, Ph.D. Thesis, Univ. of Waterloo, Waterloo, Ont., 1983.

114. Sudicky, E. A. A Natural Gradient Experiment on Solute Transport in a Sand Aquifer: Spatial Variability of Hydraulic Conductivity and Its Role in the Dispersion Process. *Water Resources Research*. **1986**. 22, 2069-2082.

115. Sutton, P.A.; Barker, J.F. Migration and Attenuation of Selected Organics in a Sandy Aquifer- A Natural Gradient Experiment. *Ground Water*. **1985**. 10-16.

116. Tetra Tech. Treatability Pilot Study Report for Valmont TCE Site. 2010. EPA Work Assignment Number 035-PTCO-031M

117. Thomson, N.R.; Hood, E.D.; Farquhar, G.J. Permanganate Treatment of an Emplaced DNAPL Source. *Ground Water Monitoring & Remediation*. **2007**. 27, 74-85.

118. Tunnicliffe, B.S.; Thomson, N.R. Mass Removal of Chlorinated Ethenes from Rough-Walled Fractures using Permanganate. *Journal of Contaminant Hydrology*. **2004**. 75, 91-114.

119. Urynowicz, M.A.; Siegrist, R.L. Interphase Mass Transfer During Chemical Oxidation of TCE DNAPL in an Aqueous System. *Journal of Contaminant Hydrology*. **2005**. 80, 93-106.

120. Vanderborght, J.; Vereecken, H. Review of Dispersivities for Transport Modeling in Soils. *Vadose Zone Journal*. **2007**. 6, 29-52.

121. Vanderkwaak, J.E.; Sudicky, E.A. Dissolution of Non-Aqueous-Phase Liquids and Aqueous-Phase Contaminant Transport in Discretely-Fractured Porous Media. *Journal of Contaminant Hydrology*. **1996**. 23, 45-68.

122. Warrick, A.W.; Nielson, D.R. Spatial Variability of Soil Physical Properties in the Field. In: Hillel, D., Applications of Soil Physics. 1980. Academic Press, New York, NY.

123. Weber, W.J. Jr.. *Environmental Systems and Processes: Principles, Modeling, and Design*. Wiley-Interscience. New York, NY, 2001.

124. West, O.R.; Cline, S.R.; Holden, F.G.; Gardner, B.M.; Schlosser, J.E.; Thate, D.E.; Pickering, D.A.; Houk, T.C. A Full-Scale Demonstration of In-Situ Chemical Oxidation Through Recirculation at X-701B Site, ORNL/TM-13556, **1997**. 1-102.

125. West, M.W.; Grant, G.P.; Gerhard, J.I.; Kueper, B.H. The Influence of Precipitate Formation of the Chemical Oxidation of TCE DNAPL with Potassium Permanganate. *Advances in Water Resources*. **2008**. 31, 324-338.

126. Wexler, E. *Analytical Solutions for One-,Two-,and Three-Dimensional Solute Transport in Ground-Water Systems with Uniform Flow.* USGS: Government Printing Office: 1992

127. Williams, J.H.; Paillet, F.L. Characterization of Fractures and Flow Zones in a Contaminated Shale at the Watervliet Arsenal, Abany County, New York. 2002. USGS Open File Report 01-385

128. Yan, Y.E.; and Schwartz, F.W. Oxidative Degradation and Kinetics of Chlorinated Ethylenes by Potassium Permanganate. *Journal of Contaminant Hydrology*. **1999**. 37, 343-365.

129. Zhang, H.; Schwartz, F.W. Simulating the In Situ Oxidative Treatment of Chlorinated Ethylenes by Potassium Permanganate. *Water Resources Research*. **2000**. 36, no. 10: 3031-3042.

130. Zhu, J.; Sykes, J.F. The Influence of NAPL Dissolution Characteristics on Field-Scale Contaminant Transport in the Subsurface. *Journal of Contaminant Hydrology*. **2000**. 41, 133–154

Vita

Adam Karl Tressler

Ph.D. Environmental Science, Rutgers University, October 2012

M.A. in Public Policy and M.S. in Environmental and Waste management, SUNY Stony Brook Fall, Fall, 2002

B.A. in Philosophy, Mansfield University, Spring, 1999
Minors in Chemistry, Environmental Studies, Math, Music, and Political Science

Environmental Health & Safety Specialist III, Rutgers University, July, 2007 – Present

Environmental Health & Safety Technician, Rutgers University, December,2007 – July, 2007

Instructor, Pennsylvania College of Technology, Fall 2005- Summer 2007

- Courses taught: Environmental Science, Introduction to Philosophy, Ethics

Instructor, Mansfield University, Fall 2005 & Summer 2006

- Courses taught: Environmental Crime and Enforcement, American Government

Instructor, St. Bonaventure University, Spring 2003

- Courses taught: Feeding the World: Food and the Environment

Environmental & Waste Coordinator, SUNY Stony Brook, November, 2000 - January, 2002

Hydrogeologist/Technician, Handex Consulting & Remediation, LLC., August, 2000 - November, 2000

Hazardous Waste Technician, Leard Environmental Services, September, 1999 to November, 2000